UAB

Universitat Autònoma de Barcelona

Ochrobactrum anthrop

UAB
Universitat Autònoma de Barcelona

FACULTAT DE BIOCIÈNCIES

DEPARTAMENT DE GENÈTICA I MICROBIOLOGIA

Heavy metal uptake in the environmental isolated bacterium *Ochrobactrum anthropi* DE2010: Morphological responses, genomic insights and cellular strategies

Eduard Villagrasa Ramírez

2021

UAB

Universitat Autònoma de Barcelona

FACULTAT DE BIOCIÈNCIES

DEPARTAMENT DE GENÈTICA I MICROBIOLOGIA

Heavy metal uptake in the environmental isolated bacterium *Ochrobactrum anthropi* DE2010: Morphological responses, genomic insights and cellular strategies

Memòria de la tesi presentada per obtenir el grau de Doctor en Microbiologia per la Universitat Autònoma de Barcelona, per Eduard Villagrasa Ramírez.

Vist i plau del director,

Dr. Antoni Solé Cornellà

Bellaterra, Gener del 2021

Amable, optimista,

precisa, paciente, incansable,

luchadora, empática,

un referente,

Para ti Isabel.

"The question "What is Life?" is a linguistic trap. To answer according to the rules of grammar, we must supply a noun, a thing. But life on Earth is more like a verb. It repairs, maintains, re-creates, and outdoes itself"

Lynn Margulis (What is life, 1995)

CONTENTS

SUMMARY

La contaminació ambiental és una de les condicions extremes que pot alterar els ecosistemes naturals i afectar tots els organismes vius. Entre els contaminants ambientals, els metalls tenen un paper rellevant degut a la seva elevada toxicitat. De fet, es pot considerar que els microorganismes que habiten zones contaminades per metalls formen freqüentment consorcis, la qual cosa els permet desenvolupar estratègies cel·lulars per sobreviure en presència de metalls evitant així els seus efectes nocius.

En els darrers anys, el nostre grup de recerca ha aïllat diferents consorcis de microorganismes dels tapets microbians del delta de l'Ebre (Tarragona). Aquests consorcis estan formats per un únic microorganisme fotòtrof i diferents heteròtrofs. En la present tesi doctoral, a partir del consorci on domina la microalga *Scenedesmus* sp. DE2009, s'ha aïllat, caracteritzat i identificat un bacteri heteròtrof com a *Ochrobactrum anthropi* DE2010. En estudis preliminars, aquest bacteri ha mostrat la capacitat per fixar nitrogen atmosfèric, presentar pleomorfisme cel·lular i resistir a antibiòtics del grups dels betalactàmics. Encara que prèviament s'ha investigat l'efecte de diversos metalls pesants en el consorci *Scenedesmus* sp. DE2009, no se sap res sobre l'efecte d'aquests en la viabilitat cel·lular d'*O. antropi* DE2010 i el seu paper en la captació de metalls pesants.

Els objectius de la present tesi s'han desenvolupat tenint en compte que *O. anthropi* DE2010 creix de manera fàcil i ràpida tant en medi líquid com sòlid, esdevenint un model adequat per a la investigació front a toxicitat per metalls pesants. A més a més, s'ha analitzat l'efecte citotòxic i la capacitat de resposta de *O. anthropi* DE2010 per superar l'estrès front a l'exposició a Cd, Pb(II), Cu(II), Cr(III) i Zn així com els patrons de localització cel·lular

d'aquests metalls i les estratègies emprades per aquest bacteri per immobilitzar-los. Aquesta tesi s'ha organitzat en diferents capítols. Concretament, el capítol 2 correspon als articles publicats on els resultats obtinguts de la investigació realitzada es troben a les seccions de la 2.1 a la 2.4 i es discuteixen globalment en el capítol 3.

Els resultats obtinguts en aquest estudi indiquen que *O. anthropi* DE2010 mostra una elevada resistència als cinc metalls assajats tolerant concentracions de fins a 20 mM de Zn i de 10 mM per a Cd, Pb(II), Cu(II) i Cr(III). A més, aquest bacteri té una gran capacitat per eliminar metalls del medi, captant fins a un 90% de Pb (II) i un 40% de Cr (III), ambdós a 10 mM. Analitzant la seqüencia del genoma d'*O. anthropi* DE2010 s'ha observat que presenta sis gens relacionats amb el metabolisme del polifosfat, i que l'anàlisi del contingut cel·lular de polyP indica que aquest bacteri el sintetitza i l'acumula de manera directament proporcional a la concentració de metall. D'altra banda, les cèl·lules d'*O. anthropi* DE2010 immobilitzen metalls pesants en grànuls i/o inclusions de polyP mitjançant tres patrons específics de localització subcel·lular: extracel·lularment en grànuls de polifosfat (Cu (II)); a l'espai periplasmàtic formant cristalls amb el fòsfor (Pb (II)), i intracel·lularment en inclusions de polifosfat (Pb (II), Cr (III) i Zn). Per tant, *O. anthropi* DE2010 genera respostes cel·lulars (estratègies de supervivència) específiques per a cada metall, com ara bioacumulació en el cas de Pb (II), Cu (II), Cr (III) i Zn, biosorció per al Cr (III) i Cd i biomineralització per al Pb (II). L'elevada resistència i la capacitat de segrestar metalls d'*O. anthropi* DE2010 posen de manifest el seu gran potencial com a possible agent bioremediador, especialment en zones contaminades per Pb i Cr.

La contaminación ambiental es una de las condiciones extremas que puede alterar los ecosistemas naturales y afectar a todos los organismos vivos. Entre los contaminantes ambientales, los metales tienen un papel relevante debido a su elevada toxicidad. De hecho, se puede considerar que los microorganismos que habitan zonas contaminadas por metales forman frecuentemente consorcios, lo que les permite desarrollar estrategias celulares para sobrevivir en presencia de metales evitando así sus efectos nocivos.

En los últimos años, nuestro grupo de investigación ha aislado diferentes consorcios de microorganismos de los tapetes microbianos del delta del Ebro (Tarragona). Estos consorcios están formados por un único microorganismo fotótrofo y varios heterótrofos. En la presente tesis doctoral, a partir del consorcio donde domina la microalga *Scenedesmus* sp. DE2009, se ha aislado, caracterizado e identificado una bacteria heterótrofa como *Ochrobactrum anthropi* DE2010. En estudios preliminares, esta bacteria ha mostrado la capacidad para fijar nitrógeno atmosférico, presentar pleomorfismo celular y resistir a antibióticos del grupo de los betalactámicos. Aunque previamente se ha investigado el efecto de varios metales pesados en el consorcio *Scenedesmus* sp. DE2009, poco se conoce del efecto de estos en la viabilidad celular de *O. antropi* DE2010 y su papel en la captación de metales pesados.

Los objetivos de la presente tesis se han desarrollado teniendo en cuenta que *O. anthropi* DE2010 crece de manera fácil y rápida tanto en medio líquido como sólido, lo que permite considerarlo como modelo para la investigación frente a la toxicidad por metales pesados. Además, se ha analizado el efecto citotóxico y la capacidad de respuesta de *O. anthropi* DE2010 para superar el estrés frente a la exposición a Cd, Pb(II), Cu(II), Cr(III) y Zn así como los patrones de localización celular de estos metales y las estrategias empleadas

por esta bacteria para inmovilizarlos. Esta tesis se ha organizado en diferentes capítulos. Concretamente, el capítulo 2 corresponde a los artículos publicados donde los resultados obtenidos se encuentran en las secciones de la 2.1 a la 2.4 y se discuten globalmente en el capítulo 3.

Los resultados obtenidos en este estudio indican que *O. anthropi* DE2010 muestra una elevada resistencia a los cinco metales ensayados tolerando concentraciones de hasta 20 mM de Zn y de 10 mM para Cd, Pb(II), Cu(II) y Cr(III). Además, esta bacteria tiene una gran capacidad para eliminar metales del medio, captando hasta un 90% de Pb (II) y un 40% de Cr (III), ambos a 10 mM. Analizando la secuencia del genoma de *O. anthropi* DE2010 se ha observado que presenta seis genes del metabolismo del polifosfato, y que el análisis del contenido celular de polyP indica que esta bacteria lo sintetiza y acumula de manera directamente proporcional a la concentración de metal. Por otro lado, las células de *O. anthropi* DE2010 inmovilizan metales pesados en gránulos y/o inclusiones de polyP mediante tres patrones específicos de localización subcelular: extracelularmente en gránulos de polifosfato (Cu (II)); en el espacio periplasmático formando cristales con el fósforo (Pb (II)), e intracelularmente en inclusiones de polyP (Pb (II), Cr (III) y Zn). Por lo tanto, *O. anthropi* DE2010 genera respuestas celulares (estrategias de supervivencia) específicas para cada metal, como bioacumulación en el caso de Pb (II), Cu (II), Cr (III) y Zn, biosorción para el Cr (III) y Cd y biomineralitzación para el Pb (II). La elevada resistencia y la capacidad de secuestrar metales de *O. anthropi* DE2010 ponen de manifiesto su gran potencial como posible agente bioremediador, especialmente en zonas contaminadas por Pb y Cr.

Environmental pollution remains as one of the extreme conditions that can disrupt the existing natural ecosystems and affect all the living organisms. Among the environmental stressors, metals play a significant role as potential toxicants. Consequently, it can be considered that the microorganisms inhabiting metal polluted areas frequently form consortia and they can develop cellular strategies to survive in the presence of heavy metals for avoid their negative effects.

In the last years, our research group has isolated different consortia of microorganisms from Ebro Delta microbial mats (Tarragona). These consortia are formed by a single type of phototrophic microorganism and different heterotrophic bacteria. In the present doctoral thesis, an heterotrophic bacteria from the consortium dominated by the microalga *Scenedesmus* sp. DE2009, have been isolated, characterized and identified as *Ochrobactrum anthropi* DE2010. In preliminary studies, this bacterium showed the ability to fix atmospheric nitrogen, present cellular pleomorphism and beta-lactam antibiotic resistance. Despite the effect of some heavy metals in the microalgae consortium had previously been investigated, nothing is known about the effect of them on the cell viability of *O. anthropi* DE2010 and the role of this bacterium in heavy metal sequestration.

The goals of this thesis have been developed taking into account the fact that *O. anthropi* DE2010 grows easily and fast in both liquid and solid media culture, which it becomes a suitable model for heavy metal experimental research. Thus, cytotoxic effects of heavy metals and cellular responses on *O. anthropi* DE2010 cultures exposed to increasing concentrations of Cd, Pb(II), Cu(II), Cr(III), and Zn, and the cellular metal localization patterns and the strategies and pathways used by this bacterium to immobilize them have extensively been analyzed. This thesis has been organized in different Chapters. Specifically,

the Chapter 2 correspond to the published articles; thus, the obtained results from the research carried out are therefore in sections from 2.1 to 2.4 and are discussed globally in Chapter 3.

The results of this study indicate that *O. anthropi* DE2010 shows high resistance to the five tested metals, supporting concentrations up to 20 mM of Zn and up to 10 mM for Cd, Pb(II), Cu(II) and Cr(III). Moreover, this bacterium has a high ability to remove metals from the environment, highlighting up to 90% for Pb(II) and 40% for Cr(III) both at 10 mM. Analyzing the sequenced genome of *O. anthropi* DE2010 it has been observed that it presents six genes linked to the metabolism of the polyphosphate and that the analysis of polyP content indicates that this bacterium synthesizes and accumulates it in a metal concentration-dependent manner. *O. anthropi* DE2010 cells immobilized heavy metals in polyP granules and/or inclusions in three metal-specific patterns for subcellular localization: extracellular in polyphosphate granules (Cu(II)); in the periplasmic space forming crystals with phosphorus (Pb(II)), and intracellular in polyphosphate inclusions (Pb(II), Cr(III) and Zn). Therefore*, O. anthropi* DE2010 generates specific cellular responses for each heavy metal as survival strategies, such as bioaccumulation for Pb(II), Cu(II), Cr(III) and Zn, biosorption for Cr(III) and Cd and biomineralization for Pb(II). The high resistance and the capacity to uptake metals evidenced by *O. anthropi* DE2010 prove its great potential as a possible candidate to bioremediate, especially Pb and Cr polluted areas.

THESIS STRUCTURE

Chapter I. Introduction

This chapter introduces the sampling site: Ebro Delta microbial mats. It covers the concept of microbial consortia, particularly the *Scenedesmus* sp. DE2009 consortium. Additionally, the environmental bacterial isolates including *Ochrobactrum anthropi* DE2010 and the effects of heavy metal pollution in natural ecosystems such as the Ebro river are described in detail. Lastly, it emphasizes the cellular strategies and pathways of microorganisms to capture and resist the heavy metal toxicity.

Chapter II. Publications

This chapter is divided into four sections 2.1 to 2.4; each of them corresponding to the accepted versions of published articles. In these articles, a combination of qualitative and quantitative microbiological, morphological, and analytical techniques was selected. It provides a comprehensive overview of the bacterium *O. anthropi* DE2010 and its cell responses to heavy metals exposure.

Chapter III. Summary of Results and General Discussion

In this chapter, all the results obtained in sections 2.1 to 2.4 are summarized and discussed.

Chapter IV. Conclusion

The last chapter covers the conclusions obtained in this thesis.

1 μm
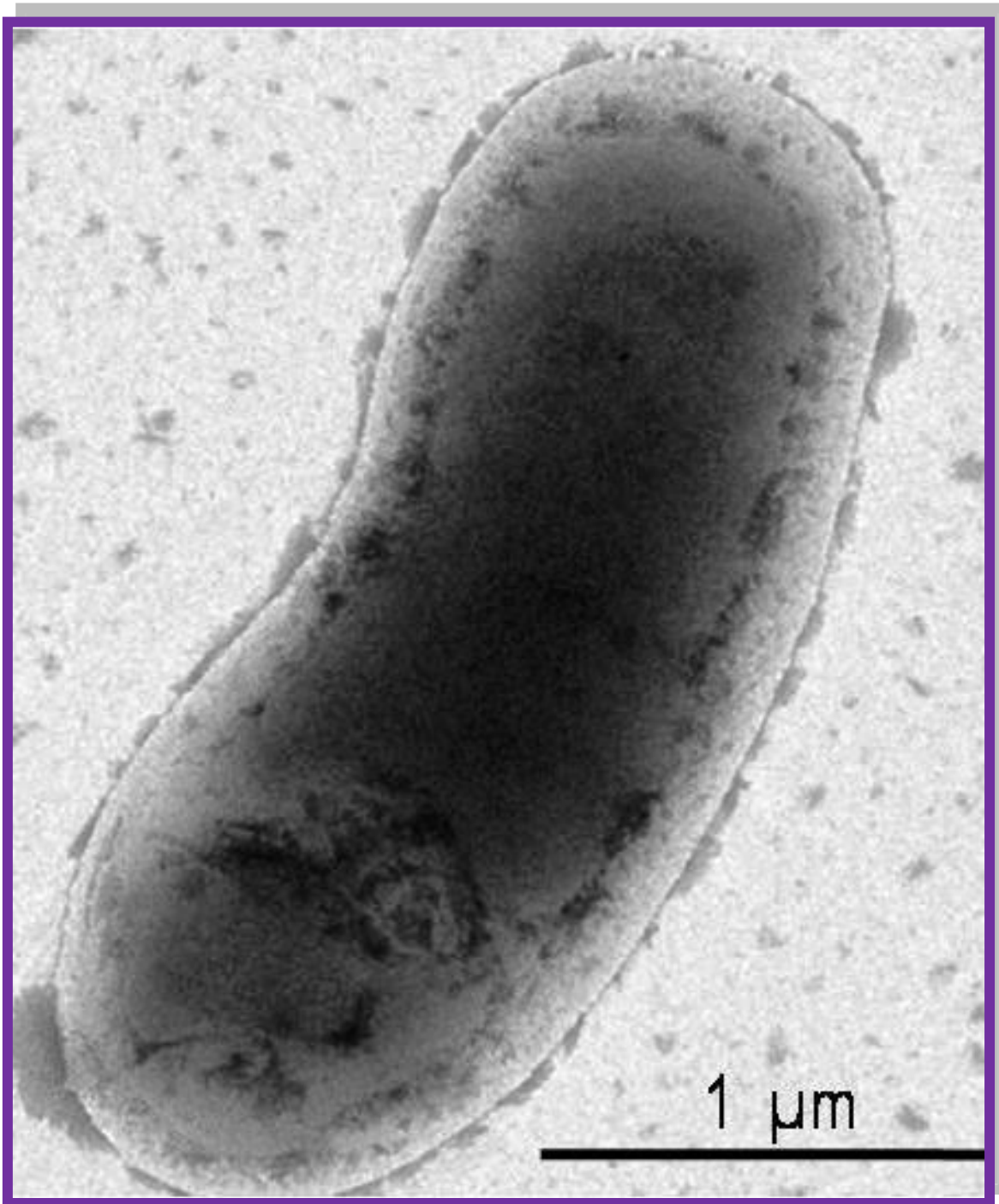
Chapter I. Introduction

A microbial consortium is a group of different species of microorganisms that act together as a community in a specific habitat. The origin of this functional unit seems to be related to its ability to survive in extreme and unfavorable conditions of the environment (Seufferheld et al. 2008; Merino et al. 2019; Yin et al. 2019a). The most common adverse environmental conditions for microorganisms include (i) high or low temperatures (hot and cold deserts, hot springs, hydrothermal vents, polar regions, and cold waters) (de los Ríos et al. 2014; Fernandez-Martínez et al. 2016), (ii) high atmospheric pressures (deep lakes) (Verma et al. 2017; Saber et al. 2019), (iii) the deviation of pH values from optimum levels (alkaline and acid hot springs or lakes) (Edwardson et al. 2014; Sakai et al. 2016), and (iv) high salinity concentrations (salt flats and hypersaline waters) (Hayashida et al. 2017; Shadrin, 2018). Several anthropogenic activities, especially those related to agriculture and industry, have continued to produce new adverse conditions for the growth of microorganisms. These activities release high amounts of toxic substances into the environment, including organic xenobiotic (oxidants, phenols) and heavy metals – the breeding ground of the microorganisms (revision in Ojuederie and Babalola, 2017; revision in Rai et al. 2019). Furthermore, microorganisms with the capability of survival and growth in natural extreme environments develop metabolic mechanisms and pathways. These mechanisms can be applied to a plethora of economic activities in the field of biotechnology, medicine, agriculture, and/or environmental protection. To this end, the isolation and characterization of novel tolerant microbial species are emerging as a key question in all economic areas.

Microbial mats are highly productive, often centimeter-thick benthic multilayered structures formed by bacteria, archaea, algae, and fungi and sometimes enriched with protozoans and sediment. Today, these ecological assemblages that grow at solid-aqueous interfaces in extreme environments (Wong et al. 2016; Reinold et al. 2019) are considered the modern equivalents of Precambrian stromatolites, the oldest ecosystem known from the fossil record (Hickman-Lewis et al. 2018; Visscher et al. 2020). Microbial mats provide a highly productive ecosystem and are widely distributed around the world (Davey and O'Toole, 2000; Abed et al. 2020). They are well documented in coastal areas such as marine waters (Esteve et al. 1992; Gontharet et al. 2017), freshwaters (Chan et al. 2016; Cardoso et al. 2019), and soils (Lavoie et al. 2017; Kobayashi et al. 2020). They can also be found in extreme environments including hypersaline ponds (Hoehler et al. 2001; Isaji et al. 2017), estuaries (Spetter et al. 2015; Serra et al. 2017), hot deserts (Abed et al. 2015; Abed et al. 2018), hot springs (Roeselers et al. 2007; Tank et al. 2017), polar regions (Jungblut et al. 2012; Prieto-Barajas et al. 2018), and hydrothermal vents in the deep ocean (Miranda et al. 2016; Zhang et al. 2019). Although they appear to be a stable ecosystem, microbial mats are exposed to highly dynamic conditions under changing light intensity, temperature, salinity, pH, sulfide (S^{2-}), carbon dioxide (CO_2), oxygen (O_2) among other physicochemical parameters (Nübel et al. 2001; Martínez-Alonso et al. 2004; Bolhuis et al. 2014; Prieto-Barajas et al. 2018; Lichtenberg et al. 2020). In these environments, the microbial mats establish the essential role of heterotrophic bacteria in the biogeochemical cycles (Reid et al. 2000; revision in Prieto-Barajas et al. 2018), especially in phototrophic consortia. In such associations, microorganisms are mostly located in the amorphous sheath that envelops

filamentous cyanobacteria and microalgae (Diestra et al. 2005; revision in Fakhimi et al. 2020).

Our research group studied the microbial mats of Ebro Delta (0°35'E–0°56'E and 40°33'N–40°47'N) located at the mouth of the Ebro River in the province of Tarragona (between Montsià and Baix Ebre counties) in Catalonia (NE Spain). In 1983, the Ebro Delta was declared a protected area which later expanded in 1986 covering an area of 7,736 hectares. Microbial mats of the Ebro Delta cover an area of 3 km^2. They occur along the coast in the narrow ephemeral ponds of the backshore, on the flanks of the storm inlets, and most commonly, on the sand flats and channels of the La Banya spit (Fig 1A). Moreover, these mats are benthic ecosystems vertically stratified in varying thick (mm to cm) colored layers (Fig 1B-C) formed by several phototrophic microorganisms such as algae, cyanobacteria, and purple sulfur bacteria, and different groups of heterotrophic bacteria (Esteve et al. 1992; Guerrero et al. 1993; Navarrete et al. 2000; Solé et al. 2003; Benaiges-Fernandez and Urmeneta, 2018; Burganskaya et al. 2019).
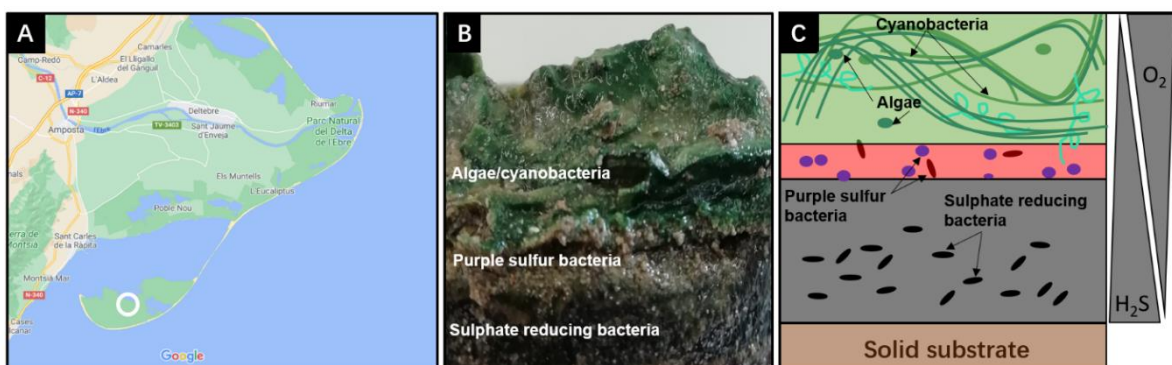
Figure 1 Ebro Delta Microbial Mats. (A) Ebro Delta area, (B) overview yz image, and (C) microbial mat graphic representation from the Ebro Delta sampling site. The white circle indicates the sampling site. Sources: (A) Google maps and (B) and (C) property of the thesis author.

Three stable consortia of microorganisms, formed by a single type of phototrophic microorganism (the most abundant) and different heterotrophic bacteria, have been isolated from Ebro Delta microbial mats (Diestra et al. 2005; Maldonado et al. 2010a; Burgos et al. 2013). Two out of the three microorganisms are filamentous cyanobacteria – *Microcoleus chthonoplastes* DE2006 (Fig 2A and D) and *Geitlerinema* sp. DE2011 (Fig 2B and E) – while the third one is a unicellular microalga - *Scenedesmus* sp. DE2009 (Fig 2C and F). These microorganisms carry out oxygenic photosynthesis using water as the electron donor and chlorophyll *a* as the key photosynthetic pigment, fixing the CO_2 through the Calvin cycle. Specifically, *Microcoleus chthonoplastes* DE2006 is a benthic cyanobacterium with trichomes of 2.5-6 mm in diameter. It has elongated intercalary cells with constrictions at the cross-walls and conical end cells and forms bundles of many closely intertwined trichomes enclosed in a common sheath (Diestra et al. 2005). *Geitlerinema* sp. DE2011 is a cyanobacterium which forms single filaments (size from 3.13 to 3.75 μm), sometimes densely packed and surrounded by a sheath (Burgos et al. 2013). Lastly, *Scenedesmus* sp.DE2009 is a microalga which forms spherical cells and grows to a diameter of 7–9 μm (Maldonado et al. 2010a).
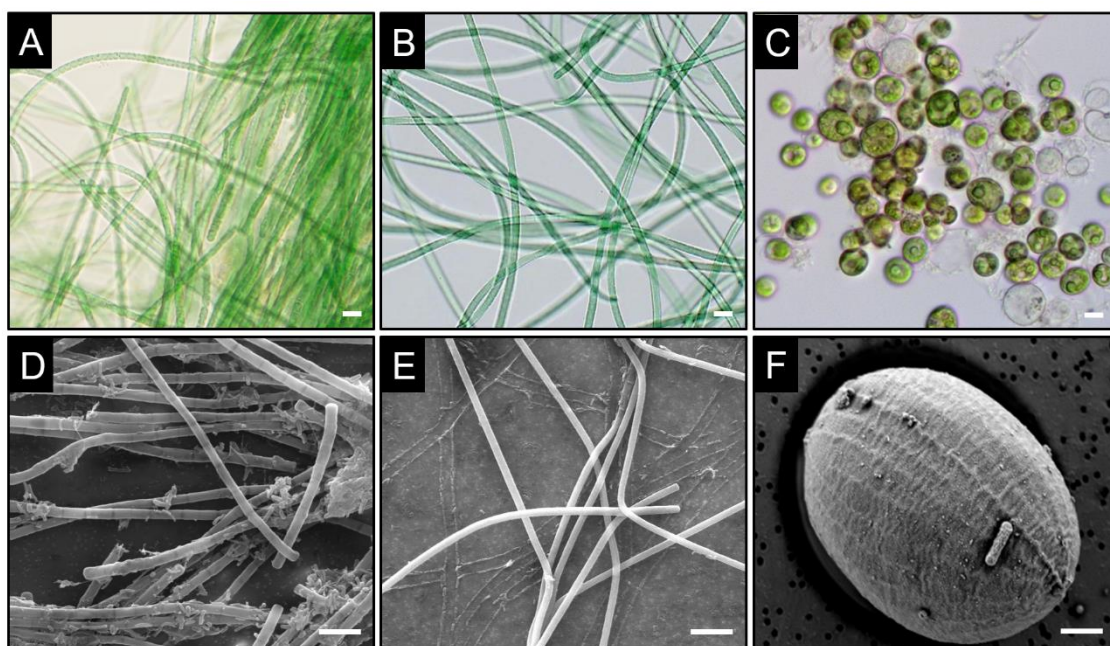
Figure 2. Optical bright-field microscopy images of (A) *Microcoleus chthonoplastes* DE2006, (B) *Geitlerinema* sp. DE2011, and (C) *Scenedesmus* sp. DE2009. Scanning electron microscopy (SEM) images of (D) *Microcoleus chthonoplastes* DE2006, (E) *Geitlerinema* sp. DE2011, and (F) *Scenedesmus* sp. DE2009. The scale bars represent 10 μm (A, B, and C) and 1 μm (D, F, and G), respectively. Sources: Courtesy of Dr. Elia Diestra (A and D) and Dr. Laia Millach (B-C and E-F).

Several heterotrophic microorganisms have also been isolated from these phototrophic consortia. Two of them have been identified by 16S rRNA sequencing as *Paracoccus* sp. DE2007 (Diestra et al. 2007) and *Micrococcus luteus* DE2008 (Maldonado et al. 2010b). The former is an aerobic, Gram-negative coccoid, 1 μm in size, non-motile, encapsulated, and non-spore-forming (Diestra et al. 2007). *Micrococcus luteus* DE2008 is an aerobic, Gram-positive coccus, 1.5 μm in size, non-motile, encapsulated, and non-spore-forming (Maldonado et al. 2010b). Additionally, a third heterotrophic bacterium, *Ochrobactrum anthropi* DE2010 (Fig 3B-D), was isolated from *Scenedesmus* sp. DE2009 consortium (Fig 3A). This bacterium has been characterized and identified in this doctoral thesis (see section 2.1). *Ochrobactrum anthropi* is described as a gram-negative, aerobic,

flagellated, oxidase- and urease-positive, non-fermentative bacilli (Vila et al. 2016). It has

been isolated from soil, water, animal, and also human sources (Kulkarni et al. 2017; Yagel

et al. 2020). In 1988, Holmes described the genus *Ochrobactrum*; considering that it is

phylogenetically related to soil and human pathogenic bacteria such as *Brucella* sp. and

Acinetobacter sp. and phenotypically to *Pseudomonadaceae* family (Teyssier et al. 2005).
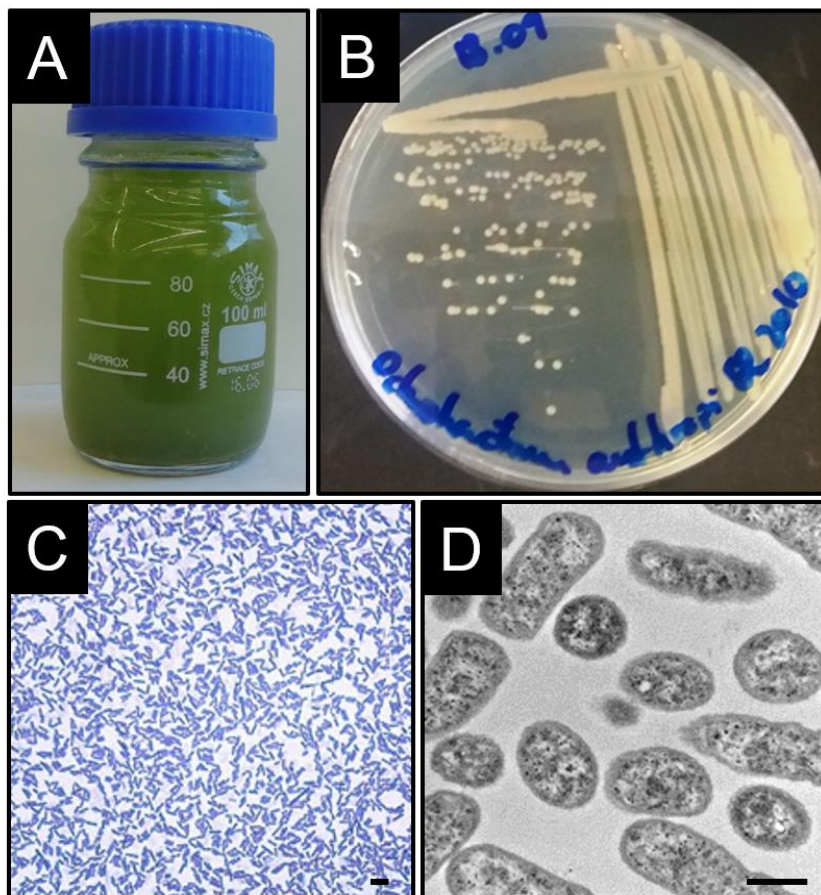
Figure 3. *Ochrobactrum anthropi* DE2010 imaging. (A) Laboratory culture of *Scenedesmus* sp. DE2009 consortium; (B) culture plate, (C) optical bright-field microscopy image, and (D) transmission electron microscopy (TEM) image of *Ochrobactrum anthropi* DE2010. The scale bars represent 10 μm (C) and 1 μm (D), respectively. Source: Property of the thesis author.

Environmental pollution remains one of the main sources of new non-natural

extreme conditions that can disrupt the existing natural ecosystems and affect all the living

organisms. Among the environmental stressors, metals play a significant role as potential toxicants. They are the major environmental pollutants resulting from anthropogenic activities (Roane et al. 2015, Masindi and Muedi, 2018). Metals are also considered a class of solid forming chemicals that are good conductors of heat and electricity. Heavy metals, in particular, are a group of metals with a higher atomic number (above 20) and greater density (5 g/cm^3). They are the key elements of the earth's crust existing as persistent environmental contaminants. These heavy metals are not completely biodegradable and can transform into nontoxic forms (Coral et al. 2005; Tchounwou et al. 2012). In recent years, ecological and global public health concerns associated with environmental contamination caused by heavy metals has increased considerably. Due to high toxicity, persistence in the environments especially in sediment, and biological accumulation in living organisms, heavy metals are emerging as a potential threat to animals and human beings even at relatively low concentrations (Şen et al. 2015; Azimi et al. 2017). Moreover, human exposure to such contaminants has risen dramatically, with an exponential increase in their use in several industrial, agricultural, domestic, and technological applications (García-Betancourt et al. 2020). Reported sources of heavy metals causing contamination in the environment include mining, different industrial sectors (such as chemical as polymers, painting, etc.), pharmaceutical, fertilizer leaching in agriculture, and domestic contamination such as sewage discharge and urban construction, besides atmospheric sources (revision in He et al. 2005; Nguyen et al. 2013; Abdel-Ghani and El-Chaghaby, 2014; Luo et al. 2017). Heavy metals can be transported as either dissolved species into water or an integral part of suspended sediments. Additionally, they can be stored in riverbed sediments or volatilized into the atmosphere (revision in Peng et al. 2018; Rügner et al. 2019). Although these

pollutants can cause significant deleterious effects on the microorganisms, they could take

up the toxic heavy metals (Figure 4) (revision in Kapahi and Sachdeva, 2019).
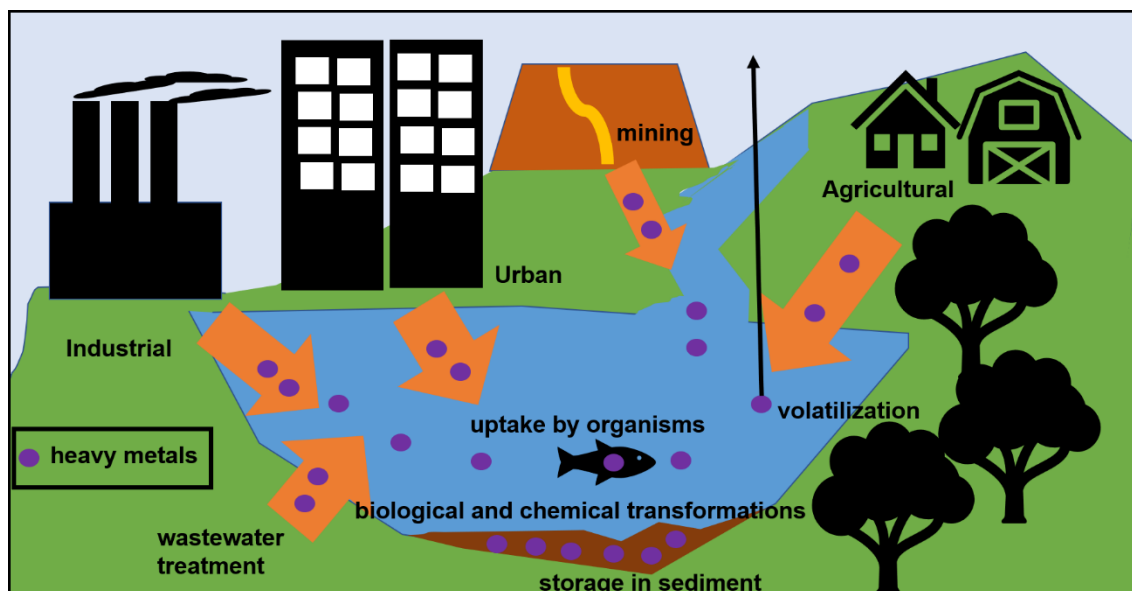
Figure 4. Global biogeochemical cycling of heavy metals in the environment. Source: Property of the thesis author.

It has been reported that metals such as cobalt (Co), copper (Cu), chromium (Cr), iron

(Fe), magnesium (Mg), manganese (Mn), molybdenum (Mo), nickel (Ni), selenium (Se), and

zinc (Zn) are essential metals (nutrients) for various biochemical and physiological cellular

functions. However, large doses of these metals may cause acute or chronic toxicities to

humans and other organisms (revision in Singh et al. 2011; Engwa et al. 2019). Other metals

such as aluminum (Al), antimony (Sb), arsenic (As), barium (Ba), beryllium (Be), bismuth (Bi),

cadmium (Cd), gallium (Ga), germanium (Ge), gold (Au), indium (In), lead (Pb), lithium (Li),

mercury (Hg), platinum (Pt), silver (Ag), strontium (Sr), tellurium (Te), thallium (Tl), tin (Sn),

titanium (Ti), vanadium (V) and uranium (U) are non-essential metals that have no

established biological functions but cause toxicities to living organisms at different levels

(Zhu et al. 2020; Madkour, 2020). This thesis is focused on relevant metals such as Cd, Pb, Cu, Cr, and Zn which have been linked with environmental pollution due to their cytotoxic effects. The discharge of large amounts of metal-contaminated wastewater from industries impairs the water quality and, in turn, affect the freshwater reservoirs. Cu, Cr, and Zn, in particular, are required in small quantities as nutrients, involved in a range of enzymatic and metabolic pathways, and act as cofactors/coenzymes. However, large quantities of such metals can become strongly inhibitory to all forms of lives including microorganisms, plants, animals, and humans (Jaishankar et al. 2014; revision in Nagaiyoti et al. 2010; Hirve et al. 2020). On the other hand, Cd and Pb are non-essential metals with no known biological role and extremely hazardous even at very low concentrations and over short exposure (Atlas and Bartha 1993; revision in Abtahi et al. 2017; revision in Yilmaz et al. 2018).

The accumulation levels and effects of Cd, Pb, Cu, Cr, and Zn in water, soil, plants, and animals in deltaic floodplains have been analyzed worldwide (Mañosa et al. 2001; Sánchez-Chardi and López-Fuster, 2009; Olawoyin et al. 2012; Xiao et al. 2012; Li et al. 2014; Dhanakumar et al. 2015; Wang et al. 2020). In Spain, the Ebro River and its delta have been widely impacted by several industrial, agricultural, and cattle farming activities. These potential pollution sources have also caused an increase in the concentration of the above-mentioned metals in water, biota, and sediments (Nadal et al. 2011; Vilavert et al. 2015). For a long time, the Microbial Ecology Laboratory of the Universitat Autònoma de Barcelona has studied the capacity of microorganisms isolated from Ebro Delta microbial mats to overcome the stress produced by contaminated heavy metals. For example, some isolated phototrophic and heterotrophic microorganisms (cited before) were tested to analyze their

cellular responses to the stress caused by metals and their ability for capturing and accumulating metals such as Cr(III), Pb(II), and Cu(II) at the cellular level (e.g. Burnat et al. 2009; Maldonado et al. 2010a,b; Puyen et al. 2012; Burgos et al. 2013; Millach et al. 2015; Millach et al. 2019). More importantly, at present, the Spanish government (through the project *Red de control de sustancias peligrosas. Conferencia hidrográfica del Ebro)* considers the Ebro river and its delta as a non-contaminated area by metals (Table 1), as relatively low values of these metals are detected in the area. Moreover, the level of metal contamination is below the safety threshold to human health risk established by the Spanish Legislation (see table 1) (*RD 1/2001*, 20th of July 2001, specifically law article 1 and 2 and 4 sections; *RD 60/2011*, 21st of January, on environmental quality standards in the field of water policy; and *RD 817/2015* establishing the criteria for monitoring and evaluating water quality). However, it does not rule out the need for their continuous assessment to assure the low level of metals in the Ebro River and its delta. Also, it must be considered that the microorganisms inhabiting these areas could have developed strategies to survive in the presence of heavy metals and avoid their negative effects. Among the negative effects of the above-mentioned metals on the microorganisms, those listed in Table 2 stand out.

Table 1. Average concentrations (24 sampling stations) of Cd, Pb(II), Cu(II), Cr (total), and Zn in water and sediment from Ebro River and human risk threshold established by Spanish legislation. Source: *Red de control de sustancias peligrosas. Conferencia hidrográfica del Ebro (Vicepresidencia cuarta. Ministerio para la Transición Ecológica)*.

Heavy metal	Water (mg/L)					Sediment (mg/kg)				
	2015	2016	2017	2018	Permitted threshold	2015	2016	2017	2018	Permitted threshold
Cd	0.00002	0.002*	0.00005	0.00005	**0.0002**	0.8	0.8	0.8	0.8	**5**
Pb(II)	0.0005	0.005	0.0005	0.0005	**0.0072**	4.0	4.0	4.0	4.0	**100**
Cu(II)	0.002	0.002	0.002	0.002	**0.04**	4.0	4.0	4.0	4.0	**100**
Cr (total)	0.002	0.002	0.002	0.002	**0.05**	10.0	10.0	10.0	10.0	**150**
Zn	0.010	0.010	0.010	0.010	**0.3**	60.0	60.0	60.0	60.0	**300**

*value out of permitted threshold

Table 2. Toxic effects on microorganisms due to Cd, Pb(II), Cu(II), Cr(total), and Zn exposure.

Heavy metal	Effects on Microorganisms	References
Cd	Denaturation of protein, degradation of nucleic acid, hinder cell division and transcription	Fashola et al. 2016
Pb(II)	Degradation of nucleic acid and protein, inhibition enzyme actions and mRNA transcription	Fashola et al. 2016
Cr(total)	Inhibition of growth, elongation of lag phase, inhibition of oxygen uptake	Cervantes et al. 2001
Cu(II)	Disruption of cellular function, inhibition enzyme activities	Fashola et al. 2016
Zn	Cellular death, decrease in biomass, inhibition of growth	Malik, 2004

A series of physicochemical technologies such as membrane ultra- and nano-filtration, ion-exchange, chemical precipitation, chemical oxidation, electrochemical treatment, reverse osmosis, coagulation-flocculation, and adsorption using active carbon has known to be developed to remove heavy metals from polluted environments (revision in Fu and Wang, 2011; revision in Tang et al. 2016; Khulbe and Matsuura, 2018; revision in Yin et al. 2019b). However, these traditional physicochemical methods have several limitations such as toxic sludge production, ineffective in terms of process cost, energy and

chemical product consumption, not eco-friendly, production of complicated material, and induction of secondary pollution (revision in Yin et al. 2019b). Thus, the use of living organisms to remove heavy metals from polluted samples appeared as a promising eco-friendly and feasible alternative that avoids the above-mentioned physicochemical disadvantages. Bioremediation processes that enable the use of bacteria, fungi, algae, and green plants provide significant advantages including low cost, simple-to-use, large availability, and high efficiencies of the removal capacity (Kanamarlapudi et al. 2018; revision in Yin et al. 2019b). Bacteria that can degrade several environmental contaminants such as heavy metals have been widely used in bioremediation. Compared to animals, plants, and fungi, bacteria can resist or tolerate environmental stresses. Besides, they grow fast and develop rapid mutations that can permit the evolution (Mehta et al. 2019; Chevallereau et al. 2019).

Strategies or mechanisms developed by microorganisms, especially bacteria, in polluted environments to remove heavy metals or obtain less harmful species include biosorption, bioaccumulation, biomineralization, and biotransformation (Table 3). Biosorption is a simple metabolic passive process involved in the binding of metal ions to the biosorbent surface of biological origin (Fomina and Gadd, 2014). Second, bioaccumulation is a metabolism-mediated active process where the metal ions are accumulated intracellularly into the living cells (Diep et al. 2018). Third, biomineralization is a biological process that induces the non-bioavailability of metals which allows an organism to create a local micro-environment favoring extracellular precipitation of metal in mineral phases (Chaparro-Acuña et al. 2018). Lastly, biotransformation is the enzyme-catalyzed

conversion of one chemical into another of the same metal that may be less toxic (Smitha

et al. 2017). A schematic representation of the previous biological strategies is presented in

a prokaryotic cell model in Figure 5.

Table 3. Heavy metal remediation strategies developed by microorganisms

Cellular strategies	Heavy metals	Microorganisms	References
Biosorption	Cu(II) and Pb(II)	Bacteria	Puyen et al. 2012
	Cu(II), Cd and Zn	Bacteria	Yue et al. 2015
	Zn	Bacteria	Magnin et al. 2014
	Cu(II), Cd and Cr	Cyanobacteria	Chojnacka et al. 2005
	Cu(II), Cr and Pb(II)	Cyanobacteria	Colica et al. 2010
	Zn	Microalga	Monteiro et al. 2009
	Cr	Microalga	Han et al. 2006
	Pb	Fungi	Xu et al. 2020
Bioaccumulation	Pb(II) and Cr	Bacteria	Shao et al. 2019
	Cr	Bacteria	Sharma and Shukla, 2020
	Zn and Pb(II)	Bacteria	Li and Ramakrishna, 2011
	Pb(II)	Cyanobacteria	Burnat et al. 2010
	Pb(II)	Microalga	Maldonado et al. 2010a
	Cd	Yeast	Andreeva et al. 2014
	Pb(II)	Fungi	Khan et al. 2019
Biomineralization	Pb(II)	Bacteria	Chen et al. 2016
	Zn	Cyanobacteria	Podda et al. 2014
	Cd, Cu(II) and Zn	Fungi	Fomina et al. 2005
Biotransformation	Cr	Bacteria	Cheng et al. 2010
	Cu	Yeast	Rajpert et al. 2013
	Cr	Fungi	Coreño-Alonso et al. 2014
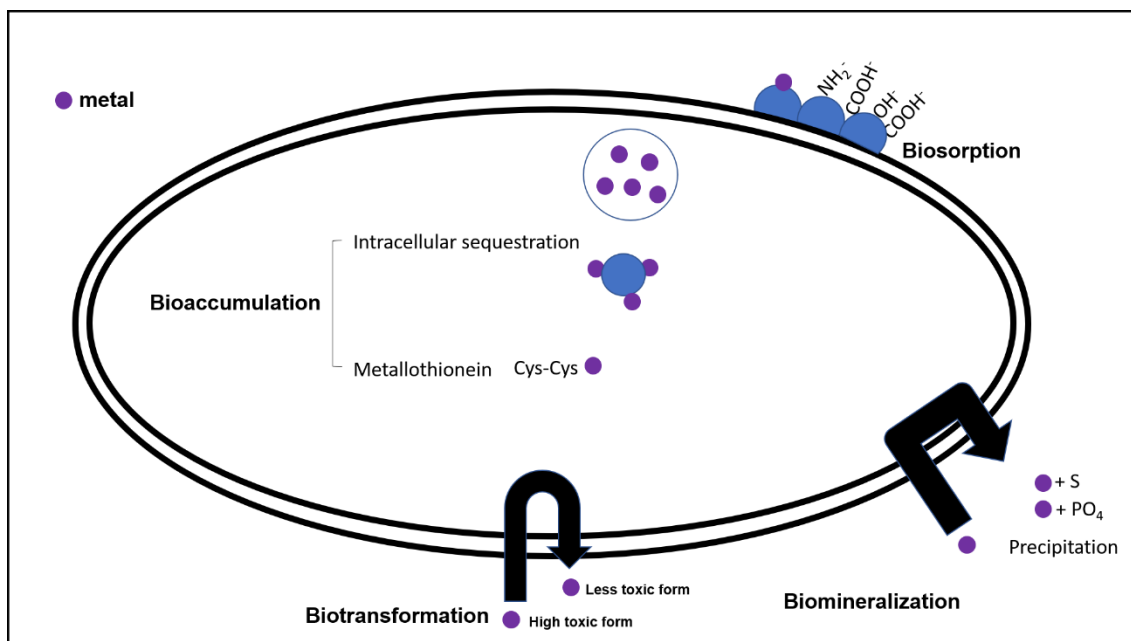
Figure 5. Cellular representation of the main heavy metal remediation strategies involving bacteria

Major bacterial detoxification pathways of heavy metal used by bacteria (Table 4) to carry out the aforementioned strategies, include extracellular and/or intracellular sequestration, active transport of heavy metal outside the cells, and enzymatic detoxification that can avoid heavy metal exposure or reduce their bioavailability. Firstly, the extracellular sequestration of heavy metals can efficiently decrease their toxicity to the rest of the microorganisms. This detoxification pathway is linked to biosorption mechanism in which heavy metals can be accumulated to various biological structures including extracellular polymeric substances (EPS), siderophores, glutathione, and biosurfactants (revision in Igiri et al. 2018). Secondly, the intracellular sequestration of heavy metal requires to cross the cell wall and enter the cytoplasm of live cells of microorganisms. It is linked to bioaccumulation mechanisms in which some specific intracellular components within the cytoplasm can sequestrate the heavy metals and prevent them from reaching the toxic level.

Following this pathway, the metals can be accumulated inside the cell forming polyphosphate complexes and/or associated with cysteine-rich proteins such as metallothionein (revision in Yin et al. 2019b). Active export of heavy metals is another process of cellular response against heavy metal stress in which cells can efficiently regulate intracellular concentrations of heavy metal with efflux systems. This detoxification pathway could be related to the biomineralization mechanism (revision in Yin et al. 2019b). Lastly, enzymatic detoxification from highly toxic heavy metals to less harmful forms contributes greatly to increasing microbial resistance to metals. It is associated with biotransformation mechanisms (revision in Liu et al. 2017).

Table 4. Heavy metal detoxification pathways developed by living and dead microorganisms.

Cellular pathway or pattern	Substance or molecule	Heavy metals	Microorganisms	References
Extracellular sequestration	Extracellular polymeric substances	Cu(II), Cd, and Zn	*Desulfovibrio desulfuricans*	Yue et al. 2015
		Cu(II) and Pb(II)	*Micrococcus luteus* DE2008	Puyen et al. 2012
		Cu(II) and Zn	*Bacillus licheniformis*	Biswas et al. 2020
		Cu(II), Cd, Cr, and Pb	*Pseudomonas aeruginosa* CPSB1 *Azotobacter chroococcum* CAZ3	Rizvi and Shagir Khan, 2019
	Siderophores	Cu(II)	*Pseudomonas aeruginosa*	Teitzel et al. 2006
Intracellular Sequestration	Polyphosphate	Cu(II)	*Sulfolobus sulfararicus*	Remonsellez et al. 2006
		Cd	*Anacystis nidulans*	Keyhani 1996
		Cr	*Ochrobactrum tritici* 5bvl1	Francisco et al. 2011
		Pb(II)	*Microcoleus* sp. DE2006	Burnat et al. 2010
		Cd	*Criptococcus humicola*	Andreeva et al. 2014
		Cd	*Criptococcus humicola*	Kulakovskaya et al. 2018
	Metallothionein	Cd and Zn	*Synechococcus* sp.	Blindauer et al. 2008
Active export	P-type efflux ATPase	Cu(II)	*Sulfolobus sulfararicus*	Soto et al. 2018
		Zn	*Sinorhizobium meliloti*	Lu et al. 2016
	ABC transporters	Cd and Zn	*Escherichia coli*	Lerebours et al. 2016
Enzymatic detoxification	Catalase, superoxid dismutase	Pb(II) and Cr	*Bacillus* sp.	Shao et al. 2019
		Zn and Pb(II)	*Pseudomonas putida*	Hussein et al. 2013
		Pb(II)	*Halomonas* sp.	Abdel-Razik et al. 2020

Interestingly, the environmental phototrophic and heterotrophic microorganisms isolated by our research group can sequester the metals externally (biosorption strategy) in extracellular polymeric substances (EPS), being especially interesting in *Micrococcus luteus*

DE2008 for Cu(II) and Pb(II) metals (Puyen et al. 2012). On the other hand, the intracellular

metal uptake (bioaccumulation strategy) in polyphosphate (polyP) inclusions is widely used

by phototrophic microorganisms such as *Microcoleus chthonoplastes* DE2006,

Scenedesmus sp. DE2009, and *Geiltherinema* sp. DE2011 (Burnat et al. 2009; Burnat et al.

2010; Millach et al. 2015). These microorganisms are of interest for bioremediation of

contaminated environments.

Despite the availability of extensive information, nothing is known about the effect

of heavy metals on the cell viability of *O. anthropi* DE2010 and the role of this bacterium in

heavy metal sequestration. As the heterotrophic bacterium – isolated from the

Scenedesmus sp. DE2009 microalgae consortium of microorganisms from Ebro Delta

microbial mats – grows easily in both liquid and solid media cultures, it becomes a suitable

model for heavy metal experimental research.

The main objectives of the current doctoral thesis are given below:

1. The phenotypic characterization and genotypic identification of strain DE2010 (*Ochrobactrum anthropi* DE2010).

2. The complete genome sequencing of *O. anthropi* DE2010 and detection of polyP and PPi metabolic genes.

3. The evaluation of cytotoxic effects of heavy metals and cellular responses on *O. anthropi* DE2010 cultures exposed to increasing concentrations of Cd, Pb(II), Cu(II), Cr(III), and Zn, including:

   a. Changes in cellular viability and biomass, in the production and composition of EPS, and in the intracellular polyP content.

   b. The metal removal capacities (%) and their respective removal efficiencies (*q*).

4. The analysis of the cellular metal localization patterns and the strategies and pathways used by *O. anthropi* DE2010 to immobilize Cd, Pb(II), Cu(II), Cr(III), and Zn.

1 μm
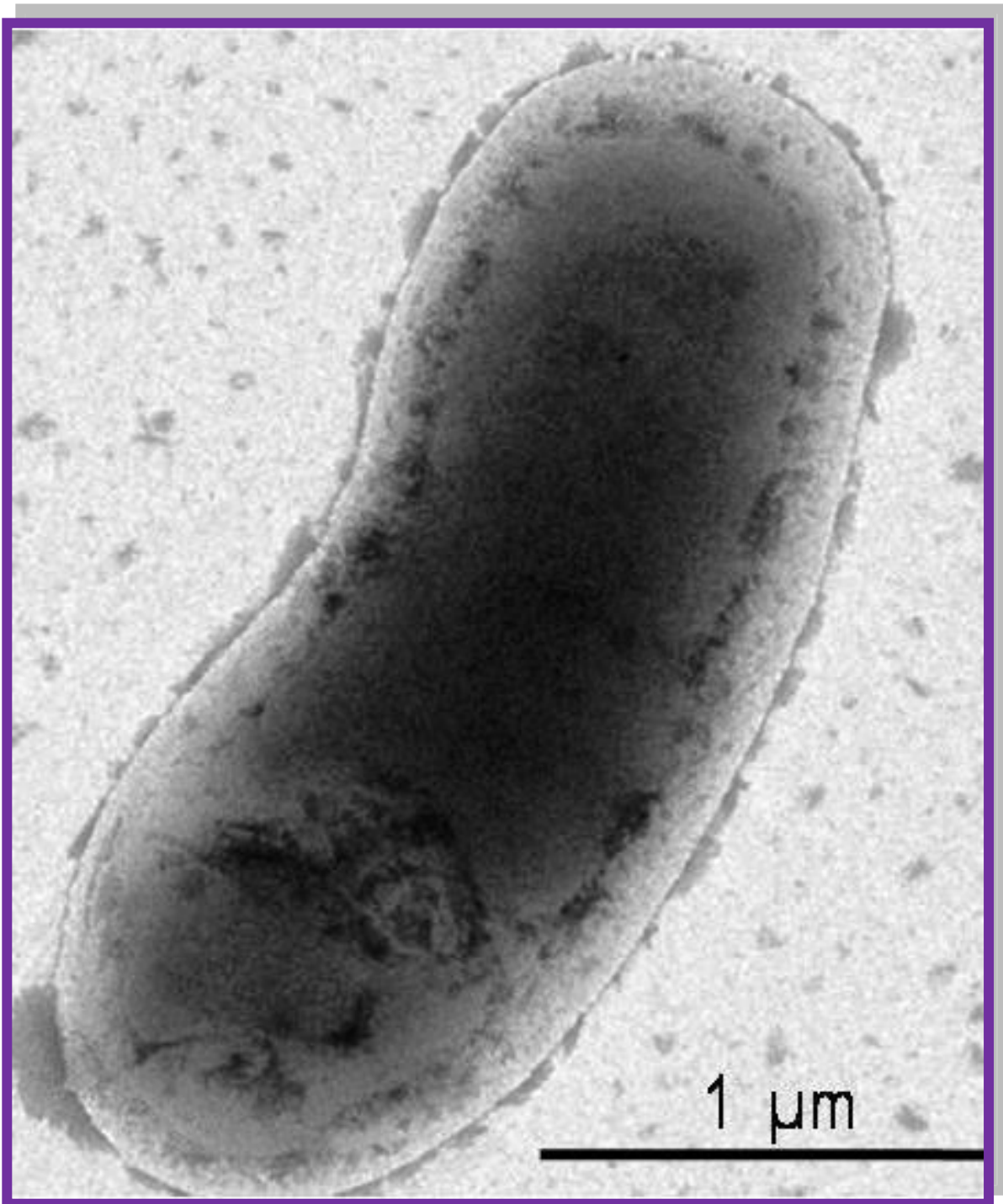
Chapter II. Publications

Section 2.1 Morphological responses to nitrogen stress deficiency of a new a heterotrophic isolated strain of Ebro Delta microbial mats.

Morphological responses to nitrogen stress deficiency of a new heterotrophic isolated strain of Ebro Delta microbial mats.

Eduard Villagrasa[1], Neus Ferrer-Miralles[1, 2, 3], Laia Millach[1], Aleix Obiol[1], Jordi Creus[1], Isabel Esteve[1] and Antonio Solé[1]

[1]*Departament de Genètica i Microbiologia. Facultat de Biociències. Universitat Autònoma de Barcelona. Bellaterra, Cerdanyola del Vallès, 08193 Barcelona, Spain*

[2]*Institut de Biotecnologia i de Biomedicina. Universitat Autònoma de Barcelona. Bellaterra, Cerdanyola del Vallès, 08193 Barcelona, Spain*

[3]*CIBER de Bioingeniería, Biomateriales y Nanomedicina (CIBER-BBN), Spain.*

Abstract

Microorganisms living in hypersaline microbial mats frequently form consortia under stressful and changing environmental conditions. In this paper, the heterotrophic strain DE2010 from a microalgae consortium (*Scenedesmus* sp. DE2009) from Ebro Delta microbial mats has been phenotypically and genotypically characterized and identified. In addition, changes in the morphology and biomass of this bacterium in response to nitrogen deficiency stress have been evaluated by correlative light and electron microscopy (CLEM) combining differential interference contrast (DIC) microscopy and transmission electron microscopy (TEM) and scanning electron microscopy (SEM). These isolated bacteria are chemoorganoheterotrophic, gram-negative and strictly aerobic bacteria that use a variety of amino acids, organic acids and carbohydrates as carbon and energy sources, and they grow optimally at 27 ºC in a pH range of 5 to 9 and tolerate salinity from 0 to 70 ‰ NaCl. The DNA sequencing analysis of the *16S rRNA* and *nuo*C and *fix*H genes and the metabolic characterization highlight that strain DE2010 corresponds to the species *Ochrobactrum anthropi*. Cells are rod shaped, 1–3 µm in length, and 0.5 µm wide, but under deprived

nitrogen conditions, cells are less abundant and become more round, reducing their length and area and, consequently, their biomass. An increase in the number of pleomorphic cells is observed in cultures grown without nitrogen using different optical and electron microscopy techniques. In addition, the amplification of the *fix*H gene confirms that *Ochrobactrum anthropi* DE2010 has the capacity to fix nitrogen, overcoming N_2-limiting conditions through a *nif*H –independent mechanism that is still unidentified.

1. Introduction

Microbial mats are highly productive ecosystems growing at solid-aqueous interfaces and can be found around the world, more frequently in shallow and extreme environments, which are subjected to regular and strong changes in environmental parameters (Millach et al., 2017 and Ramos et al., 2017). The focus of the current study is the hypersaline microbial mats located in the Ebro Delta, which are benthic ecosystems that have strong interactions between microorganisms, mostly prokaryotes, and the sediment and are vertically stratified in millimeter-thick colored layers of several functional groups of microorganisms, such as photo- and chemo-autotrophic and heterotrophic microorganisms, which are distributed along vertical physicochemical gradients, mainly for light, oxygen and sulfides, among others (Revsbech et al., 1983, Esteve et al., 1992 and Martínez-Alonso et al., 2004). These mats cover an area of 3 km^2 and are a few millimeters thick. They usually show a brown-green layer, on the mat surface, corresponding to microalgae and unicellular and filamentous cyanobacteria (oxygenic photoautotrophic microorganisms); a thin red layer often found below, mainly composed of purple sulfur

bacteria (anoxygenic photoautotrophic bacteria) and a thick black third layer formed by sulfate-reducing bacteria (anaerobic heterotrophic bacteria) at a greater depth (Mir et al., 1991, Guerrero et al., 1993, Solé et al., 2003). Cyanobacteria and microalgae constitute the most important populations found in these mats, playing an important role in the stabilization of deltaic sediments and have been described as the chief primary producers, using light as a source of energy and water as an electron donor. It is known that these phototrophic microorganisms are frequently associated with heterotrophic bacteria in nature and that they form consortia (Paerl 1977 and Diestra et al., 2005). Many autotrophic microorganisms grow more efficiently in co-cultures with heterotrophic bacteria than in axenic cultures, especially through remineralization of organic carbon by heterotrophic bacteria, which alleviates cyanobacterial and microalgal carbon limitations, improving their nutrient and vitamin (vitamin B_{12}) acquisition (Cole 1982 and Shen at al., 2011). These interspecies interactions exert globally significant impacts upon biochemical cycles, such as nitrogen and carbon cycling, which favors microbial adaptation and survival under stressful conditions (Xie et al., 2013 and Cole et al., 2014).

In the last decade, our working group has isolated, from Ebro Delta microbial mats, three different stable consortia of microorganisms, each formed by a single type of phototrophic microorganism (the most abundant) and different heterotrophic bacteria. Two of these are filamentous cyanobacteria, *Microcoleus chthonoplastes* DE2006 (Diestra et al., 2005) and *Geitlerinema* sp. DE2011 (Burgos et al., 2013), and the other one is a microalga, *Scenedesmus* sp. DE2009. Three heterotrophic microorganisms have also been isolated from these consortia, and two of them have been identified as *Paracoccus* sp. DE2007 (Diestra et al., 2007) and *Micrococcus luteus* DE2008 (Maldonado et al., 2010). In this paper,

another heterotrophic bacterium isolated from a *Scenedesmus* sp. DE2009 consortium has been identified as a member of the *Ochrobactrum* genus (strain DE2010).

Some species of the *Ochrobactrum* genus are considered as nitrogen-fixing microorganisms, and this activity is closely related to cellular pleomorphism. The modern definition of pleomorphism, in the context of bacteriology, is the ability of some bacteria to modify the cell size and shape in response to specific environmental conditions. Cell pleomorphism has been described in pure cultures of free-living microorganisms incubated in nitrogen-limited medium (Bal et al., 1980). Many alphaproteobacteria interact with other photosynthetic organisms (cyanobacteria, microalgae and plants), functioning as symbionts, with some of them fixing nitrogen (Batut et al., 2004). Nitrogen fixation can be considered as one of the most interesting microbial activities as it makes the recycling of nitrogen on earth possible and makes a fundamental contribution to nitrogen homeostasis in the biosphere (Aquilantia et al., 2004). Several authors have used CLEM to visualize structures at different scales of magnitude, including studies related to cellular pleomorphism (Vancová et al., 2017). This methodological imaging approach allows for the generation of new and valuable information because images can be obtained from the same sample using different microscopy techniques. Certain fluorescent structures or cells can be first localized by light microscopy and then re-localized later by electron microscopy, with light microscopy performed before or after the embedding of the samples to be analyzed at the highest resolution (Perkovic et al., 2014; Wrede et al., 2008).

The current study is focused on the identification of strain DE2010, and changes in the morphology and biomass of this microorganism in response to nitrogen deficiency

stress have also been studied. For this, the images obtained were studied by CLEM imaging combining DIC microscopy and TEM.

2. Materials and methods

2.1 Environmental sampling and isolation of strain DE2010

The strain DE2010 was isolated from *Scenedesmus* sp. DE2009 from a consortium formed by microalgae and different heterotrophic microorganisms isolated from Ebro Delta microbial mats located in Tarragona (0°35'E–0°56'E; 40° 33'N–40°47'N), Spain. These mats occur all along the coast in the narrow ephemeral ponds of the backshore, on the flanks of the storm inlets and, most commonly, on the sand flats and channels of the La Banya spit. The temperature of water covering these microbial mats ranges from 12 to 30 °C, conductivity from 59 to 105 mS/cm, salinity from 40 to 75 ‰, and pH from 7.5 to 9.0 (Esteve et al. 1994; Guerrero et al. 1999). Cultures of this microalgae consortium were grown in liquid mineral Pfennig medium and maintained at 27 °C in a growth chamber under continuous illumination with a light intensity of 6-8 μEm^{-2}·s^{-1} (Millach et al., 2015). Then, 100 µL of these cultures were plated in solid Luria–Bertani (LB) medium containing tryptone (10.0 g/L), yeast extract (5.0 g/L), sodium chloride (10.0 g/L) and bacteriological agar (15.0 g/L) at pH 7.0 and grown in darkness at 27 °C for 24 hours. Later, the isolated strain was subcultured on LB medium at 27 °C and preserved in *cryoinstant* vials (Thermo Fisher scientific) at -80 °C.

2.2 Phenotypic strain DE2010 characterization

The characterization of the strain DE2010 was performed from cultures grown in LB medium for 24 h at 27 °C. The morphological cell characteristics were examined with an

Olympus BH2 (Olympus, Japan) conventional light microscope. Gram and Wirtz-Conklin staining were performed according to Doetsch (1981) and Hamouda et al. (2002), respectively. The growth of the isolated strain under different selected environmental stress conditions, such as temperature (4, 27 and 37 °C), pH range (2 - 10) and NaCl concentrations (0 - 80 % NaCl), was determined following the method described by Dalgaard et al. (1994). The biochemical characteristics were analyzed by means of BioMerieuxTM API™ 10S Clinical Diagnostic Kits, BioMerieux™ API™ 2O E Clinical Diagnostic Kits, BioMerieux™ API™ 2O NE Clinical Diagnostic Kits, BioMerieux™ API™ 50CH Clinical Diagnostic Kits and BioMerieux™ API™ ZYM Microbial Identification Strip microsystems (BioMérieux®sa, Marcy-l'Etoile, France) following the manufacturer's recommendations. Oxidase and catalase activities were determined using oxidase strips (Oxoid Ltd, Basingstoke, UK) and measurements of the formation of enzyme-generate oxygen bubbles after soaking in 3 % (v/v) H_2O_2 solution on a colony of strain DE2010 respectively (Holt et al 1994). DNase activity and degradation of Tween 80 were analyzed following the methods described by Hansen and Sørheim (1991).

The growth of strain DE2010 was also evaluated, after 1 day of incubation at 27 °C, in different solid media: LB, Minimal Salinity (MS; Sigma-Aldrich, Germany), Vogel-Bonner E (VBE; Southern Group Laboratory, UK), Reasoner's 2A (R-2A; Sigma-Aldrich, Germany), Reasoner's 3A (R-3A; Sigma-Aldrich, Germany), mannitol-salt and McConkey (Scharlau, Spain). Moreover, anaerobic growth was tested on LB agar plates in an Anaerocult system (Merck KGaA, Darmstadt, Germany) for 1 week and hemophilic activity in blood agar plates (Scharlau, Spain) was test for 24 h at 27 °C. Additionally, colonies of strain DE2010 grown in LB agar were place in VBE/glucose without a nitrogen source in the agar plate medium

at 27 ºC for 48-72 h. Under these stress conditions, the expression of clusters of nitrogen

fixing genes is induced to allow the fixation of atmospheric nitrogen. Finally, an antibiotic

susceptibility test of the strain DE2010 was carried out on Mueller Hinton Agar containing

beef extract (2.0 g/L), acid hydrolysate of casein (17.5 g/L), starch (1.5 g/L) and

bacteriological agar (17.0 g/L) at pH 7.3, using the Kirby Bauer disc diffusion method (Sayah

et al. 2005). In this study, the antibiotics and the concentrations used were as follows:

nalidixic acid - 30 μg, chloramphenicol - 30 μg, tetracycline - 30 μg, erythromycin - 15 μg

and ampicillin - 10 μg. The growth curve measurements for strain DE2010 were also

determined. In this case, cultures were grown in 150 μL LB medium in 96-well microplates

maintained at 150 rpm and 27 °C for 24 h in the dark. Triplicate negative control samples

were included in the microplates by adding 150 μL of bacteria-free LB medium to the wells.

During incubation, the OD (λ = 600 nm) was measured every 30 min with a microtiter plate

photometer (Thermo Scientific Variokan® Flash, Waltham, USA). Before the measurements,

the microtiter plate was shaken for 5 s at 120 rpm following the method described by Hall

et al. 2014. The specific growth rate (μ) and the generation time (g) in LB medium at 27 ºC

were calculated using the following formulas:

$$\mu = \frac{\ln OD_2 - \ln OD_1}{t_2 - t_1} \qquad\qquad g = \frac{\ln 2}{\mu}$$

where OD_2 and OD_1 represent the optical density (600 nm) of the cultures at the final (2)

and initial (1) measures of the experiment, and t_2 and t_1 represent their homologous times

(h). The results are expressed in h^{-1} (μ) and in h (g).

2.3 Genotypic strain DE2010 characterization

Total genomic DNA of strain DE2010 was obtained using the UltraClean Microbial DNA isolation Kit (MO BIO Laboratories, Inc, Carlsbad, USA). Template DNA concentration was determined by measuring absorbance at 260 nm with an Ultrospect 1100 Pro UV/Vis spectrophotometer. PCR cycling was performed in a Techne FTC 3G/02 thermal cycler using a hotstart protocol. A total reaction volume of 25 μL was used, containing 125 ng of DNA. The PCR cycling conditions were set as follows: an initial denaturing step of 5 min at 95 °C, followed by 35 cycles of 1 min at 95 °C, 2 min at the optimized annealing temperature for each gene, 2 min at 72 °C, and a final extension of 10 min at 72 °C. All positive samples were detected in a 1.2 % agarose gel in 1X TAE buffer and further purified with ExoSAP-IT PCR Product Cleanup (Affymetrix) for DNA sequencing of the PCR products with the corresponding specific forward primer at the UAB Scientific Technical Service "Servei de Genòmica i Bioinformàtica" (http://sct.uab.cat/genomica-bioinformatica). Sequence analysis of partial gene amplicons of *16S* rRNA and *nuo*C and *fix*H genes were performed using MEGA version 7 (http://www.megasoftware.net) to eliminate ambiguous data and were deposited in GenBank/ENA sequence databases (Table 1). The verified sequences were then compared to those present in the NCBI database and were matched with available references (www.ncbi.nlm.nih.gov) using the BLAST software (https://blast.ncbi.nlm.nih.gov/Blast.cgi) and, only for *16S rRNA*, the Ribosomal Database Project at Michigan State University (RDP-II) (http://rdp.cme.msu.edu/) (Cole et al., 2014). Multiple alignments were performed using the CLUSTALW software (Thompson et al., 1997), and phylogenetic and molecular evolutionary analyses were conducted using MEGA version 7 (www.megasoftware.net) (Kumar et al., 2016). The evolutionary distances were calculated and clustering determined using the maximum-likelihood and neighbor-joining

methods, and a phylogenetic tree was reconstructed with the neighbor-joining method (Saitou and Nei 1987) using the Tamura three-parameter model (Tamura 1992) for *16S rRNA* and the Jukes-Cantor model (Jukes et al., 1969) for *nud*C. Bootstrap analysis was used to evaluate the tree topologies of the neighbor-joining data by performing 1000 replications (Felsenstein 1985). The *16S rRNA* gene tree was rooted using the *16S rRNA* gene sequence of *Rhizobium rhizogenes* strain 163C (GenBank accession number AY206687), and the *nud*C gene was rooted using the *nud*C gene sequence of *Escherichia coli* str.K-12 (GenBank accession number NC000913)

2.4 SEM and TEM

SEM and TEM were used to reveal morphological features of the isolated microorganisms. For SEM images, an overnight culture of bacteria on LB liquid medium was centrifuged at 4000 *g* for 10 minutes in a refrigerated Eppendorf 5804R centrifuge (Eppendorf, Hamburg, Germany). Samples of DE2010 cultures were fixed in 2.5 % glutaraldehyde in Millonig phosphate buffer (Millonig et al., 1961) for 2 h and washed four times in the same buffer. They were then dehydrated in successively increasing concentrations of ethanol (30, 50, 70, 90, and 100 %) and dried by critical-point drying following the method described by Maldonado et al. 2010. Finally, all samples were mounted on metal stubs and coated with gold. A Jeol JSM-6300 scanning electron microscope (Jeol, Tokyo, Japan) was used to view the images. For TEM images (negative stain), 8 µL of strain DE2010 culture was loaded onto glow-discharged carbon-coated 400-mesh copper grids and mixed with 8 µL of 2 % (w/v) phosphotungstic acid (Sigma-Aldrich QUIMICA S.L). All grids were observed and recovered by a JEOL JEM-1400 transmission electron microscope (Jeol, Tokyo, Japan).

2.5 CLEM imaging

CLEM microscopy was applied to evaluate the morphological responses of cells to the effect of nitrogen availability. Therefore, overnight cultures of the strain DE2010 grown on LB and VBE/glucose without a nitrogen source were centrifuged at 4000 g for 10 minutes in a refrigerated Eppendorf 5804R centrifuge (Eppendorf, Hamburg, Germany). The same pellets were viewed by (i) differential interference contrast (DIC) microscopy, using a methylene blue stain to examine the morphological characteristics of bacteria with a Leica LEITZ DMRB microscope at 1000A, and (ii) TEM to determine ultrastructural features. For that, pellets were fixed in 2.5 % glutaraldehyde in Millonig phosphate buffer (Millonig et al., 1961) for 2 h, washed in the same buffer, post-fixed in 1 % OsO_4 at 4 ºC for 2 h, and washed again. They were then dehydrated in a graded series of acetone (30, 50, 70, 90, and 100 %) and embedded in Spurr's resin. Ultrathin 70-nm sections were mounted on carbon-coated 400-mesh copper grids and stained with uranyl acetate and lead citrate (Maldonado et al., 2010). All the grids were observed and recovered by a Hitachi H-7000 transmission electron microscope (Hitachi, Tokyo, Japan).

2.6 Image analysis

DIC images of strain DE2010 grown in LB agar and in VBE/glucose without nitrogen agar were acquired at 1024x1024 pixels, digitized and stored. Later, these images were binarized using the image processing and analysis software ImageJ 1.40g (Wayne Rasband, NIH, USA). To measure several morphological parameters (area, length and circularity) of every cell present in each generated image and to obtain biomass values from these black and white images by means of the Voxel Counter plugin, the method described by Puyen

et al. 2012 was applied. Morphological parameters are expressed in µm^2 (area) or µm (length and circularity), and biomass is expressed in µg C/cm^3.

3. Results

3.1 Strain DE2010 characterization

Ochrobactrum anthropi DE2010 is gram-negative, non-spore forming, rod shaped, 1–3 µm in length, 0.5 µm wide and motile, with peritrichous flagella. This microorganism grows optimally at a temperature of 27 ºC, in a pH range from 5 to 9, and tolerates salinity from 0 to 70 ‰ NaCl. The growth rate and generation time of strain DE2010 on LB liquid medium at 27 ºC was 0.17 h^{-1} and 4.02 h, respectively. Colonies grown on LB plate medium for 24 h at 27 ºC are circular, convex, smooth and opaque, with entire margins, no pigmentation, and a diameter of 0.8-1 mm. Cells are oxidase and catalase positive and exhibit and strictly aerobic chemoorganoheterotrophic metabolism, using a variety of amino acids, organic acids and carbohydrates as carbon and energy sources. This strain is able to grow on VBE, R-2A and R-3A media, but not on MS and mannitol-salt media after 24 h at 27 ºC. On McConkey medium, colonies become red at 48 hours of growth, indicating that this organism is lactose positive, and it increases its beta-hemolytic capacity after a long period of incubation on blood agar. Finally, *O. anthropi* DE2010 also grows on VBE/glucose medium without nitrogen after 72 h at 27 ºC, indicating that it is able to fix atmospheric nitrogen.

Taking into account the results of the APIZYM, API10S and API20E kit tests, strain DE2010 show positive enzymatic activities related to esterase (C4), lipase (C14), urease and α-glucosidase and negative results for acid and alkaline phosphatase, protease (gelatin

hydrolysis), β-glucosidase (esculin hydrolysis), β-galactosidase, DNase (DNA hydrolysis) and esterase-lipase (C8) activities. With regard to the API 20NE test, positive results were obtained with glucose, malate, mannitol, citrate, gluconate, mannose and arabinose assimilation, and negative results were obtained with adipic acid and phenylacetic acid. For the API50CHB test, positive results were obtained for ribose, xylose, adonitol, arabinose, fucose, inositol, erythritol, glycerol and dulcitol oxidation, and negative results were obtained for lactose, glucose, arbutin and arabitol. The isolated strain is negative for indole and H_2S production, but positive for nitrate and nitrite reduction. The antibiogram results indicate that it is resistant to chloramphenicol, tetracycline and ampicillin and sensitive to nalidixic acid and erythromycin. A summary of the characterization of the isolated strain DE2010 is shown in Table 2.

3.2 Identification of strain DE2010

To identify the strain DE2010, genomic DNA was purified to amplify the *16S rRNA* gene. The concentration of the resulting DNA solution was 2.43 µg/ml with a 260/280 ratio of 1.93. The DNA band obtained from the PCR cycling using the universal primers for eubacteria (27F and 1492R, Table 1) was resolved in a 1.2 % agarose gel (Figure 1) and further purified and sequenced. The refined sequence was then entered in the Ribosomal Database Project website at Michigan State University (RDP-II) (https://rdp.cme.msu.edu/classifier/classifier.jsp). The sequence analysis of the strain DE2010 shows that it belongs to the genus *Ochrobactrum* with a 100 % probability. The sequence was then introduced in BLAST (Basic Local Alignment Search Tool) (https://blast.ncbi.nlm.nih.gov/Blast.cgi) and was found to have a high degree of gene sequence similarity with *Ochrobactrum anthropi* ATCC49188^T (99.85 %), *Ochrobactrum*

anthropi strain AOB[T] (99.85 %), *Brucella melitensis* bv. 1str16M[T] (98.38 %), *Ochrobactrum pseudogrignonense* strain K8[T] (98.02 %) and *Sinorhizobium fredii* NGR234[T] (96.39 %). The Tamura three-parameter model neighbor-joining phylogenetic tree constructed from *16S rRNA* sequences of strain DE2010 and from other *Ochrobactrum* and *Brucella* species, with *Rhizobium rhizogenes* used as an outgroup, indicated that the strain DE2010 clearly belongs to the genus *Ochrobactrum* and is closely related to the species *O. anthropi* (Figure 2*a*). On the other hand, to further characterize the strain DE2010, the *nud*C gene was amplified from the genomic DNA. The *nud*C gene encodes for a NADH pyrophosphatase, which is a key player in the decay of messenger RNA in bacteria (Cahová et al., 2015) and could be therefore considered as a housekeeping gene in bacteria. In addition, previous studies have shown that the expression of the *nud*C gene plays an important role in drug tolerance and resistance to toxicity (Wang et al., 2011 and O'Toole et al., 2014). The DNA band was resolved in an agarose gel (Figure 1), purified and sequenced. The refined sequence was introduced in BLAST, and, as with the results obtained for the *16S rRNA* gene sequence of the isolated strain, a high degree of gene sequence similarity was found with *O. anthropi* ATCC49188[T] (99.85 %). The Jukes-cantor model neighbor-joining phylogenetic tree constructed from *nud*C sequences of DE2010 and other species from different genus (*Ochrobactrum, Rhizobium, Agrobacterium, Sinorhizobium, Mycobacterium, Geobacter, Pseudomonas*), with *Escherichia coli* used as the outgroup, corroborated that the isolated strain is closely related to the species *O. anthropi* (Figure 2*b*).

The capacity of symbiotic microorganisms to grow in nitrogen-limiting conditions has been related to the presence of plasmid-linked nitrogen-fixing genes such as *nif*H. In the case of *O. anthropi DE2010*, the purification of the genomic DNA renders a unique DNA

fragment (Figure 1) with no traces of extrachromosomal DNA. In addition, the PCR mixture using the specific primers for DNA band amplification from *nif*H (Table 1) confirms the absence of this gene (data not shown). Therefore, the presence of the genomic nitrogen-fixing gene *fix*H was confirmed using specific primers (Table 1 and Figure 1). The DNA sequence of this gene also confirms the identity of the isolated strain as belonging to the species *O. anthropi*.

3.3 Morphological responses to nitrogen deficiency

The morphological traits of *Ochrobactrum anthropi* DE2010 were assessed by SEM. The results indicate that the morphology of the cells, when grown in LB medium, are similar to those obtained for other described strains of *O. anthropi*. The cells, which reproduce by binary fission, are rod shaped and surrounded by an extracellular polymeric substance (EPS). In addition, as indicated above, they have a width of 0.5 μm and a length ranging from 1 to 3 μm. The same traits were obtained by negative staining when they are observed by TEM (Figure 3).

As the strain DE2010 is able to grow in the absence of N_2, changes in cell morphology under these conditions were also studied. For this, samples of this bacterium grown in both media (LB and VBE-glucose without nitrogen) were analyzed by microscopy. The images show the presence of cells with an altered morphology (Figure 4), as has been widely reported for symbiotic nitrogen-fixing bacteria (Haynes et al., 2004 and Cheng et al., 2007). In the DIC images corresponding to *O. anthropi* DE2010 grown in LB medium (Figure 4a), cells maintained the rod-shaped morphology shown in SEM images (Figure 3). However, under nitrogen deficient growth conditions, cells have a smaller size and exhibit different morphological types, on one hand, the typical rod shape, and on the other hand,

bulging or branched forms shaped like the letter L or V (Figure *4b*). The DIC images were also used to assess the effect of nitrogen deprivation on the shape and biomass of *O. anthropi* DE2010 with the *ImageJ* program. The results are summarized in Table 3. The biomass of *O. anthropi* DE2010 varies significantly depending on the growth medium used (LB or VBE without nitrogen source), showing a difference of 39.08 % in biomass depending on the medium used. A reduction in length of 46.4 % and in area of 34 %, as well as a change of 31 % in circularity, were observed in nitrogen-deprived conditions, are shown in DIC images. These results agree with those obtained by other authors when microorganisms were grown under unfavorable conditions (Chakravarty et al., 2008 and Justice et al., 2008).

Finally, similar results were obtained in cells grown in LB medium when they were analyzed simultaneously by DIC microscopy and TEM, but in the latter, more structural details are apparent, including (i) the typical bacterial cell wall of a gram-negative bacterium, (ii) the homogeneous cytoplasm occupied by numerous ribosomes and (iii) the presence of some peripheral electron-dense inclusions (Figure *4c*). On the other hand, TEM images of the microbial cells grown in the nitrogen-deficient medium show similar traits but present smaller lengths and pleomorphic morphologies when compared with cells grown in medium with nitrogen (Figure *4d*).

4. Discussion and conclusions

4.1 Phenotypic and genotypic characteristics of Ochrobactrum anthropi DE2010

The alphaproteobacterial *Ochrobactrum* genus, a member of the *Brucellaceae* family branch within rRNA superfamily IV, was established by Holmes et al. (1988). Currently, this microbial genus consists of eighteen species: *Ochrobactrum anthropi*, *O. ciceri*, *O. cytisi*,

O. daejeonense, *O. gallinifaecis*, *O. grignonense*, *O. haematophilum*, *O. intermedium*, *O. lupini*, *O. oryzae*, *O. pectoris*, *O. pituitosum*, *O. endophyticum*, *O. pseudintermedium*, *O. pseudogrignonense*, *O. rhizosphaerae*, *O. thiophenivorans* and *O. tritici*. These species have been isolated from a diverse range of sources, including soil (Lebuhn et al., 2006), plants and rhizospheres (Imran et al., 2010), industrial environments (Huber et al., 2010), animals (Kämpfer et al., 2011), humans (Teyssier et al., 2007) and sludge (Woo et al., 2011). The *Ochrobactrum* genus is phylogenetically related to other soil pathogenic bacteria and to the human pathogens *Brucella* and *Acinetobacter*, and phenotypically, it could be related to the genera *Alcaligenes* and *Achromobacter* or to the members of the *Pseudomonadaceae* family (Teyssier et al., 2005). *Ochrobactrum anthropi* is a gram-negative, aerobic, flagellated, oxidase- and urease-positive, non-fermentative and non-fastidious bacilli (Kern et al., 1993), and it can cause potentially serious opportunistic and nosocomial infections (Romano et al., 2009). In previous phenotypic studies using biochemical probes, *Ochrobactrum* strains exhibited negative results for indole, H_2S, carbohydrate fermentation and assimilation of adipate and phenylacetate and positive results for oxidase, catalase and assimilation of glucose, arabinose, mannose and malate (Teysser et al., 2005 and Huber et al., 2010). According to this information, the results obtained in this work demonstrated that *O. anthropi* DE2010 met all the phenotypic characteristics previously identified. Moreover, it is also known that the isolated *O. anthropi* and the type strains were highly resistant to all β-lactams (Kulkarni et al., 2017), and in this case, *O. anthropi* DE2010 exhibited resistance to ampicillin. All these results confirm that the strain described in this paper is *O. anthropi*.

4.2 Microalgae Scenedesmus sp. DE2009 and Ochrobactrum anthropi DE2010 interactions

The heterotrophic microorganism *Ochrobactrum anthropi* DE2010 was isolated from the microalgal *Scenedesmus* sp. DE2009 consortium of the Ebro Delta microbial mats. It is well-known that microbial autotroph-heterotroph interactions influence biogeochemical cycles (Cole et al., 2014), and understanding these interactions is critical for maintaining diversity in microbial communities in aquatic environments (Paerl et al., 2000). Some of these interactions involve (i) the molecular oxygen from algal photosynthesis, which is used as an electron acceptor by bacteria to degrade organic matter (Subashchandrabose et al., 2011); (ii) the carbon dioxide (CO_2) from bacterial mineralization that completes the photosynthetic cycle (Rier at al., 2002); (iii) the acquisition of vitamin B12 by algae through a symbiotic relationship with heterotrophic microorganisms because algae cannot synthesize vitamin B12 de novo (Croft et al., 2005); and (iv) the typical algal exudates, which are rich in carbohydrates and can be readily consumed by heterotrophic microorganisms (Rodriguez-Celma et al., 2013). All these interactions explain the cohabitation and microalgae-bacteria interrelationships in the same habitat.

In microbial mats, it is established that heterotrophic bacteria are very important for the community's cycles (Reid, et al., 2000), especially in consortia where these microorganisms are mostly located in the amorphous sheath that envelops the filamentous cyanobacteria and microalgae (Diestra et al., 2005). The microbial formation of consortia may be a possible explanation for microbes surviving in extreme environments under unfavorable conditions (Seufferheld et al., 2008). Thus, these heterotrophic communities often provide a new source of nitrogen for non-nitrogen fixing phototrophic

microorganisms. From the results obtained, it can be concluded that *Ochrobactrum anthropi* DE2010 probably plays an important role in providing a nitrogen source for the microalgal *Scenedesmus* sp. DE2009 in natural habitats.

4.3 Pleomorphism and nitrogen fixation

Nitrogen fixation in microbial mats has been described mainly in symbiotic bacteria and in free-living cyanobacteria, also known as diazotroph microorganisms (Stal, 1995). The contribution of cyanobacteria to nitrogen fixation in microbial mats seems to occur under light conditions since no nitrogenase activity is detected in the dark (Berrendero et al., 2016). Therefore, the metabolic demand of fixed nitrogen could be supplemented by associated heterotrophs. In fact, it has been described that bacteria related to the isolated strain DE2010, *O. anthropi* and *O. oryzae*, fix nitrogen and act as endosymbionts in artichoke and rice plants (Tripathi et al., 2006 and Meng et al., 2014). The nitrogen fixation activity has been linked to the presence of the nitrogenase activity encoded by the *nif* operon, being the *nif*H gene, which encoded the nitrogenase enzyme. The presence of *nif*H has been demonstrated in diazotrophs, and it has been specifically located in plasmids. Since the isolated strain DE2010 was able to grow under stressful conditions lacking N_2, we analyzed the presence of plasmids coding for the *nif*H gene. The isolated DNA gave a unique DNA band corresponding to the supercoiled genomic DNA (Figure 1), and the PCR analysis using the *nif*H primers failed to give a specific *nif*H-containing DNA band. The lack of the *nif*H gene in nitrogen-fixing bacteria has been associated with the genus *Ochrobactrum* and specifically with *O. oryzae* (Tripathi et al, 2006). Therefore, the nitrogenase activity might be associated with genomic operons in *O. anthropi* DE2010. Some operons are involved in the regulation of nitrogenase activity in diazotrophs. The *fix*

operon is essential for nitrogen fixation (Edgren et al., 2004) because it takes part in the regulation and metabolism of oxygen. The *fix* gene family is commonly found in three core operon structures: *fix*ABCX, *fix*GHIS and *fix*NOPQ (Black et al., 2012). The *fix*H gene is predicted to control genes involved in nitrogen metabolism and electron transport, and it is present in a V region of common clusters analyzed in nitrogen-fixing bacteria. We amplified part of the *fix*H gene of *O. anthropi* DE2010 in order to analyze the ability of this strain of microorganism to regulate nitrogen-fixing activity (Figure 1), and a prominent DNA band confirmed the presence of this gene after DNA sequencing. In general, bacteria have developed complex genetic and biochemical programs to maintain their classical shapes. However, despite these strict control mechanisms, bacteria have also retained genes that encode proteins dedicated to the purposeful alteration of overall bacterial cell length under certain circumstances, such as metabolic stress, including nitrogen deprivation (Young 2006). To understand the morphological response of *O. anthropi* DE2010 when exposed to nitrogen stress conditions, we used a CLEM approach (Figures 3 and 4). This approach enables, after a 24 h-period of growth with or without nitrogen, one to visualize cell structures in their respective state under two microscopy techniques, DIC and TEM. This makes it possible to measure and analyze the changes in cellular morphometric parameters and biomass under normal and stressful growth conditions using, as indicated by Cushnie et al., 2016, the open source software *ImageJ*. Cells under nitrogen-deprived conditions are less abundant and undergo cell rounding, reducing their length and area and, consequently, their biomass (Figure 4). In spite of that, incremental variation in the number of cellular types is demonstrated in cultures grown without a nitrogen source by the different microscopy techniques applied here. This pleomorphism and the amplification of

part of the *fix*H gen confirm that *O. anthropi* DE2010 has the capacity to fix nitrogen in normal growing conditions. Most likely, *O. anthropi* DE2010, as a member of the *Scenedesmus* sp. DE2009 consortium, provides nitrogen to the microalgae, and these organisms, in turn, provide organic matter and oxygen to the bacteria, favoring the interaction between both microorganisms in natural environments, as in this case in the Ebro Delta microbial mats. To the best of our knowledge this study is the first to describe the presence of a non-symbiotic nitrogen-fixing *O. anthropi* DE2010 in microbial mats.

In conclusion, the strain DE2010 from the *Scenedesmus* sp. DE2009 consortium corresponds to a member of the *Ochrobactrum* genus. Specifically, the sequencing analysis of the *16S rRNA* and *nuo*C and *fix*H genes show that this strain corresponds to the species *Ochrobactrum anthropi*. In addition, the biochemical characterization of this microorganism confirms previous molecular results. Furthermore, *O. anthropi* DE2010 is able to overcome N_2-limiting conditions through a *nif*H–independent mechanism still not identified, showing at the same time changes in shape and size and a greater abundance of pleomorphic cells. With regard to future research, it is important to highlight the role of consortia in studying the symbiotic relationships between microorganisms living in extreme habitats, such as the deprived nitrogen conditions assessed in this paper. To this end, our research group is now studying the effect of other stress factors, such us changes in environmental parameters and metal pollution, on consortia and on *Ochrobactrum anthropi* DE2010.

Acknowledgements
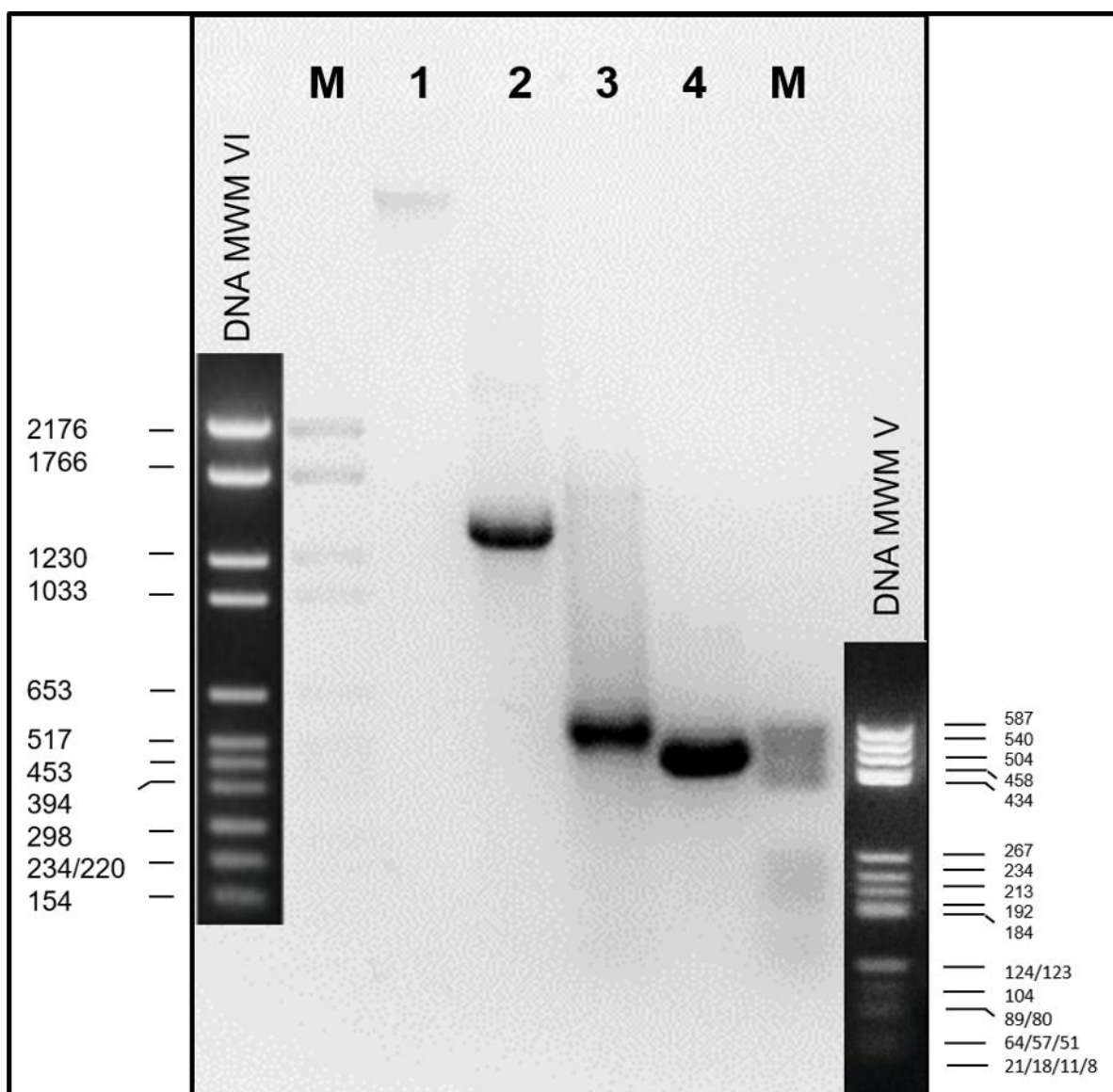
Fig. 1 Agarose gel (1.2%) analysis of the PCR products for *16S* rRNA and *nuo*C and *fix*H gene detection. Lanes 1 and 6, indicated with M, are DNA molecular weight markers (Roche) VI and V, respectively; and lanes 2, 3, 4 and 5 show genomic DNA, *16S* rRNA, *nuo*C and *fix*H, respectively, for PCR bands of *Ochrobactrum anthropi* DE2010.
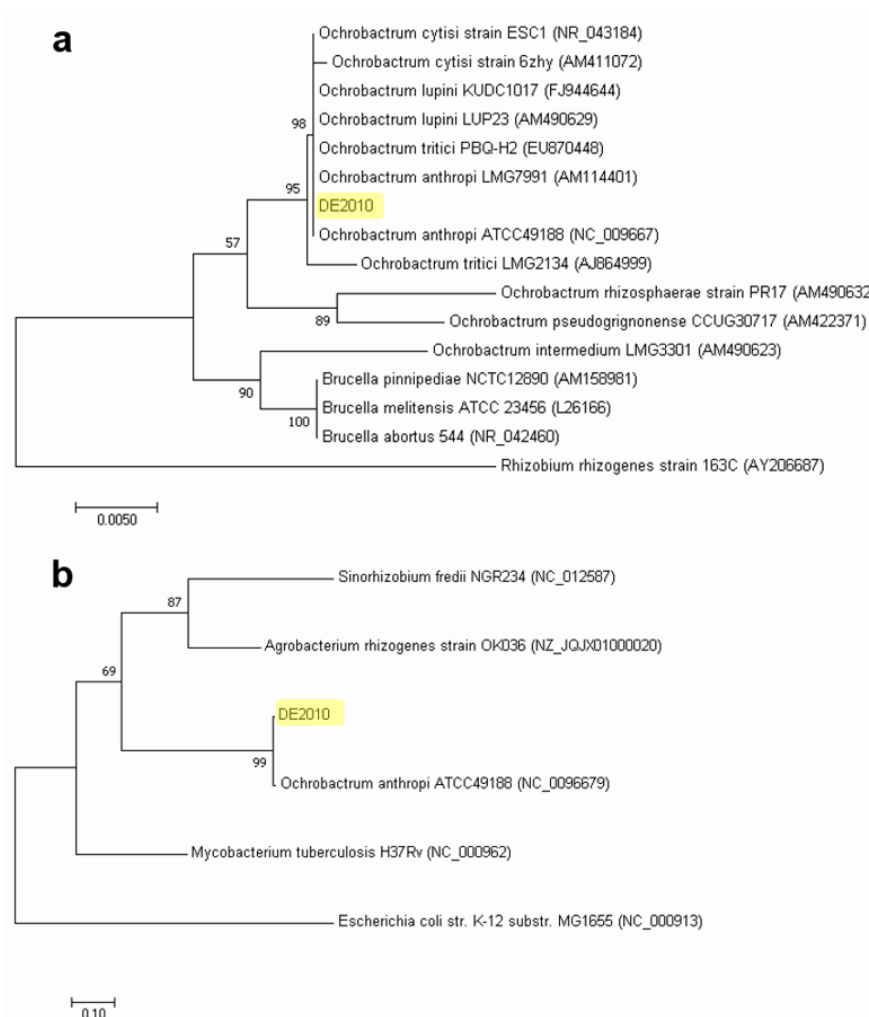
Fig. 2 Neighbor-joining trees based on 16S rRNA (a) and nudC (b) gene sequence relationships between Ochrobactrum anthropi DE2010 and the type strains of Ochrobactrum, Brucella species, Pseudomonas, Geobacter, Agrobacterium, Sinorhizobium and Mycobacterium. Numbers at the nodes are percentage bootstrap values based on 1000 resampled datasets. Bar represents 0.005 substitutions per nucleotide position on 16S rRNA and 0.2 substitutions per nucleotide position on nudC. The root positions of the trees for 16S rRNA and nudC were determined using Rhizobium rhizogenes and Escherichia coli, respectively, as the outgroups.
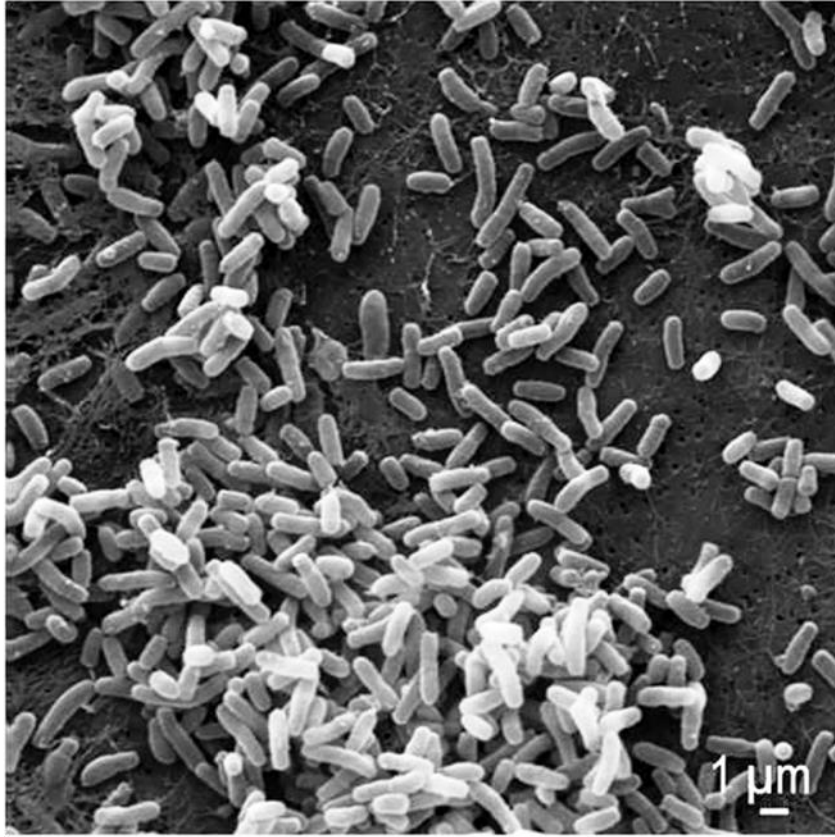
Fig. 3 SEM micrograph of *Ochrobactrum anthropi* DE2010 grown in LB culture medium.
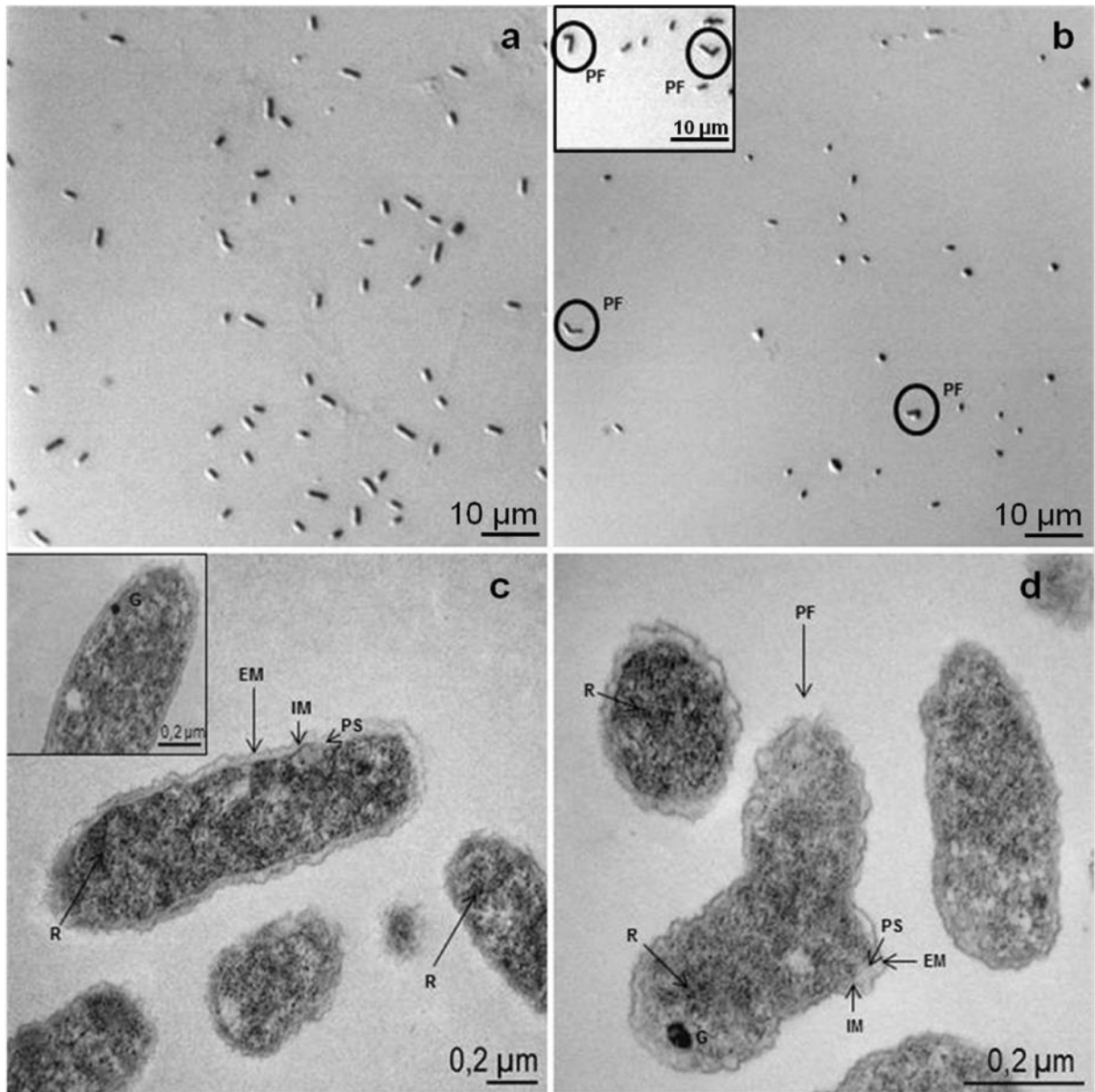
Fig. 4 DIC and TEM images of Ochrobactrum anthropi DE2010 grown in LB culture medium (a and c) and VBE–glucose culture medium without a nitrogen source (b and d), respectively. External membranes (EMs), granules (Gs), internal membranes (IMs), pleomorphic forms (PFs), periplasmic spaces (PSs) and ribosomes (Rs).

Table 1 Forward and reverse primers, annealing temperature (AT), amplicon size (bp) and accession number (AN) of the PCR products from *16S rRNA*, *nud*C, *fix*H and *nif*H genes.

Forward primer (5'–3')	Reverse primer (5'–3')	AT (°C)	Amplicon size (bp)/AN
Universal primer 27F AGAGTTTGGATCMTGGCTCAG	Universal primer 1492R GGTTACCTTGTTACGACTT	54	1,359/ KY575285
*nud*C-F CTAGCCATGGATCGTATAATTGAAAAATTAG	*nud*C-R CAGGGATCCTCACTCATACTCTGCCCGACAC	60	530/ MF179012
*fix*H-F ATGTCGATCAAGTCGAAAACC	*fix*H-R TCATAGTATCCTCCCGTCC	50	459/ MF363123
*nif*H-F GTCTCCTATGACGTGCTCGG	*nif*H-R GCTTCCATGGTGATCGGGGT	60	ND*

*ND: Not detected

Table 2 Phenotypic characterization of the *Ochrobactrum anthropi* DE2010.

Characters	*Ochrobactrum anthropi* DE2010	Characters	*Ochrobactrum anthropi* DE2010
Cell morphology	rod shaped	Erythritol	+
Spore formation	-	Glicerol	+
Motility	+	Dulcitol	+
Catalase	+	Inositol	+
Oxidase	+	Arbutine	-
Nitrate reduction (nitrite production)	+	Lactose	-
Nitrite reduction (amonium production)	+	Arabitol	-
Indole production	-		
H$_2$S production	-	**Enzymatic activity**	
Assimilation (API20NE)		Urease	+
Citrate	+	Acid and alkaline phosphatase	-
Glucose	+	Esterase (C4)	+
Gluconate	+	Esterase-lipase (C8)	-
Arabinose	+	α-glucosidase	+
Mannitol	+	β-glucosidase	-
Mannose	+	β-galactosidase	-
Malate	+	Lipase (C14)	+
Phenylaceticacid	-	DNase (hydrolysis of DNA)	-
		Protease (hydrolysis of gelatin)	-
Oxidation (API50CHB)			
D-Ribose	+	**Antibiotic resistance**	
L-Xilose	+	Chloramphenicol	R
D-Adonitol	+	Tetracycline	R
D-Glucose	-	Ampicillin	R
L-Arabinose	+	Nalidixic acid	S
D-Fucose	+	Erythromycin	S

+: positive, -: negative, R: resistant and S: sensitive.

Table 3 Cellular morphometric parameters from the *Ochrobactrum anthropi* DE2010 cultures grown in LB and VBE-glucose without nitrogen source media.

Culture medium	Length (µm)	Circularity (µm)	Area (µm^2)	Biomass (µg C/ cm^3)
LB	5.41 ± 0.22	0.61 ± 0.02	20.04 ± 1.21	16.17*
VBE without nitrogen source	2.51 ± 0.19	0.92 ± 0.01	6.81 ± 0.86	6.32*

* for the biomass analysis the average of relative standard deviation (RSD) was < 10 %.

References:

Aquilantia L, Favilib F, Clementi F (2004) Comparison of different strategies for isolation and preliminary identification of *Azotobacter* from soil samples. Soil Biol Biochem 36:1475-1483

Bal AK, Shantharam S, Verma DPS (1980) Changes in the outer cell wall of *Rhizobium* during development of root nodule symbiosis in soybean. Can J Microbiol 26:1096-1103

Batut J, Andersson SG, O'Callaghan D (2004) The evolution of chronic infection strategies in the alphaproteobacteria. Nat Rev Microbiol 2:993-945

Berrendero-Gómez E, Johansen JR, Kaštovský J, Bohunická M, Čapková K (2016) *Macrochaetegen.* nov. (Nostocales, Cyanobacteria), a taxon morphologically and molecularly distinct from *Calothrix*. J Phycol 52:638–655

Black M, Moolhuijzen P, Chapman B, Barrero R, Howieson J, Hungria M, Bellgard M (2012) The Genetics of Symbiotic Nitrogen Fixation: Comparative Genomics of 14 Rhizobia Strains by Resolution of Protein Clusters. Genes 3(1):138-166

Burgos A, Maldonado J, De los Rios A, Solé A, Esteve I (2013) Effect of copper and lead on two consortia of phototrophic microorganisms and their capacity to sequester metals. Aquat Toxicol 140–141:324–336

Cahová H, Winz ML, Höfer K, Nübel G, Jäschke A (2014) NAD captureSeq indicates NAD as a bacterial cap for a subset of regulatory RNAs. Nature 519:374–377

Chakravarty R and Banerjee PC (2008) Morphological changes in an acidophilic bacterium induced by heavy metals. Extremophiles 12: 279

Chen W, de Faria S, James E, Elliott G, Lin K, Chou J, Sheu S, Cnockaert M, Sprent J, Vandamme P (2007) *Burkholderia nodosa* sp. nov., isolated from root nodules of the woody Brazilian legumes *Mimosa bimucronata* and *Mimosa scabrella*. Int J Syst Evol Microbiol 57(5):1055-1059

Cole JJ. Interactions Between Bacteria and Algae in Aquatic Ecosystems (1982) Annu Rev Ecol Syst 13(1): 291-314

Cole JR, Wang Q, Fish JA, et al. (2014). Ribosomal Database Project: Data and tools for high throughput rRNA analysis. Nucleic Acids Res 42: D633-42

Cole JK, Hutchison JR, Renslow RS, Kim YM, Chrisler WB, Engelmann HE, Dohnalkova AC, Hu D, Metz TO, Fredrickson JK, Lindemann SR (2014) Phototrophic biofilm assembly in microbial-mat-derived unicyanobacterial consortia: model systems for the study of autotroph-heterotroph interactions. Front Microbiol 5:109

Croft MT, Lawrence AD, Raux-Deery E, Warren MJ, Smith AG (2005) Algae acquire vitamin B12 through a symbiotic relationship with bacteria. Nature 438: 90-93

Cushnie TPT, O'Driscoll NH, Lamb AJ (2016) Morphological and ultrastructural changes in bacterial cells as an indicator of antibacterial mechanism of action. Cell Mol Life Sci 73:4471–4492

Dalgaard P, Ross T, Kamperman L, Neumeyer K, McMeekin TA (1994) Estimation of bacterial growth rates from turbidimetric and viable count data. Int J Food Microbiol 23(3-4):391-404

Diestra E, Solé A, Martí M, Garcia De Oteyza T, Grimalt JO, Esteve I (2005) Characterization of an oil-degrading *Microcoleus* consortium by means of confocal scanning microscopy, scanning electron microscopy and transmission electron microscopy. Scanning 27:176–180

Diestra E, Esteve I, Burnat M, Maldonado J, Sole A (2007) Isolation and characeritzation of heterotrophic bacterium able to grow in different environmental stress conditions, including crude oil and heavy metals. In: A Menendez-Vilas (Ed) Communicating Current Research and Educational Topics in Applied Microbiology, 7th edn. pp 90-99

Doetsch RN (1981) Determinative methods of light microscopy. In: P. Gerhardt, R. G. E. Murray, R. N.Costilow, E. W. Nester, W. A. Wood, N. R. Krieg, and G. B.Phillips (ed.) Manual of methods for general bacteriology. American Society for Microbiology, Washington, D.C. p. 21-33

Edgren T and Nordlund S (2004) The *fix*ABCX Genes in *Rhodospirillum rubrum* Encode a Putative Membrane Complex Participating in Electron Transfer to Nitrogenase. J Bacteriol 2052–2060

Esteve I, Martínez-Alonso M, Mir J, Guerrero R (1992) Distribution, typology and structure of microbial mat communities in Spain: a preliminary study. Limnetica 8:185–195

Esteve I, Ceballos D, Martínez-Alonso M, Gaju N, Guerrero R (1994) Development of versicolored microbial mats: Succession of microbial communities. In: Stal L.J., Caumette P. (eds) Microbial Mats. NATO ASI Series (Series G: Ecological Sciences), vol 35. Springer, Berlin, Heidelberg.

Felsenstein J (1985) Confidence limits on phylogenies: an approach using the bootstrap. Evolution 39:783–791

Guerrero R, Urmeneta J, Rampone G (1993) Distribution of types of microbial mats at the Ebro Delta, Spain. Biosystems 31:135–144

Guerrero R, Haselton A, Solé M, Wier A, Margulis L (1999) *Titanospirillum velox*: A huge, speedy, sulfur-storing spirillum from Ebro Delta microbial mats. Proceedings of the National Academy of Sciences of the United States of America, 96(20):11584–11588

Hall BG, Acar H, Nandipati A, Barlow M (2014) Growth rates made easy. Mol Biol Evol 31(1):232-238

Hamouda T, Shih AY, Baker Jr. JR (2002) A rapid staining technique for the detection of the initiation of germination of bacterial spores. Lett Appl Microbiol 34:86–90

Haynes JG, Czymmek KJ, Carlson CA, Veereshlingam H, Dickstein RD, Sherrier J (2004) Rapid analysis of legume root nodule development using confocal microscopy. New Phytol 163: 661–668

Holmes B, Popoff M, Kiredjian M, Kersters K (1988) *Ochrobactrum anthropi* gen. nov., sp. nov. from Human Clinical Specimens and Previously Known as Group Vd. Int J Syst Bacteriol 38(4):406-416

Holt JG, Krieg RN, Sneath PHA, Staley JT, Williams ST (1994) Bergey's Manual of Determinative Bacteriology, 9th ed., Williams and Wilkins, Baltimore.

Høvik Hansen G, Sørheim R (1991) Improved method for phenotypical characterization of marine bacteria. J Microbiol Meth 13:231–241

Huber B, Scholz HC, Kámpfer P, Falsen E, Langer S, Busse HJ (2010) *Ochrobactrum pituitosum* sp. nov., isolated from an industrial environment. Int J Syst Evol Microbiol 60:321–326

Imran A, Hafeez FY, Frühling A, Schumann P, Malik KA, Stackebrandt E (2010) *Ochrobactrum ciceri* sp. nov., isolated from nodules of *Cicer arietinum*. Int J Syst Evol Microbiol 60:1548–1553

Jukes TH, Cantor C.R. (1969) Evolution of Protein Molecules. New York: Academic Press. pp. 21–132

Justice SS, Hunstad DA, Cegelski L, Hultgren SJ (2008) Morphological plasticity as a bacterial survival strategy. Nat Rev Microbiol 6:162‑168

Kämpfer P, Scholz HC, Huber B, Falsen E, Busse HJ (2007) *Ochrobactrum haematophilum* sp. nov.and *Ochrobactrum pseudogrignonense* sp. nov., isolated from human clinical specimens. Int J Syst Evol Microbiol 57:2513–2518

Kern W V, Oethinger M, Marre R, Kaufhold A, Rozdzinski E (1993) *Ochrobactrum anthropi* bacteremia: Report of four cases and short review. Infection 21(5):306‑310

Kulkarni G, Gohil K, Misra V, Kakrani AL, Misra PS, Patole M, Shouche Y, Dharne M. (2017) Multilocus sequence typing of *Ochrobactrum* spp. isolated from gastric niche. Volume 10, Issue 2, 201–210.

Kumar S, Stecher G, and Tamura K (2016) MEGA7: Molecular Evolutionary Genetics Analysis version 7.0 for bigger datasets. Mol Biol Evol 33:1870‑1874

Lebuhn M, Bathe S, Achouak W, Hartmann A, Heulin T & Schloter M (2006) Comparative sequence analysis of the internal transcribed spacer 1 of *Ochrobactrum* species. System Appl Microbiol 29:265‑275

Maldonado J, Diestra E, Huang L, Domènech AM, Villagrasa E, Puyen ZM, Duran R, Esteve I, Solé A (2010) Isolation and identification of a bacterium with high tolerance to lead and copper from a marine microbial mat in Spain. Ann Microbiol 60(1):113–120

Martínez‑Alonso M, Mir J, Caumette P, Gaju N, Guerrero R, Esteve I (2004) Distribution of phototrophic populations and primary production in a microbial mat from the Ebro Delta, Spain. Int Microbiol 7(1):19‑25

Meng X, Yan D, Long X, Wang C, Liu Z, Rengel, Z (2014) Colonization by endophytic *Ochrobactrum anthropi* Mn1 promotes growth of Jerusalem artichoke. Microb Biotechnol 7: 601–610

Millach L, Solé A, Esteve I (2015) Role of *Geitlerinema* sp. DE2011 and *Scenedesmus* sp. DE2009 as Bioindicators and Immobilizers of Chromium in a Contaminated Natural Environment. Biomed Res Int Article ID 519769

Millach L, Obiol A, Solé A, Esteve I (2017) A novel method to analyse in vivo the physiological state and cell viability of phototrophic microorganisms by confocal laser scanning microscopy using a dual laser. J Microsc-Oxford 268(1):53–65

Milloning G (1961) A modified procedure for lead staining of thin sections. J Biophys Biochem Cytol 11:736-739

Mir J, Martínez-Alonso M, Esteve I, Guerrero R (1991) Vertical stratification and microbial assemblage of a microbial mat in Ebro Delta (Spain). FEMS Microl Ecol 86:59–68

O'Toole RF, Johari BM, Mac Aogáin M, Rogers TR, Bower JE, Basu I, Freeman JT (2014) Draft Genome Sequence of the First Isolate of Extensively Drug-Resistant *Mycobacterium tuberculosis* in New Zealand. Gen Announ 2:4–5

Paerl HW (1977) Role of heterotrophic bacteria in promoting N2 fixation by *Anabaena* in aquatic habitats. Microb Ecol 4(3):215-231

Paerl HW, Pinckney JL, Steppe TF (2000) Cyanobacterial-bacterial mat consortia: Examining the functional unit of microbial survival and growth in extreme environments. Environ Microbiol 2(1):11-26

Perkovic M, Kunz M, Endesfelder U, Bunse S, Wigge C, Yu Z, Hodirnau VV, Scheffer MP, Seybert A, Malkusch S, Schuman EM, Heilemann M, Frangakis AS (2014) Correlative Light- and Electron Microscopy with chemical tags. J Struct Biol 186:205–213

Ramos VMC, Castelo-Branco R., Leão PN, Martins J, Carvalhal-Gomes S, Sobrinho da Silva F, Mendonça Filho JG, Vasconcelos VM (2017) Cyanobacterial Diversity in Microbial Mats from the Hypersaline Lagoon System of Araruama, Brazil: An In-depth Polyphasic Study. Front Microbiol 8:1233

Reid RP, Visscher PT, Decho AW, Stolz J F (2000) The role of microbes in accretion, lamination and early lithification of modern marine stromatolites. Nature 406(6799):989-92

Revsbech NP, Barker Jmgensen, B, Blackburn TH, Cohen Y, Steinitz H (1983) Microelectrode studies of the photosynthesis and O2, H2S, and pH profiles of a microbial mat. Limnol Oceanogr 28:1062–1074

Rier ST, Stevenson RJ (2002) Effects of light, dissolved organic carbon, and inorganic nutrients [2pt] on the relationship between algae and heterotrophic bacteria in stream periphyton. Hydrobiologia 489:179–184

Rodríguez-Celma J, Lin WD, Fu GM, Abadía J, López-Millán AF, Schmidt W (2013) Mutually Exclusive Alterations in Secondary Metabolism Are Critical for the Uptake of Insoluble Iron Compounds by *Arabidopsis* and *Medicago truncatula*. Plant Physiology 162 (3):1473-1485

Romano S, Aujoulat F, Jumas-Bilak E, Masnou A, Jeannot JL, Falsen E, Marchandin,H, Teyssier C (2009) Multilocus sequence typing supports the hypothesis that *Ochrobactrum anthropi* displays a human-associated subpopulation. BMC Microbiol 9:267

Sayah RS, Kaneene JB, Johnson Y, Miller R (2005) Patterns of antimicrobial resistance observed in *Escherichia coli* isolates obtained from domestic- and wild-animal fecal samples, human septage, and surface water. Appl Environ Microbiol 71(3):1394-1404

Saitou N, Nei M (1987) The neighbor-joining method: a new method for reconstructing phylogenetic trees. Mol Biol Evol 4(4):406-25

Seufferheld MJ, Alvarez HM, Farias ME (2008) Role of polyphosphates in microbial adaptation to extreme environments. Appl Environ Microbiol 74:5867–5874

Shen H, Niu Y, Xie P, Tao M, Yang X (2011) Morphological and physiological changes in *Microcystis aeruginosa* as a result of interactions with heterotrophic bacteria. Freshwater Biol 56:1065–1080

Solé A, Gaju N, Esteve I (2003) The biomass dynamics of cyanobacteria in an annual cycle determined by confocal laser scanning microscopy. Scanning 25(1):1-7

Stal JL (1995) Physiological ecology of cyanobacteria in microbial mats and other communities. New Phytol 131:1-32

Subashchandrabose S R, Ramakrishnan B, Megharaj M, Venkateswarlu K, Naidu R (2011) Consortia of cyanobacteria/microalgae and bacteria: Biotechnological potential. Biotechnol Adv 29(6):896-907

Tamura K (1992) Estimation of the number of nucleotide substitutions when there are strong transition-transversion and G+C content biases. Mol Biol Evol 9 (4): 678–687

Teyssier C, Marchandin H, Jean-Pierre H, et al (2005) Molecular and phenotypic features for identification of the opportunistic pathogens *Ochrobactrum* spp. J Med Microbiol 54(10):945-953

Teyssier C, Marchandin H, Jean-Pierre H, Masnou A, Dusart G, Jumas-Bilak E (2007) *Ochrobactrum pseudintermedium* sp. nov., a novel member of the family Brucellaceae, isolated from human clinical samples. Int J Syst Evol Microbiol 57:1007–1013

Thompson JD, Gibson TJ, Plewniak F, Jeanmougin F, Higgins DG (1997) The CLUSTAL X windows interface: Flexible strategies for multiple sequence alignment aided by quality analysis tools. Nucleic Acids Res 25:4876–4882

Tripathi A, Verma S, Chowdhury S, Lebuhn M, Gattinger A, Schloter M (2006) *Ochrobactrum oryzae* sp. nov., an endophytic bacterial species isolated from deep-water rice in India. Int J Syst Evol Microbiol 56(7):1677-1680

Vancová M, Rudenko N, Vaněček J, Golovchenko M, Strnad M, Rego ROM, Tichá L, Grubhoffer L, Nebesářová J (2017) Pleomorphism and viability of the Lyme disease pathogen *Borrelia burgdorferi* exposed to physiological stress conditions: A correlative cryo-fluorescence and cryo-scanning electron microscopy study. Front Microbiol 8:596

Wang XD, Gu J, Wang T, Bi LJ, Zhang ZP, Cui ZQ, Wei HP, Deng JY, Zhang XE (2011) Comparative analysis of mycobacterial NADH pyrophosphatase isoforms reveals a novel mechanism for isoniazid and ethionamide inactivation. Mol Microbiol 82:1375–1391

Woo SG, Ten LN, Park J, Lee J (2011) *Ochrobactrum daejeonense* sp. nov., a nitrate-reducing bacterium isolated from sludge of a leachate treatment plant. Int J Syst Evol Microbiol 61:2690–2696

Wrede C, Heller C, Reitner J, Hoppert M (2008) Correlative light/electron microscopy for the investigation of microbial mats from Black Sea Cold Seeps. J Microbiol Meth 73:85–91

Xie B, Bishop S, Stessman D, Wright D, Spalding MH, Halverson LJ (2013) *Chlamydomonas reinhardtii* thermal tolerance enhancement mediated by a mutualistic interaction with vitamin B12-producing bacteria. ISME J 7(8):1544-1555

Young KD (2006) The Selective Value of Bacterial Shape. Microbiol. Mol Biol Rev 70(3): 660-703

Complete bibliographical reference of article from 2.1 thesis section:

Villagrasa, E., Ferrer-Miralles, N., Millach, L., Obiol, A., Creus, J., Esteve, I., Solé, A., 2019. Morphological responses to nitrogen stress deficiency of a new heterotrophic isolated strain of Ebro Delta microbial mats. Protoplasma. 256 (1):105-116. https://doi.org/10.1007/s00709-018-1263-8.

Section 2.2 Multi-approach analysis to assess the chromium(III) immobilization by *Ochrobactrum anthropi* DE2010

Multi-approach analysis to assess the chromium(III) immobilization by *Ochrobactrum anthropi* DE2010

Eduard Villagrasa[1], Belén Ballesteros[2], Laia Millach[1], Aleix Obiol[1], Isabel Esteve[1] and Antonio Solé[1]

[1]*Departament de Genètica i Microbiologia. Facultat de Biociències. Universitat Autònoma de Barcelona. Bellaterra, Cerdanyola del Vallès, 08193 Barcelona, Spain*

[2]*Catalan Institute of Nanoscience and Nanotechnology (ICN2), CSIC and BIST, Campus UAB, Bellaterra, 08193 Barcelona, Spain*

Abstract

Ochrobactrum anthropi DE2010 is a microorganism isolated from Ebro Delta microbial mats and able to resist high doses of chromium(III) due to its capacity to tolerate, absorb and accumulate this metal. The effect of this pollutant on *O. anthropi* DE2010 has been studied assessing changes in viability and biomass, sorption yields and removal efficiencies. Furthermore, and for the first time, its capacity for immobilizing Cr(III) from culture media was tested by a combination of High Angle Annular Dark Field (HAADF) Scanning Transmission Electron Microscopy (STEM) imaging coupled to Energy Dispersive X-ray spectroscopy (EDX).

The results showed that *O. anthropi* DE2010 was grown optimally at 0-2 mM Cr(III). On the other hand, from 2 to 10 mM Cr(III) microbial plate counts, growth rates, cell viability, and biomass decreased while extracellular polymeric substances (EPS) production increases. Furthermore, this bacterium had a great ability to remove Cr(III) at 10 mM (q= 950.00 mg g^{-1}) immobilizing it mostly in bright polyphosphate inclusions and secondarily on the cellular surface at the EPS level. Based on these results, *O. anthropi* DE2010 could be considered as a potential agent for bioremediation in Cr(III) contaminated environments.

1. Introduction

The increase in industrial and anthropogenic activities has largely contributed towards the introduction of heavy metals and other pollutants into the environment (Gupta et al., 2014; Bhattacharya et al., 2015). Pollution by heavy metals has become a serious threat to the environment and public health, since, in general, they are highly toxic and accumulate throughout the food chain (Feng et al., 2012; Xu et al., 2014). Chromium is one of the earth crust's most abundant elements (Mohana and Pittman, 2006) and it is a redox active 3d transition metal with different oxidation states ranging from 2+ to 6+ (Greenwood and Earnshaw, 1998; Srivastava and Thakur, 2007). The trivalent (Cr(III)) and hexavalent (Cr(VI)) forms, from industrial by-products or by being part of phosphate fertilizers used in agriculture (Nziguheba and Smolders, 2008; Manahan, 2009) among other chromium sources, are stable in the majority of terrestrial surface and aquatic environments (Kimbrough et al., 1999; Ihsanullah et al., 2016). Cr(III) is considered to be an essential element (micronutrient) with known cellular biological functions (Balk et al., 2007; Evert et al., 2013). However, with long-term exposure it can produce toxic effects in the cells, but at a much lower degree than Cr(VI), which is more toxic and unhealthy for living beings and the environment (Shanker et al., 2005; Francisco et al., 2011; Ihsanullah et al., 2016). Even so, Cr(III) is involved in some human diseases such as: structural perturbation in erythrocyte membrane and cancer (Kusiak et al., 1993; Suwalsky et al., 2008; Figgit et al., 2010).

In the last decade, our research group has isolated different heterotrophic and phototrophic (cyanobacteria and algae) microorganisms from the Ebro Delta microbial mats (Tarragona, Spain). One of these microorganisms, *Ochrobactrum anthropi* DE2010, was isolated from the microalgae *Scenedesmus* sp. DE2009 consortium from the same ecosystems, and recently was characterized and identified by means of microbiological, biochemical and molecular methods. Furthermore, the analysis of the effect of deprived nitrogen source conditions on this heterotrophic bacterium demonstrate that it is able to overcome this limiting condition through a still unknown *nif*H–independent mechanism, although there were changes in shape, size, and abundance of pleomorphic cells (Villagrasa et al., 2019).

The aims of this work are: (i) to evaluate the cytotoxic effect of chromium and the capacity of *Ochrobactrum anthropi* DE2010, growing in axenic cultures, to remove it; (ii) to determine changes in total biomass and cellular viability and in composition and production of EPS in cultures exposed to this metal and (iii) to determine the Cr(III) uptake efficiency of *Ochrobactrum anthropi* DE2010 and its ability to capture chromium(III) extra and/or intracellularly. With this in mind, an analytical multi-approach combining classical microbial plate counts, growth methods, optical microscope techniques, and biochemical and chemical analysis besides high resolution microscopy techniques have been applied.

2. Materials and methods

2.1 Microorganism, chromium(III) stock solutions and culture conditions

O. anthropi DE2010 (accession number DDBJ/ENA/GenBank, KY575285) isolated from a *Scenedesmus* sp. DE2009 consortium from Ebro Delta microbial mats (Villagrasa et

al., 2019) was grown at 27 °C in Luria–Bertani (LB) agar medium, containing tryptone (10.0 g L^{-1}), yeast extract (5.0 g L^{-1}), NaCl (10.0 g L^{-1}) and agar (15.0 g L^{-1}), and preserved in Cryoinstant® vials (Thermo Fisher Scientific) at -80 ºC.

Chromium(III) stock solution was prepared as $Cr(NO_3)_3 \cdot 9H_2O$ salt (Sigma-Aldrich, Bellefonte, PA, USA). The 2,600 mg L^{-1} (50 mM) Cr(III) stock solution was made by dissolving the exact quantities of $Cr(NO_3)_3$ in double deionized water and sterilized by filtration through a 0.2 µm filter (Millipore, Merck Millipore). The Cr(III) working concentrations of 0 (control experiment), 0.5, 2, 5, 7, and 10 mM (equivalent to 0, 26, 104, 260, 364, and 520 mg L^{-1}, respectively) were obtained by serial dilution. The Cr(III) stock and serial working solutions were prepared just before use and its pH were adjusted at 6.5.

Unpolluted (0 mM) and polluted (0.5, 2, 5, 7 and 10 mM) cultures were prepared at the same conditions in the following manner: 2 mL of a 24 h culture of *O. anthropi* DE2010 grown in LB (OD_{600} between 1.4-1.6, approximately 10^{10} cfu mL^{-1}) was inoculated into 18 mL of LB liquid medium with the different tested Cr(III) concentrations. These cultures were used for all experiments and were incubated in an orbital shaker (Infors HT, Ecotron) (150 rpm) at 27 ºC for 24 h. Triplicate cultures were grown for eh heavy metal concentration.

2.2 Bacterial plate counts and growth curves

To determine the concentration of bacterial cells, 0.1 mL from 24 h cultures grown at different Cr(III) concentrations were spread onto LB agar plates also supplemented with the same final chromium working concentrations: 0, 0.5, 2, 5, 7, and 10 mM. In addition, in order to evaluate the number of dormant *O. anthropi* DE2010 cells, 0.1 mL from each 24 h culture polluted with Cr(III) was spread onto new LB agar plates without Cr(III). The plates were incubated at 27 ºC for 2 d in darkness. The viability counts were expressed in cfu/mL,

and 8 replicates were performed for each experiment. The dormant cell counts were determined using the following formula (Sachidanandham et al., 2009):

$$DC = [100 - (\frac{CC}{CC+RC} \times 100)]$$

where DC is the dormant cells relative ratio; CC is the cultivable cells grown with Cr (III) count (cfu mL^{-1}) and RC is the resurrected cells count (cfu mL^{-1}) and corresponds to the difference between cfu mL^{-1} obtained without and with Cr (III).

For growth curve measurements, *Ochrobactrum anthropi* DE2010 culture was grown in LB medium at 27 °C for 24 h in the dark. After this incubation time, a 96-well microplate was prepared by inoculating 20 µL of the above-mentioned over-night culture in microplate columns 2, 4, 6, 8, 10, and 12 filling all the wells. Working Cr(III) concentrations 0, 0.5, 2, 5, 7, and 10 mM at a final volume of 200 µL were used. Blank media samples were considerate by adding bacteria-free LB medium uncontaminated and contaminated with Cr(III) using the same working concentrations in microplate columns 1, 3, 5, 7, 9, and 11, respectively. OD (λ = 600 nm) was measured every 30 min during 24 h with a microtiter plate photometer (Thermo Scientific Variokan® Flash, Waltham, USA). Before each measurement, microtiter plate was shaken for 5 s at 120 rpm. Eight replicates were analyzed for each heavy metal concentration.

2.3 Cell viability and biomass analysis by Confocal Laser Microscopy (CLSM)

Biomass and viability of *O. anthropi* DE2010 cells at different Cr(III) concentrations were determined according to the fluorochromes-confocal laser scanning-image analysis method (FLU-CLSM-IA) described by Puyen et al. (2012a) with some modifications introduced for this particular study. This method combined the use of specific

fluorochromes, CLSM, and image analysis using the ImageJ/FIJI v.1.46r software (Schneider et al., 2012).

For this experiment, 1 mL from each 24 h culture contaminated with a different Cr(III) working concentration was centrifuged at 2000xg for 10 min at 4 ºC (Eppendorf 5804R refrigerated centrifuge). Then, the obtained pellets were stained with a mixture of 100 μL of two fluorochromes, SYTOX® Green (5 μM) and Hoechst 33342 (64.9 μM) for 30 min at room temperature in the dark. Subsequently, 25 μL of these stained pellets were smeared onto Polylysine® slides (ThermoFisher Scientific, USA), producing a sticky surface and preventing cell movement, mounted in BacLight mounting oil (ThermoFisher Scientific, USA) and immediately covered and sealed with coverslips (24x24 mm). Stained cells were observed with a confocal microscope (Leica TCS SP5; Leica Microsystems CMS GmbH, Mannheim, Germany) using a HCX PL APO lambda blue 63.0x1.40 OIL UV at 2 zoom. In this study, *xyz* CLSM images were taken in a sequential scan in two channels to distinguish the fluorescence emitted by Hoechst 33342 (414-485 nm) and SYTOX Green (515-580 nm), respectively. In order to differentiate between living and dead cells, they were stained with Hoechst 333429 or SYTOX Green respectively, blue (live cells) and green (dead cells) pseudo-colors were used. In each bacterial culture, once the 20 blue and green CLSM images (1024x1024 pixels) were acquired, the corresponding CLSM binary images (black/white) were generated by means of the ImageJ/FIJI v.1.46r program. In addition, Voxel counter plugin of this software was applied to assess the cellular viability and biomass at each Cr(III) concentration (Puyen et al., 2012a).

2.4 Extraction and Biochemical analysis of the total EPS

Total EPS of *O. anthropi* DE2010 from all analyzed cultures were extracted using the physico-chemical method described by Adav and Lee (2008), with some modifications. For this analysis, 20 mL from each contaminated (0.5, 2, 5, 7, and 10 mM Cr(III)), and non-contaminated (control) culture were centrifuged at 2000xg for 10 min at 4 °C (Eppendorf 5804R refrigerated centrifuge), and pellets were resuspended in 10 mL of sterile double deionized water. Cellular suspensions were mixed with 60 μL of ultra-pure formamide (ThermoFisher Scientific, USA) and incubated on ice for 60 min. Then, 4 mL of 1N NaOH was added and the resulting mixtures were incubated for 40 min on ice, and afterward were subjected to ultrasound at 120 W for 5 min on ice in an ultrasonic bath (Sonorex, Bandelin). All sonicated suspensions were centrifuged at 10000xg for 20 min at 4 °C. The supernatants obtained were filtered, to avoid the presence of cells, through 0.22 μm pore size filters (Millipore, Merck Millipore) to collect the total EPS. Aliquots of 5 mL of each of the EPS extracts were stored at -20 °C until further analysis. Biochemical composition of each EPS extract was determined using various colorimetric methods as follows: total carbohydrate content with the phenol–sulphuric acid method (Dubois et al., 1956), using glucose (1 mg mL^{-1}, Merck) as standard; protein content by the Bradford method (Bradford, 1976), with bovine serum albumin (2 mg mL^{-1}, Pierce) as standard, and the uronic acids content by the *m*-hydroxyphenyl method (Kintner and Van Buren, 1982), using galacturonic acid (1 mg mL^{-1}, Fluka) as standard. The cell lysis caused by EPS extraction was evaluated by quantification of the DNA present in the extracts by the diphenylamine colorimetric method (Burton, 1956) using salmon sperm DNA (1 mg mL^{-1}, Sigma) as standard. Low content of DNA (1-1.2%) indicates that the EPS extracted are not contaminated by intracellular substances (Liu and Fang, 2002). A total of 15 replicates for each EPS extract were analyzed,

with the aid of a Beckman Coulter DU® 730 spectrophotometer (Beckman Coulter, Harbor Blvd., Fullerton CA, USA). All calculations were expressed in ppm (parts per million) corresponding to 1 microgram of EPS component (protein, total carbohydrates or uronic acid) per milliliter of total EPS extract (μg mL^{-1}).

On the other hand, the production of EPS was expressed as a percentage of the total concentration of EPS in relation to cell concentration.

2.5 Inductively Coupled Plasma Optical Emission Spectrometer (ICP-OES)

Cr (III) removal capacity of *O. anthropi* DE2010 was analyzed by ICP-OES and the specific metal removal (*q*), expressed as mg of chromium/g of dry weight, was calculated using the following formula (Chakravarty and Banerjee, 2012):

$$q = \frac{V(Ci - Cf)}{m}$$

where V is the sample volume (L); Ci and Cf are the initial and final metal concentrations (mg L^{-1}), and m is the dry culture biomass (g).

After 24 h, *O. anthropi* DE2010 cultures growing at each tested concentration were centrifuged at 2000x*g* for 10 min at 4 °C (Eppendorf 5804R refrigerated centrifuge). Samples from the resulting supernatants and liquid samples from the initial Cr(III) working concentrations (without microorganism) were analyzed by ICP-OES. Pellets were resuspended in 10 mL of sterile double deionized water and the corresponding EPS extracts were obtained using the same method as that described above (Adav and Lee, 2008). These extracts and samples from the same cellular suspensions but without EPS were also analyzed by ICP-OES, in order to detect the presence of chromium immobilized into the cells. Before chemical assays, all samples were digested with HNO$_3$ in a 600 W microwave digestion system to remove all organic matter. Chromium analysis at 267.716 nm was

carried out on the resultant digestions using an ICP-OES spectrometer Optima 4300DV (Perkin Elmer LLC, 761 Main Avenue, Norwalk, USA), in quadruplicate assays.

2.6 Energy dispersive X-ray spectroscopy (EDX) analysis coupled to Scanning transmission electron microscope (STEM) imaging

Metal sorption capability of *O. anthropi* DE2010 was confirmed by STEM EDX. Samples were prepared following the TEM-EDX protocol described by Maldonado et al. (2010). To this end, a sample from each 24 h culture contaminated with a Cr(III) working concentration was centrifuged at 4000x*g* for 5 min at 4 ºC (Eppendorf 5804R refrigerated centrifuge). The resulting pellets were included in soft agar and subsequently fixed in 2.5% glutaraldehyde diluted in Millonig phosphate buffer (Millonig, 1961) for 2 h and washed four times (15 min) in the same buffer. Then samples were post-fixed in 1% OsO_4 at 4 °C for 2 h and washed again in the same buffer. They were then dehydrated in a graded series of acetone (50, 70, 90, 95, and 100%), and embedded in Spurr's resin. Semi-fine sections (200 nm thick) were mounted on a titanium grid covered with a thin carbon layer without additional staining (lead citrate and uranyl acetate). High angle annular dark field scanning transmission electron microscopy (HAADF-STEM) images and STEM EDX profiles were acquired using a FEI Tecnai G2 F20 microscope operated at 200 kV and equipped with an EDAX super ultra-thin window (SUTW) X-ray detector (FEI, Hillsboro, Oregon, USA).

2.7 Data analysis

Statistical analysis was carried out by one-way analysis of variance (ANOVA) and Tukey multiple comparison *post-hoc* test. Significant differences in ANOVA and Tukey's test were accepted at $p \leq 0.05$. The analyses were performed using SPSS software (version 20.0 for Windows 7).

3. Results and discussion

In this study, several analytical methods were applied to batch cultures in order to evaluate the cytotoxic effect of Cr(III) on *O. anthropi* DE2010, and the capacity of this bacterium to remove it.

3.1 Changes in plate counts, cell viability and biomass

The changes in plate counts, growth curves, cell viability, and biomass in the presence of chromium are shown in Figure 1 (Log_{10} cfu mL^{-1} of total and cultivable cells, and growth curves), and Figure 2 (FLU–CLSM–IA imaging, live and dead cells%, mg C $(cm^3)^{-1}$, and DC%). The effect of Cr(III) on *O. anthropi* DE2010 varied significantly depending on the concentration, although is more evident at the highest metal concentrations. This is evidenced by a reduction in the number of cfu mL^{-1}, cell viability and biomass, and an increase in DC% and duplication time.

The maximum values of the four biological parameters were obtained at 0 mM Cr(III) ($9.26x10^9$ cfu mL^{-1} of cultivable cells, 4.02 h duplication time, 99.82% of live cells and 46.76 mg C $(cm^3)^{-1}$ of biomass) and the minimum were recovered out for 7 mM (<10 cfu mL^{-1} of cultivable cells, 21 h duplication time, 62.72% of live cells and 3.30 mg C $(cm^3)^{-1}$ of biomass) (Fig 1, and Fig 2). Statistically significant differences were obtained, ranging from 0 mM (control) to 7 mM Cr(III) for viability (F= 213.434) (p <0.05) and biomass (F= 212.253) (p <0.05) results. Using the Tukey multiple comparisons *post-hoc* test, statistically significant differences (p <0.05) were observed among all the metal concentrations tested for cell viability and biomass (Fig 2). On one hand, decreasing values from 0 mM to 7 mM Cr (III) corresponding to reductions in cfu mL^{-1} of 99.99%, cell viability of 37.1% and biomass of

92.94%, were also noted. On the other hand, results of cell viability and biomass at 10 mM Cr(III) could not be determined from FLU-CLSM images due to the formation of cellular aggregates (Fig 2), but a minimal cfu mL^{-1} value was achieved at this concentration (Fig 1). Comparing these results with those obtained by different phototrophic microorganisms, *Scenedesmus* sp. DE2009 and *Geitlerinema* sp. DE2011 (Millach et al., 2015) and *Chroococcus* sp. PCC 9106 (Puyen et al., 2017) and the yeast *Pichia stipitis* (Yilmazer and Saracoglu, 2008), it can be demonstrated that *O. anthropi* DE2010 shows a great tolerance and resistance to this metal at higher concentrations, even at 10 mM.

It is important to highlight that at 7 mM Cr(III) a high percentage of cells remain alive (FLU-CLSM-IA method) despite minimal viable cells being detected in plate counts. A possible explanation for this fact is the presence of dormant cells (DC) in cultures contaminated with Cr(III) that are unable to grow in plates. Lewis (2010) defined DC as a small sub-population of cells that spontaneously enter a dormant, non-dividing, and resistant state. In this paper, to study the role of DC, 24 h cultures of *O. anthropi* DE2010 grown at the different tested Cr(III) concentrations were also spread onto LB agar without metal (Fig 1A, cfu mL^{-1} of total cells). These results are shown in Figure 2. The number of DC increases as the metal concentration increases. Results were significant at 5 mM Cr(III), with a relative ratio of dormant cells of 96.68%. This can be seen even more clearly at 7 mM and 10 mM Cr(III), where the values were 99.98% and 99.89%, respectively.

3.2 Changes in the EPS composition and production

The results concerning the biochemical analysis of EPS extracts from *O. anthropi* DE2010 cultures grown with Cr(III) at different concentrations are shown in Table 1. Changes in the EPS composition were observed as a response to an increase in Cr(III) concentration.

At lower concentrations of Cr(III) (0-2 mM) the major EPS component is carbohydrates (88-89%), followed by proteins (5-7%) and uronic acids (3-5%). However, at 5 mM Cr(III) the most drastic metal effect was assessed. At this concentration, a considerable increase of 37.88% in proteins was observed in contrast to a significant reduction in 35.45% in carbohydrates, with as well as a slight decrease in uronic acid content. Guibaud et al. (2003) demonstrated that the protein played a major role in the complexation of metal ions and the number of binding sites (alcohol, carboxyl and amino groups) for heavy metals. This change in the EPS composition coincide with that described by Seng et al. (2005), who indicate that the content of extracellular proteins increased when bacteria were grown in adverse environmental conditions, and Yin et al. (2011), who report that the presence of heavy metals resulted in a higher production of proteins than total carbohydrates and uronic acids in the EPS. A decreasing value in carbohydrates and proteins content is observed from 7 mM Cr(III), reaching a similar value between both EPS components, although a slight increase was observed at 10 mM, as result of cell aggregation. Regarding the uronic acids content, in this study its role in *O. anthropi* DE2010 is less clear, although different authors have been demonstrated the active role of this EPS components in heavy metals chelation (Guibaud et al., 2005; Morillo Pérez et al., 2008; Pal and Paul, 2008). The results showed in Table 1 demonstrated that the concentration of uronic acid decreases from 0 to 5 mM and it is maintained at higher Cr(III) concentrations, especially at 7 mM, when the carbohydrates and proteins reach the lowest values. This data coincides with the formation of cellular aggregates, which probably indicates that under these conditions, uronic acid could contribute to chromium immobilization. Statistically significant differences were found among all the metal concentrations assayed for carbohydrates (F= 271.15) (p <0.05),

proteins (F= 471.14) (p <0.05), and uronic acids (F= 130.28) (p <0.05). Using the Tukey

multiple comparisons post-hoc test, statistically significant differences (p <0.05) were

labelled in Table 1.

As regards the EPS production, a maximum increase in EPS concentration in relation

to cell concentration (7.82%) was obtained from 0 mM (10.17%) to 5 mM (17.99%) Cr(III)

coinciding with the increment in the protein content. It is well known that the EPS generally

contains high molecular weight compounds with charged functional groups with adsorptive

and adhesive properties. These functional groups provide binding sites for heavy metals, as

demonstrated by Decho (1990) and more recently by other authors (More et al., 2014; Yue

et al., 2015). These results could explain the increase in total amount of EPS at high

concentrations of Cr(III) in *O. anthropi* DE2010.

As previously mentioned the most important cytotoxic effect of Cr(III) on *O. anthropi*

DE2010 is produced at 5 mM Cr(III). At this concentration, the percentage of dead cells

increases, provoking a drop in viability and biomass. This is linked to an enhancement in

the cellular synthesis of EPS by *O. anthropi* DE2010 to protect the cells themselves from

chromium toxicity, increasing, in turn, the protein content and reducing the amount of

carbohydrate and uronic acids.

3.3 Removal capacity for Cr(III) of *O. anthropi* DE2010

Quantitative chemical data for the ability of *O. anthropi* DE2010 cells to capture

Cr(III) and the corresponding cellular uptake efficiency (q) are shown in Table 2. These

results indicate that there is a strong correlation between the initial concentration of metal

and the total of chromium taken from the cells, reaching maximum values of removal of

40.83% at 7 mM and of 38.38% at 10 mM Cr(III). In addition, practically all the chromium

removed was detected inside the cells (cytoplasm), with values ranging between 97% and 99%, depending on the metal concentration, with the rest of the metal being found in the EPS extracts (1-3%). These results indicate that *O. anthropi* DE2010 is able to immobilize chromium in both the EPS and the cytoplasm of the cells. The q values also increase by increasing the initial metal concentration, and a maximum value of 950 mg g^{-1} was reached at 10 mM Cr(III). However, the most notable increase in q values (590 mg g^{-1}) was observed from 5 mM to 7 mM Cr(III). The highest q value reported here could be related to the cellular aggregation monitored by CLSM imaging at 10 mM. This cellular organization is more efficient to capture Cr(III) and to protect the cells from the cytotoxic effect of the metal than the individual cells observed at the other metal concentrations. Statistically significant differences for q values (F= 1,596.45) (p <0.05) were found among all the metal concentrations assayed. Using the Tukey multiple comparisons *post-hoc* test, statistically significant differences (p <0.05) were observed from 5 mM Cr(III) and were included in Table 2. The specific removal efficiency (q) of *O. anthropi* DE2010 is higher with respect to those obtained by other prokaryotic: 120 mg g^{-1} in *Sphaerotilus natans* (Solisio et al., 2000), 185 mg g^{-1} in *Spirullina* sp. (Chojnacka et al., 2005), and 14.28 mg g^{-1} in *Rhodococcus opacus* (Calfa et al., 2008); and eukaryotic microorganisms: 11.30 mg g^{-1} in *Saccharomyces cerevisiae* (Ksheminska et al., 2005), and 41.18 mg g^{-1} in *Chlorella miniata* (Han et al., 2006). For this reason, it can be considered that *O. anthropi* DE2010 show a higher capacity to sequestrate chromium into the cells than other microorganisms and is, therefore, a great candidate to bioremediate natural/artificial environments polluted with chromium.

3.4 Cr(III) localization at cellular structure level

Electron microscopy imaging, SEM and TEM, have become a crucial tool to visualize the ultrastructure of microorganisms (Rachel et al., 2010; Golding et al., 2016; Solé et al., 2019) and coupled to an EDX detector to analyze the elemental composition and its distribution in the samples (Maldonado et al., 2011, Burgos et al., 2013; Coreño-Alonso et al., 2014; Millach et al., 2015; Povedano-Priego et al., 2017). Although, these techniques have been very useful in this regard, we applied for the first time the HAADF-STEM EDX for locating, at the nanoscale level, heavy metals immobilized on different cellular structures (Fig 3) evidencing whether specific microorganisms have a capacity to immobilize them inside and/or outside cells in the same semi-fine section.

HAADF-STEM images exhibited discernible changes (changes in cell morphology, an increase in bright inclusions, and the appearance of cellular pleomorphic forms) in cells (Fig 3 A1, B1, and C1) due to the Cr (III), mainly at the highest concentration (10 mM Cr(III)). EDX microanalyses shows that chromium was not detectable, either externally or internally, in control samples (0 mM) and up to 2 mM Cr(III). However, results obtained from 5 mM to 10 mM indicated that the chromium signal was detected in the cellular structure. Figures 3 A2, B2, and C2 show the STEM EDX chromium and phosphorous composition line profiles that were taken along a bright inclusion from a semi-fine section micrograph of *O. anthropi* DE2010 grown at 0, 5, and 10 mM Cr(III). When compared the image intensity profile, with an increased signal in the bright inclusion, it is clear that the most part of chromium was located in the bright inclusions, together with an important phosphorous signal, and secondarily on the cellular surface at the EPS level.

It is known that microorganisms play an important role in heavy metal immobilization processes (Cheng et al., 2010) either at extra-cellular (biosorption) and/or

intra-cellular (bioaccumulation) levels (Guibaud et al., 2005; Guine et al., 2006; Kothe et al., 2010; Puyen et al., 2012b; Esteve et al., 2013; Burgos et al., 2013; Gutiérrez-Corona et al., 2016). On the other hand, Velásquez and Dussan, (2009) demonstrated the relation between external capture and passive process (live or dead cells) and internal bioaccumulation and active process (live cells).

The present STEM EDX results demonstrate that *O. anthropi* DE2010 accumulates Cr(III) externally in EPS, and internally mainly in cytoplasmic polyphosphate inclusions. Therefore, the chromium removal via sorption and accumulation mechanisms in this bacterium was demonstrated using STEM EDX.

Conclusions

Our results indicate that *O. anthropi* DE2010 is able to (i) tolerate and resist the presence of high Cr(III) concentrations, showing changes in production and EPS composition and increasing the number of dormant cells, (ii) capture chromium at higher removal efficiencies, and (iii) immobilize it mainly inside the cell in polyphosphate inclusions (bioaccumulation process), as well as externally in the EPS (biosorption process).

As a future perspective, *O. anthropi* DE2010 could be considered as a potential agent for bioremediation in Cr(III) contaminated environments since it shows a great ability to tolerate and efficiently remove Cr(III) from polluted cultures.

Acknowledgments

Fig 1. Growth parameters of *O. anthropi* DE2010 growing at different Cr(III) concentrations. (A) Plate counts (cfu mL-1) from total (grown on LB agar without Cr(III)) and cultivable cells (grown on LB agar with Cr(III)). $p < 0.01$**: 0.5, 2, 5, 7, and 10 mM treatments vs. control (0 mM). (B) Growth curves at different Cr(III) working concentrations. In both graphics, data are expressed as mean ±SD (n= 8).
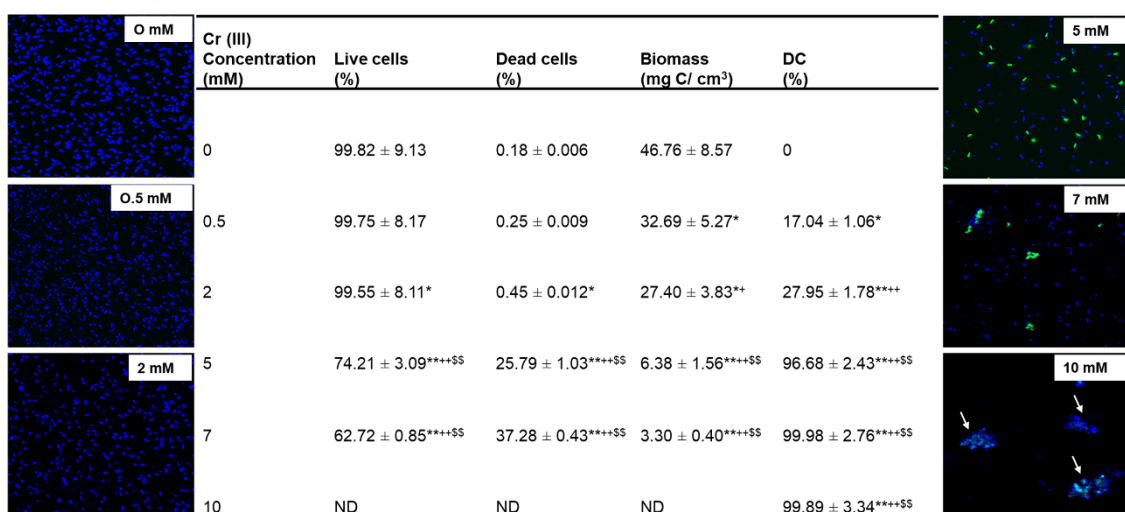
Cr (III) Concentration (mM)	Live cells (%)	Dead cells (%)	Biomass (mg C/ cm³)	DC (%)
0	99.82 ± 9.13	0.18 ± 0.006	46.76 ± 8.57	0
0.5	99.75 ± 8.17	0.25 ± 0.009	32.69 ± 5.27*	17.04 ± 1.06*
2	99.55 ± 8.11*	0.45 ± 0.012*	27.40 ± 3.83*+	27.95 ± 1.78**++
5	74.21 ± 3.09**++$$	25.79 ± 1.03**++$$	6.38 ± 1.56**++$$	96.68 ± 2.43**++$$
7	62.72 ± 0.85**++$$	37.28 ± 0.43**++$$	3.30 ± 0.40**++$$	99.98 ± 2.76**++$$
10	ND	ND	ND	99.89 ± 3.34**++$$

Fig 2. Cytotoxic effect of Cr(III) in the *O. anthropi* DE2010 cultures. *$p < 0.05$, **$p < 0.01$: 0.5, 2, 5, and 7 mM treatments vs. control (0 mM). $^+p < 0.05$, $^{++}p < 0.01$: 2, 5, and 7 mM treatments vs. 0.5 mM treatment. $^{$$}p < 0.01$: 5, and 7 mM treatments vs. 2 mM treatment. Data are expressed as mean ±SD (n= 20).

Fig 3. HAADF STEM analysis of *O. anthropi* DE2010 cells grown at 0 (A), 5 (B), and 10 mM (C) of Cr(III). (A1, B1, and C1) HAADF STEM imaging, and (A2, B2, and C2) HAADF STEM-EDX analysis and line profiles (250 nm) along the black line showing the intensity of the HAADF image (top), phosphorus (middle) and chromium (bottom).

Table 1 Variations in the production and composition of the EPS of *Ochrobactrum anthropi* DE2010 due to the effect of Cr(III)

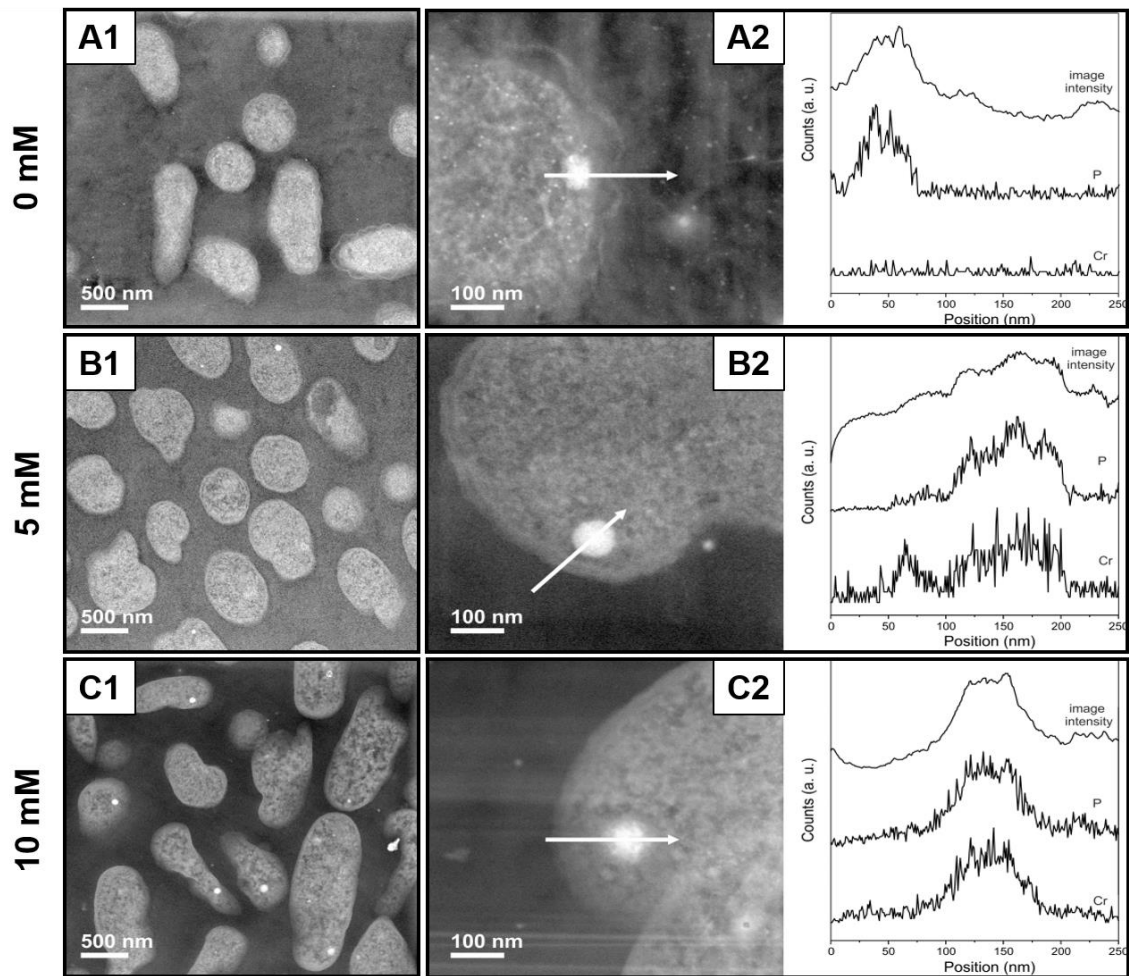| Cr(III) concentration (mM)	[DNA] (ppm)	[Carbohydrates] (ppm)	[Proteins] (ppm)	[Uronic acids] (ppm)	[Cell concentration] (ppm)	EPS concentration vs. cell number (%)
0	0.28 ± 0.02	148.12 ± 4.94	9.98 ± 0.71	8.40 ± 0.71	1640 ± 8.84	10.17 ± 0.34
0.5	0.58 ± 0.02**	150.50 ± 2.09	11.95 ± 0.52	6.30 ± 0.34**	1580 ± 15.21	10.85 ± 0.16
2	0.91 ± 0.02**[++]	133.28 ± 5.44	11.89 ± 0.88	6.02 ± 0.20**	1505 ± 15.55**	10.11 ± 0.41
5	1.20 ± 0.02**[++$$]	45.36 ± 0.95**[++$$]	39.37 ± 0.44**[++]	1.35 ± 0.16**[++$$]	485 ± 24.39**[++$$]	17.99 ± 0.38**[++$$]
7	0.87 ± 0.03[a]**[++&&]	12.46 ± 0.15**[++$$&&]	10.72 ± 1.16[&&]	0.97 ± 0.07**[++$$&&]	255 ± 4.61**[++$$&&]	9.81 ± 0.12[+&&]
10	1.27 ± 0.03[a]**[++$$^^]	17.36 ± 0.24**[++$$&&]	12.47 ± 4.36*[&&]	1.37 ± 0.26**[++$$^^]	220 ± 4.73**[++$$&&]	14.76 ± 0.21**[++$$&&^^]

[a] values out of range indicating cell lysis due to Cr(III)

Data are expressed as mean ±SD (n= 15)

*p <0.05; **p <0.01: 0.5, 2, 5, 7 and 10 mM treatments vs. control (0 mM)

[+]p <0.05; [++]p <0.01: 2, 5, 7, and 10 mM treatments vs. 0.5 mM treatment

[$$]p <0.01: 5, 7, and 10 mM treatments vs. 2 mM treatment

[&&]p <0.01: 7, and 10 mM treatments vs. 5 mM treatment

[^^]p <0.01: 7 treatment mM vs. 10 mM treatment

Table 2 Removal Cr(III) capacity by *Ochrobactrum anthropi* DE2010 in the EPS and cytoplasm

Cr(III) concentration (mM)	Culture Medium (C_i) (mg L^{-1})	Supernatant (C_f) (mg L^{-1})	Total metal removed (mg L^{-1})	Metal in EPS (mg L^{-1})	Metal in cells without EPS (mg L^{-1})	Dry weight (m) (g)	q (mg g^{-1})
0	0	0	0	0	0	0.033 ± 0.005	0
0.5	24 ± 1.15	16.50 ± 0.57	7.50 ± 1.73	0.20 ± 0.006	7.30 ± 1.71	0.031 ± 0.003	4.84 ± 0.37
2	99 ± 2.30	83.50 ± 1.73	15.50 ± 4.04	0.21 ± 0.010	15.29 ± 4.03	0.030 ± 0.004	10.33 ± 1.15*
5	257 ± 2.31	199 ± 3.46	58 ± 1.15	0.52 ± 0.015	57.48 ± 1.14	0.010 ± 0.002	116.00 ± 11.54**[++&&]
7	360 ± 3.46	212.50 ± 2.89	147.50 ± 0.58	1.85 ± 0.045	145.15 ± 0.54	0.005 ± 0.001	590.00 ± 11.55**[++&&$$]
10	495 ± 9.24	305 ± 8.08	190 ± 8.99	5.10 ± 0.095	184.90 ± 0.90	0.004 ± 0.001	950.00 ± 46.19**[++&&$$^^]

Data are expressed as mean ±SD (n= 4)

*p <0.05, **p <0.01: 0.5, 2, 5, 7 and 10 mM treatments vs. control (0 mM)

[++]p <0.01: 2, 5, 7, and 10 mM treatments vs. 0.5 mM treatment

[$$]p <0.01: 5, 7, and 10 mM treatments vs. 2 mM treatment

[&&]p <0.01: 7, and 10 mM treatments vs. 5 mM treatment

[^^]p <0.01: 7 treatment mM vs. 10 mM treatment

References:

Adav, S.S., Lee, D.J., 2008. Extraction of extracellular polymeric substances from aerobic granule with compact interior structure. J. Hazard. Mater. 154 (1-3), 1120-1126. https://doi.org/10.1016/j.jhazmat.2007.11.058.

Balk, E.M., Tatsioni, A., Lichtenstein, A.H., Lau, J., Pittas, A.G., 2007. Effect of chromium supplementation on glucose metabolism and lipids: a systematic review of randomized controlled trials. Diabetes Care 30 (8), 2154–2163. https://doi.org/10.2337/dc06-0996.

Bhattacharya, A., Dey, P., Gola, D., Mishra, A., Malik, A., Patel, N., 2015. Assessment of Yamuna and associated drains used for irrigation in rural and peri-urban settings of Delhi NCR. Environ. Monit. Assess. 187, 4146. https://doi.org/10.1007/s10661-014-4146-2.

Bradford, M., 1976. A rapid and sensitive method for the quantification of microgram quantities of protein utilizing the principle of protein– dye binding. Anal. Biochem. 72, 248–254. https://doi.org/10.1016/0003-2697(76)90527-3.

Burgos, A., Maldonado, J., De los Rios, A., Solé, A., Esteve, I., 2013. Effect of copper and lead on two consortia of phototrophic microorganisms and their capacity to sequester metals. Aquat. Toxicol. 140–141, 324–336. https://doi.org/10.1016/j.aquatox.2013.06.022.

Burton, K., 1956. A study of the conditions and mechanism of the diphenylamine reaction for the colorimetric estimation of deoxyribonucleic acid. Bioch. 62, 315-323.

Calfa, BA., Torem, ML., 2008. On the fundamentals of Cr(III) removal from liquid streams by a bacterial strain. Miner. Eng. 21 (1), 48-54. https://doi.org/10.1016/j.mineng.2007.08.001.

Chakravarty, R., Banerjee, P.C., 2012. Mechanism of cadmium binding on the cell wall of an acidophilic bacterium. Bioresour.Technol.108, 176-183. https://doi.org/10.1016/j.biortech.2011.12.100.

Cheng, Y., Yan, F., Huang, F., Chu, W., Pan, D., Chen, Z., Zheng, J., Yu, M., Lin Z., Wu, Z., 2010. Bioremediation of Cr (VI) and immobilization as Cr (III) by *Ochrobactrum anthropi.* Environ. Sci. Technol. 44 (16), 6357–6363. https://doi.org/10.1021/es100198v.

Chojnacka, K., Chojnacki, A., Górecka, H., 2005. Biosorption of Cr^{3+}, Cd^{2+} and Cu^{2+} ions by blue–green algae *Spirulina* sp.: kinetics, equilibrium and the mechanism of the process. Chemosphere 59 (1), 75-84. https://doi.org/10.1016/j.chemosphere.2004.10.005.

Coreño-Alonso, A., Solé, A., Diestra, E., Esteve, I., Gutiérrez-Corona, J.F., Reyna López, G.E., Fernández, F.J., Tomasini, A., 2014. Mechanisms of interaction of chromium with *Aspergillus niger* var tubingensis strain Ed8. Bioresour. Technol. 158, 188–192. https://doi.org/10.1016/j.biortech.2014.02.036.

Decho, A.W., 1990. Microbial exopolymer secretions in ocean environments: Their role(s) in food webs and marine processes. Oceanogr. Mar. Biol. Annu. Rev. 28 (7), 73-153. https://doi.org/10.1016/j.carbpol.2018.04.126.

Dubois, M., Gilles, K.A., Hamilton, J.K., Rebers, P.A., Smith, F., 1956. Colorimetric method for determination of sugars and related substances. Anal. Chem. 28 (3), 350-356.

Esteve, I., Maldonado, J., Burgos, A., Diestra, E., Burnat, M., Solé, A., 2013. Confocal laser scanning and electron microscopic techniques as powerful tools for determining the in vivo effect and sequestration capacity of lead in cyanobacteria. Cyanobacteria: Ecology, Toxicology and Management.

Evert, A.B., Boucher, J.L.B., Cypress, M., Dunbar, S.A., Franz, M.J., Mayer-Davis, E.J., Neumiller, J.J., Nwankwo, R., Verdi, C.L., Urbanski, P., Yancy, W.S., 2013. Nutrition therapy recommendations for the management of adults with diabetes. Diabetes Care 36 (11), 3821-3842. http://doi.org/10.2337/dc13-2042.

Feng, S., Mai, B., Wei, G., Wang, X., 2012. Genotoxicity of the sediments collected from Pearl River in China and their polycyclic aromatic hydrocarbons (PAHs) and heavy metals. Environ. Monit. Assess. 184, 5651–5661. http://doi.org/10.1007/s10661-011-2369-z.

Figgitt, M., Newson, R., Leslie, I.J., Fisher, J., Ingham, E., Case, C.P., 2010. The genotoxicity of physiological concentrations of chromium (Cr(III) and Cr(VI)) and cobalt (Co(II)): An in vitro study. Mutat. Res. 688, 53–61. http://doi.org/10.1016/j.mrfmmm.2010.03.008.

Francisco, R., de Abreu, P., Plantz, B.A., Schlegel, V.L., Carvalho, R.A., Vasconcelos-Morais, P., 2011. Metal-induced phosphate extracellular nanoparticulate formation in *Ochrobactrum tritici* 5bvl1. J. Hazard. Mater. 198, 31-39. https://doi.org/10.1016/j.jhazmat.2011.10.005.

Golding, C.G., Lamboo, L.L., Beniac, D.R., Booth, T.F., 2016. The scanning electron microscope in microbiology and diagnosis of infectious disease. Sci. Rep. 6, 26516. https://doi.org/10.1038/srep26516

Greenwood, N.N., Earnshaw, A., 1997. Chemistry of the elements, 2nd ed. Butterworth–Heinemann, Oxford.

Guibaud, G., Tixier, N., Bouju, A., Baudu, M., 2003. Relation between extracellular polymers' composition and its ability to complex Cd, Cu and Pb. Chemosphere 52(10),1701-1710. https://doi.org/10.1016/S0045-6535(03)00355-2.

Guibaud, G., Comte, S., Bordas, F., Dupuy, S., Baudu, M., 2005. Comparison of the complexation potential of extracellular polymeric substances (EPS), extracted from activated sludges and produced by pure bacteria strains, for cadmium, lead and nickel. Chemosphere 59 (5), 629-638. http://doi.org/10.1016/j.chemosphere.2004.10.028.

Guiné, V., Spadini, L., Sarret, G., Muris, M., Delolme, C., Gaudet, J.P., Martins, J.M.F., 2006. Zinc sorption to three gram-negative bacteria: combined titration, modeling, and EXAFS study. Environ. Sci. Technol. 40 (6),1806–1813. https://doi.org/10.1021/es050981l.

Gupta, S.K., Chabukdhara, M., Kumar, P., Singh, J., Bux, F., 2014. Evaluation of ecological risk of metal contamination in river Gomti, India: a biomonitoring approach. Ecotoxicol. Environ. Saf. 110, 49–55. http://doi.org/10.1016/j.ecoenv.2014.08.008.

Gutiérrez-Corona, J.F., Romo-Rodríguez, P., Santos-Escobar, F., Espino-Saldaña, A.E., Hernández-Escoto, H., 2016. Microbial interactions with chromium: basic biological processes and applications in environmental biotechnology. World. J. Microbiol. Biotechnol. 32 (12), 191. https://doi.org/10.1007/s11274-016-2150-0.

Han, X., Wong, YS., Tam, NFY., 2006. Surface complexation mechanism and modeling in Cr(III) biosorption by a microalgal isolate, *Chlorella miniate*. J. Colloid Interface Sci. 303 (2), 365-371. https://doi.org/10.1016/j.jcis.2006.08.028.

Ihsanullah, Abbas, A., Al-Amer, A.M., Laoui, T., Al-Marri, M.J., Nasser, M.S., Khraisheh, M., Atieh, M.A., 2016. Heavy metal removal from aqueous solution by advanced carbon nanotubes: Critical review of adsorption applications. Sep. Purif. Technol. 157 (8), 141-161. https://doi.org/10.1016/j.seppur.2015.11.039.

Kimbrough, D.E., Cohen, Y., Winer, A.M., Creelman, L., Mabuni, C., 1999. A Critical assessment of chromium in the environment. Crit. Rev. Environ. Sci. Technol. 29 (1), 1-46. https://doi.org/10.1080/10643389991259164.

Kintner, P.K., van Buren, J.P.,1982. Carbohydrate Interference and Its Correction in pectin analysis using the *m*-Hydroxydiphenyl method. J. Food Sci. 47, 756-759. https://doi.org/10.1111/j.1365-2621.1982.tb12708.x.

Kothe, E., Dimkpa, C., Haferburg, G., Schmidt, A., Schmidt, A., Schütze, E., 2010. Streptomycete heavy metal resistance: extracellular and intracellular mechanisms, in: Sherameti, I., Varma, A., (Eds.). Soil Heavy Metals, Soil Biology. https://doi.org/10.1007/978-3-642-02436-8_10.

Ksheminska, H., Fedorovych, D., Babyak, L., Yanovych, D., Kaszycki, P., Koloczek, H., 2005. Chromium (III) and (VI) tolerance and bioaccumulation in yeast: A survey of cellular chromium content in selected strains of representative genera. Process Biochemistry. 40, 1565-1572. https://doi.org/10.1016/j.procbio.2004.05.012.

Kusiak, R.A., Ritchie, A.C., Springer, J., Muller, J., 1993. Mortality from stomach cancer in Ontario miners. Br. J. Med. 50,117–126.

Lewis K., 2010. Persister Cells. Annu. Rev. Microbiol. 64, 357–372.

Liu, H., Fang, H.P.H., 2002. Extraction of extracellular polymeric substances (EPS) of sludges. J. Biotechnol. 95 (3), 249-256. https://doi.org/10.1016/S0168-1656(02)00025-1.

Maldonado, J., Diestra, E., Domènech, A.M., Villagrasa, E., Puyen, Z.M, Esteve, I., Solé, A., 2010. Isolation and identification of a bacterium with high tolerance to lead and copper from a marine microbial mat in Spain. Ann. Microbiol. 60 (1), 113-120. https://doi.org/10.1007/s13213-010-0019-2.

Maldonado, J., Solé, A., Puyen, Z.M., Esteve, I., 2011. Selection of bioindicators to detect lead pollution in Ebro delta microbial mats, using high-resolution microscopic techniques. Aquat.Toxicol.104, 135–144. http://doi.org/10.1016/j.aquatox.2011.04.009.

Manahan, S.E., 2009. Environmental chemistry, 9th edition. Boca Raton: CRC Press, Florida.

Millach, L., Solé, A., Esteve, I., 2015. Role of *Geitlerinema* sp. DE2011 and *Scenedesmus* sp. DE2009 as bioindicators and immobilizers of chromium in a contaminated natural environment. BioMed Research International, Article ID 519769. https://doi.org/10.1155/2015/519769.

Millonig, G.,1961. A modified procedure for lead staining of thin sections. J Biophys. Biochem. Cytol. 11 (3), 736–739.

Mohana, D., Pittman, C.U., 2006. Activated carbons and low cost adsorbents for remediation of tri- and hexavalent chromium from water. J. Hazard. Mater. 137 (2), 762-811. https://doi.org/10.1016/j.jhazmat.2006.06.060.

More, T.T., Yadav, J.S.S., Yan, S., Tyagi, R.D., Surampalli. R.Y., 2014. Extracellular polymeric substances of bacteria and their potential environmental Applications. J. Environ. Manage. 144, 1-25. https://doi.org/10.1016/j.jenvman.2014.05.010.

Morillo Pérez, J.A., García-Ribera, R., Quesada, T., Aguilera, M., Ramos-Cormenzana, A., Monteoliva-Sánchez M., 2008. Biosorption of heavy metals by the exopolysaccharide produced by *Paenibacillus jamilae*. World J. Microbiol. Biotechnol. 24, 2699. https://doi.org/10.1007/s11274-008-9800-9.

Nziguheba, G., Smolders, E., 2008. Inputs of trace elements in agricultural soils via phosphate fertilizers in European countries. Sci. Total. Environ. 390 (1), 53-57. https://doi.org/10.1016/j.scitotenv.2007.09.031.

Pal, A. and Paul, A.K., 2008. Microbial extracellular polymeric substances: central elements in heavy metal bioremediation. Indian J. Microbiol. 48, 49-64.

Povedano-Priego, C., Martín-Sánchez, I., Jroundi, F., Sánchez-Castro, I., Merroun, M.L., 2017. Fungal biomineralization of lead phosphates on the surface of lead metal. Miner. Eng. 106, 46–54. https://doi.org/10.1016/j.mineng.2016.11.007.

Puyen, Z.M., Villagrasa, E., Maldonado, J., Esteve, I., Solé, A., 2012a. Viability and biomass of *Micrococcus luteus* DE2008 at different salinity concentrations determined by specific fluorochromes and CLSM-image analysis. Curr. Microbiol. 64 (1), 75-80. https://doi.org/10.1007/s00284-011-0033-z.

Puyen, Z.M., Villagrasa, E., Maldonado, J., Diestra, E., Esteve, I., Solé, A., 2012b. Biosorption of lead and copper by heavy-metal tolerant *Micrococcus luteus* DE2008. Bioresour. Technol. 126, 233–237. https://doi.org/10.1016/j.biortech.2012.09.036.

Puyen, Z. M., Villagrasa, E., Millach, L., Esteve, I., Maldonado, J., Solé, A., 2017. Multi-approach microscopy techniques to evaluate the cytotoxic effect of chromium(III) on the cyanobacterium *Chroococcus* sp. PCC 9106. in: Menendez-Vilas, A. (Ed). Microscopy and imaging science: practical approaches to applied research and education. Formatex Research Center, Badajoz, pp. 602-609.

Rachel, R., Meyer, C., Klingl, A., Gürster, S., Heimerl, T., Wasserburger, N., Burghardt, T., Küper, U., Bellack, A., Schopf, S., Wirth, R., Huber, H., Wanner G., 2010. Chapter 3 - Analysis of the Ultrastructure of Archaea by Electron Microscopy, Editor(s): Thomas Müller-Reichert.

Methods in Cell Biology. Academic Press. Vol(96), pages: 47-69. https://doi.org/10.1016/S0091-679X(10)96003-2.

Sachidanandham, R., Yew-Hoong Gin, K., 2009. A dormancy state in nonspore-forming bacteria. Appl. Microbiol. Biotechnol. 81, 927. https://doi.org/10.1007/s00253-008-1712-y.

Schneider, C.A., Rasband, W.S., Eliceiri, K.W., 2012. NIH Image to ImageJ: 25 years of Image Analysis. Nat. Methods 9 (7), 671–675.

Shanker, A.K., Cervantes, C., Loza-Tavera, H., Avudainayagam, S., 2005. Chromium toxicity in plants. Environ. Int. 31 (5), 739-753. https://doi.org/10.1016/j.envint.2005.02.003.

Sheng, G.P., Yu, H.Q., Yue, Z.B., 2005. Production of extracellular polymeric substances from *Rhodopseudomonas acidophila* in the presence of toxic substances. Appl. Microbiol. Biotechnol. 69 (2), 216-222. https://doi.org/10.1007/s00253-005-1990-6.

Sole, A., Calvo, M.A., Lora, M.J., Sánchez-Chardi, A., 2019. Chapter 12 - Electron microscopy techniques applied to bioremediation and biodeterioration studies with molds. Editor(s): Araceli Tomasini Campocosio and Hector Hugo Leon Santiesteban. Fungal bioremediation: fundamentals and applications. CRC press. pages: 354. https://doi.org/10.1201/9781315205984.

Solisio, C., Lodi, A., Converti, A., Del Borghi, M., 2000.The effect of acid pre-treatment on the biosorption of chromium(III) by *Sphaerotilus natans* from industrial wastewater. Water Res. 34 (12), 3171-3178. https://doi.org/10.1016/S0043-1354(00)00059-2.

Srivastava, S., Thakur, I.S., 2007. Evaluation of biosorption potency of *Acinetobacter* sp. for removal of hexavalent chromium from tannery effluent. Biodegradation 18 (5), 637–646. https://doi.org/10.1007/s10532-006-9096-0.

Suwalsky, M., Castro, R., Villena, F., Sotomayor, C.P., 2008. Cr(III) exerts stronger structural effects than Cr(VI) on the human erythrocyte membrane and molecular models. J. Inorg. Biochem. 102, 842–849. https://doi.org/10.1016/j.jinorgbio.2007.11.020.

Velásquez, L., Dussan, J., 2009. Biosorption and bioaccumulation of heavy metals on dead and living biomass of *Bacillus sphaericus*. J. Hazard. Mater. 167 (1-3), 713–6. https://doi.org/10.1016/j.jhazmat.2009.01.044.

Villagrasa, E., Ferrer-Miralles, N., Millach, L., Obiol, A., Creus, J., Esteve, I., Solé, A., 2019. Morphological responses to nitrogen stress deficiency of a new heterotrophic isolated strain of Ebro Delta microbial mats. Protoplasma. 256 (1), 105-116. https://doi.org/10.1007/s00709-018-1263-8.

Xu, X., Zhao, Y., Zhao, X., Wang, Y., Deng, W., 2014. Sources of heavy metal pollution in agricultural soils of a rapidly industrializing area in the Yangtze Delta of China. Ecotoxicol. Environ. Saf. 108, 161–167. https://doi.org/10.1016/j.ecoenv.2014.07.001.

Yilmazer, P., Saracoglu, N., 2009. Bioaccumulation and biosorption of copper(II) and chromium(III) from aqueous solutions by *Pichia stipitis* yeast. J. Chem. Technol. Biotechnol. 84, 604–610. https://doi.org/10.1002/jctb.2088.

Yin, Y., Hu, Y., Xiong, F., 2011. Sorption of Cu (II) and Cd (II) by extracellular polymeric substances (EPS) from *Aspergillus fumigates*. Int. Biodeterior. Biodegrad., 65, 1012-1018. https://doi.org/10.1016/j.ibiod.2011.08.001.

Yue, Z.B., Li, Q., Li, C.C., Chen, T.H., Wang, J., 2015. Component analysis and heavy metal adsorption ability of extracellular polymeric substances (EPS) from sulfate reducing bacteria. Bioresour. Technol. 194, 399-402. https://doi.org/10.1016/j.biortech.2015.07.042.

Complete bibliographical reference of article from 2.2 thesis section:

Villagrasa, E., Ballesteros, B., Obiol, A., Millach, L., Esteve, I., Solé, A. 2020. Multi-approach analysis to assess the chromium(III) immobilization by *Ochrobactrum anthropi* DE2010. Chemosphere 238:124663. https://doi.org/10.1016/j.chemosphere.2019.124663

Section 2.3 Genomic and biotechnological insights on stress-linked polyphosphate production induced by chromium(III) in *Ochrobactrum anthropi* DE2010

Genomic and biotechnological insights on stress-linked polyphosphate production induced by chromium(III) in *Ochrobactrum anthropi* DE2010

Eduard Villagrasa[1], Raquel Egea[2], Neus Ferrer-Miralles[1,3,4] and Antonio Solé[1*]

[1] *Departament de Genètica i Microbiologia. Facultat de Biociències. Universitat Autònoma de Barcelona. Bellaterra, Cerdanyola del Vallès, 08193 Barcelona, Spain.*

[2] *Servei de Genòmica i Bioinformàtica. Institut de Biotecnologia i de Biomedicina -Parc de Recerca UAB - Mòdul B. Universitat Autònoma de Barcelona. Bellaterra, Cerdanyola del Vallès, 08193 Barcelona, Spain.*

[3] *Institut de Biotecnologia i de Biomedicina. Universitat Autònoma de Barcelona. Bellaterra, Cerdanyola del Vallès, 08193 Barcelona, Spain.*

[4] *CIBER de Bioingeniería, Biomateriales y Nanomedicina (CIBER-BBN), Bellaterra, Cerdanyola del Vallès, 08193 Barcelona, Spain*

Abstract

The resistance of microorganisms to heavy metals in polluted environments is mediated by genetically determined mechanisms. One such mechanism includes the intracellular sequestration of heavy metals in polyphosphate (polyP) inclusions. In Cr(III) contaminated mediums, *Ochrobactrum anthropi* DE2010 is able to bind and sequester Cr(III) in polyP inclusions. In order to further study the relationship between Cr(III) tolerance and polyP production in *O. anthropi* DE2010, we carried out whole genomic sequencing, analysis of single nucleotide polymorphisms (SNPs), polyP chemical quantification, and determination of the relative abundance and morphometry of polyP inclusions. In the *O. anthropi* DE2010 genome, six polyP and pyrophosphate (PPi) metabolic genes were found. Furthermore, genomic analysis via SNPs calling revealed that *O. anthropi* ATCC49188 and DE2010 strains had average variations of 1.51% in their whole genome sequences and 1.35% variation associated with the principal polyP metabolic gene cluster. In addition, the

accumulation of polyP in the DE2010 strain and number of polyP inclusions found were directly correlated with the concentration of Cr(III) in contaminated cultures. The results presented in this study may enhance the understanding of polyP production in response to Cr(III) toxicity in the *O. anthropi* DE2010 strain. This knowledge may facilitate the successful removal of Cr(III) from the natural environment.

Keywords: chromium(III); cytoplasmic inclusions; genome sequencing; *Ochrobactrum anthropi* DE2010; polyphosphate production

1. Introduction

Chromium occurs in nature in bound forms in the earth's crust (Jacobs and Testa, 2005). Although it exists in several oxidation states, the most common and stable forms are the Cr(0), trivalent Cr(III), and hexavalent Cr(VI) species (Oliveira 2012). Human activities have harmed the natural environment, leading to large increases in the levels of toxic metals (e.g., - 108 -embrana in Ali et al. 2013; Masindi and Muedi, 2018). Cr(III) is found in air, soil, and - 108 -embr after being released from industries that use chromium. This metal is also released into the environment from the burning of natural gas, oil, or coal (Wilbur et al. 2012). The permanence of its soluble forms that act as long term pollutants poses a serious threat, since they can be reoxidised to Cr(VI), which is carcinogenic (Chourey et al. 2006). For this reason, it is relevant to study the immobilisation of Cr(III) (Cheng et al. 2010; Millach et al. 2015). Cr(III) is considered - 108 -em toxic - 108 -em Cr(VI), but it can cause DNA damage and topoisomerase inhibition. Besides, it is involved in some human and animal diseases with respiratory, reproductive, immunological, and development effects (Wilbur et al. 2012; Fatima and Rao, 2018). Moreover, this metal has antibacterial and antifungal due

to its oxidative damage-causing and biotoxic functions (Plaper et al. 2002; Paez et al. 2013). Microbial cells have adapted to the presence of heavy metal ions in their - 109 -embran by displaying specific resistance mechanisms. These mechanisms include cell - 109 -embran bioabsorption, bioaccumulation outside or inside the cell, and biotransformation to - 109 -em toxic forms (Chojnacka 2010; Hansda et al. 2016). One of the strategies to bioaccumulate heavy metals inside the cells involves capturing them within the - 109 -embranas- 109 -ar inclusions of polyphosphate (polyP) (Kulakovskaya, 2018a).

In a previous study, our research group isolated a strain from the Ebro Delta microbial mats (Tarragona, Spain), which was identified as *Ochrobactrum anthropi* DE2010 using the genotypic and phenotypic techniques (Villagrasa et al. 2019). *O. anthropi* DE2010 is a - 109 -emb-negative, non-spore, rod shaped, marine, heterotrophic bacterium. In addition, *O. anthropi* DE2010 immobilises Cr(III) in cytoplasmic inclusions of polyP (Villagrasa et al. 2020). Under conditions of nutrient starvation and stress, such as the presence of heavy metals, some microorganisms can accumulate polyP via gene-regulated mechanisms (Baxter and Jensen, 1980; Jensen et al. 1986; Kuroda et al. 2001; Narancic et al. 2012; Burgos et al. 2013; Millach et al. 2015). The potential for using heavy metal tolerant microorganisms in bioremediation prompted us to further characterise the response of *O. anthropi* DE2010 to Cr(III) exposure.

Inorganic polyPs are polymers of orthophosphate residues linked by phosphoanhydride P-O-P bonds (Albi and Serrano, 2016). They are present in most organisms, including bacteria, archaea, and eukaryotes (Harold 1966; Kornberg et al. 1999; Rao et al. 2009). Metabolic and biological functions of polyP in bacteria and yeast are detailed elsewhere (Aschar-Sobbi et al. 2008; Oehmen et al. 2010; Rubio-Rincón et al. 2017). Inorganic polyP was initially

considered a phosphate and energy storage molecule that seemed to be involved in diverse physiological and regulatory mechanisms in bacteria (Kornberg et al. 1999; Brown and Kornberg, 2004; Rao et al. 2009). Among these is the bioaccumulation of heavy metals in intracytoplasmic inclusions (Gerber et al., 2016, Kulakovskaya, 2018[a]). The main enzyme related to polyP biosynthesis is polyphosphate kinase 1 (PPK1, EC 2.7.4.1) (Akiyama et al. 1993; Rao and Kornberg, 1996). However, a subsequent characterisation of the pathway indicated the involvement of two PPKs (PPK1 and PPK2) in the process. PPK1 is mainly involved in polyP synthesis by catalysing the reversible transfer of phosphate residues from ATP to polyP and from polyP to ADP. On the other hand, PPK2 participates in the synthesis of polyP from GTP and is frequently associated with polyP degradation (Zang et al. 2002). Further, an exopolyphosphatase (PPX, EC 3.6.1.11) and its homologue exopolyphosphatase/guanosine pentaphosphate phosphohydrolase (PPX/GPPA, EC 3.6.1.40), hydrolyse polyP, liberate inorganic phosphate (Pi) and transform GDP into GTP (Akiyama et al. 1993). These PPK enzymes have been purified from *Escherichia coli* and their genes are found in several bacteria (Kornberg et al. 1999; Alvarez and Jerez, 2004). Other enzymes involved in polyP metabolism include inorganic pyrophosphatases (Ppases, EC 3.6.1.1), which are organised in two groups, namely, soluble (coding gene, *ppa*) and membrane embedded (coding gene, *hppa*). Soluble Ppases (sPPases) are ubiquitous proteins with roles in the removal of the inorganic pyrophosphate (Ppi) produced by anabolic reactions (Lahti et al. 1988). Membrane-bound, proton translocating, inorganic pyrophosphatases (H^+-Ppases) - 110 -embran Ppi hydrolysis as the driving - 110 -embr for the movement of H^+ across biological - 110 -embranas (Rea and Poole, 1993). Although some studies have proposed several roles for polyP in microbial metabolism, the

mechanism by which Ppi is transported from polyP inclusions remains unknown. Ruiz et al. (2001), however, found that Ppi initiates polyP chain synthesis.

In the current study, we use genomic sequencing and the annotation of the environmentally isolated *O. anthropi* DE2010 to correlate polyP production and Cr(III) concentration with the following aims: (i) to detect the presence of polyP and Ppi metabolic genes within the *O. anthropi* DE2010 genome; (ii) to apply an SNPs calling study between *O. anthropi* DE2010 and *O. anthropi* ATCC49188 to determine the overall differences in their genomic architectures and, in particular, polyP metabolic genes; (iii) to quantify the polyP in response to Cr(III); and (iv) to determine the relative abundance and morphometric characteristics of polyP cytoplasmic inclusions in Cr(III) contaminated cultures.

2. Materials and methods

2.1 Culture conditions, genome sequencing, assembly and annotation of O. anthropi DE2010

O. anthropi DE2010 was cultured on Luria-Bertani (LB) agar (tryptone (10.0 g/L), yeast extract (5.0 g/L), sodium chloride (10.0 g/L), and bacteriological agar (15.0 g/L) at pH 7.0 and 27ºC and preserved in *cryoinstant* vials (Thermo Fisher Scientific) at -80ºC. Genomic DNA for whole genome sequencing (WGS) was extracted and isolated using the Puregene Core Kit A (Qiagen Sciences, Valencia, CA, USA) according to the manufacturer's instructions. This genomic DNA was sequenced by Illumina MiSeq (https://www.illumina.com/systems/sequencing-platforms/miseq) which produced 19,362,809 paired-end reads with about 1,160-fold coverage. The reads were filtered, assembled, scaffolded, and validated using FastQC 0.11.3

(https://www.bioinformatics.babraham.ac.uk/projects/fastqc/), SPADES 3.12.0 (Bankevich et al. 2012), and BLAST (https://blast.ncbi.nlm.nih.gov/Blast), respectively. The genomic sequence was annotated using the Prokaryotic genome annotation pipeline (PGAP) (https://www.ncbi.nlm.nih.gov/genome/annotation_prok/).

2.2 Identification of single-nucleotide polymorphisms (SNPs) and protein alignment

For this analysis, the *O. anthropi* ATCC49188 genome was used as the reference to call single-nucleotide polymorphisms (SNPs). Sequences with accession numbers NC_009667.1 and NC_009668.1 were retrieved from the NCBI database (https://www.ncbi.nlm.nih.gov/genome/) (Sayers et al. 2019). Filtered reads were mapped to the *O. anthropi* ATCC49188 reference genome using the Bowtie 2.3.3.1 software package (http://bowtie-bio.sourceforge.net/bowtie2/index.shtml) (Langmead and Salzberg, 2012). Results were processed with Samtools v1.9 (http://www.htslib.org/doc/samtools.html) (Li et al. 2009) and duplicated reads were removed using Picard (https://broadinstitute.github.io/picard/). Further, variant calling was performed using GATK v3.8 (https://software.broadinstitute.org/gatk/). Finally, the PPK and PPX protein sequences of the *O. anthropi* ATCC49188 and DE2010 strains were compared through a high-quality multiple sequence alignment created using Clustal Omega (https://www.ebi.ac.uk/Tools/msa/clustalo/) (Sievers and Higgins, 2018).

2.3 Cr(III) stock solutions and O. anthropi DE2010 contaminated culture conditions

For this study, a Cr(III) stock solution (50 mmol/L) was prepared by dissolving the 1.002 g of chromium nitrate salt (Sigma-Aldrich, Bellefonte, PA, USA) in 50 mL of double deionised water. The stock was sterilised by filtration through a 0.2 μm filter (Millipore,

Merck Millipore). The Cr(III) stock was prepared just before use and its pH was adjusted at 6.5.

Cr(III) tested concentrations of 0.5, 2, 5, 7, and 10 mmol/L were obtained through the serial dilution of the 50 mmol/L stock solution. Uncontaminated (0 mmol/L) and contaminated cultures were prepared at the same conditions. To do so, 2 mL of a 24 h culture of *O. anthropi* DE2010 grown in LB (OD$_{600}$ between 1.4 and 1.6, approximately 10^{10} cfu/mL) was inoculated into 18 mL of the LB liquid medium with the various tested Cr(III) concentrations (20 mL final volume) and further, its pH was adjusted at 6.5 to prevent metal precipitation. These cultures were used for all experiments and grown in an orbital shaking incubator (Infors HT Ecotron, Boston Laboratory) at 27ºC for 24 h.

2.4 Cell lysis and polyphosphate quantification in Cr(III) contaminated cultures

After being incubated for 24 h at 27ºC, all *O. anthropi* DE2010 cultures (non-contaminated and contaminated with 0.5, 2, 5, 7, and 10 mmol/L of the Cr(III) solution) were centrifugated at 5,500 x g for 15 min at 4ºC (Eppendorf 5804R refrigerated centrifuge) and the supernatants were discarded. Further, all the obtained pellets of bacteria cultures were resuspended in a 50 mmol/L Tris-HCl buffer (pH 7.0). All the suspensions of pellets were ultrasonicated with a SONOREX (Bandelin, Berlin) system for 15 min in an ice bath, followed by centrifugation at 5,500 x g for 20 min at 4ºC to remove cell debris. Finally, the resultant supernatants were treated with a protease inhibitor cocktail tablet (Roche).

To determinate the polyP content (PPK activity), each sample was analysed using methods described by Anschutz and Deborde (2016) that involve the reaction of molybdenum blue with soluble reactive phosphorus. Assays were performed in triplicate for each sample and results were obtained following the protocol described by Eixler et al.

(2005) as well as by considering the previously described relationship between total and soluble cellular phosphorus.

2.5 Transmission electron microscopy (TEM) coupled with (EDX) analysis and TEM imaging *of O. anthropi DE2010 Cr(III) cultures*

To describe this stage of research in brief, 20 mL of cultures were incubated with Cr(III) (0, 0.5, 2, 5, 7, and 10 mmol/L). Cellular pellets were obtained by carrying out centrifugation at 5,500 x g for 15 min at 4ºC. Further, they were fixed for 2 h in the Millonig buffer (Millonig 1961), supplemented with 2.5% glutaraldehyde, and washed in the same buffer several times. Afterwards, cells were post-fixed in 1% OsO_4 at 4ºC for 2 h. All the samples were then dehydrated in a graded series of acetone (30, 50, 70, 90, and 100%) and embedded in Spurr's epoxy resin (Maldonado et al. 2010). Consecutively, ultrathin sections (70 nm thickness) were obtained with a Leica EM UCG ultramicrotome (Leica microsystems GmbH, Heidelberg, Germany). For TEM coupled with energy dispersive X-ray spectroscopy (EDX) analysis, the ultrathin sections were mounted on carbon-coated, 400-mesh titanium grids without contrast and examined with a JEOL-JEM 2011 TEM (Jeol, Tokyo, Japan). To determine the semiquantitative elemental composition of samples, EDX measurements were performed with an X-ray detector EDX spectrophotometer Link Isis-200 (Oxford Instruments, Bucks, England) and analysed with INCA 4.15 EDS software (Oxford Instruments, Bucks, England). For TEM imaging, the ultrathin sections were mounted on 200-mesh copper grids with contrast (uranile acetate and lead citrate) and examined under a JEOL-JEM 1400 TEM (Jeol, Tokyo, Japan). The obtained TEM images of *O. anthropi* DE2010 non-contaminated and Cr(III) contaminated cultures were binarised using the image analysis software ImageJ 1.40g (Wayne Rasband, NIH, USA). To perform this process,

100 cells from each case were analysed to quantify the number of electrodense inclusions and their diameters, areas, volumes, and circularities.

2.6 Statistical analysis

Statistical analyses were performed using ANOVA, Student's t test, and Tukey post-hoc test. Significant differences in ANOVA, Student's t test, and Tukey's test values were considered significant when $p \leqslant 0.05$. The results were expressed as the arithmetic mean for non-transformed data ± the standard deviation ($\bar{x} \pm$ SD). The statistical analysis and graphical representations were obtained using SPSS software (version 20.0 for Windows 7) and Sigmaplot 12.0 software, respectively.

3. Results

3.1 O. anthropi DE2010 genome sequencing and gene detection of polyP and PPi metabolisms

This whole genome shotgun project has been deposited at INSDC (DDBJ/ENA/GenBank) under the accession number QMFN00000000. The version described in this paper is version QMFN01000000. All raw reads were deposited in the sequencing read archive (SRA) of NCBI with the accession number SRR7459269. The bioproject and biosample used in this study were also deposited at INSDC under the accession numbers PRJNA475095 and SAMN09379566, respectively.

The genomic assembly of *O. anthropi* DE2010 had a total length of 4.9 Mb, consisting of 26 contigs with an N_{50} length of 688,210 bp. Its GC content was 56.52% and it contained 4,683 genes. Further, six genes related to polyP and PPi metabolism were found. The annotation of this genome revealed features that have been summarised in Table 1. The list of the identified genes is described in Table 2.

3.2 Comparison of SNPs and protein alignment between O. anthropi ATCC49188 and O. anthropi DE2010

The SNP calling of *O. anthropi* DE2010 against *O. anthropi* ATCC49188 revealed 72,465 SNPs (1.51% of the total genome length). From these variants, 2,527 positions were polymorphic within the DE2010 strain.

The *ppx* and *ppk* genes are located in the same operon (Keasling et al. 1993; Lee et al. 2006) and were found to be essential for polyP metabolism in bacteria. The SNP calling of *O. anthropi* ATCC49188 and DE2010 in this operon revealed a great degree of similarity with respect to *ppx* and *ppk1* sequences. Further, 51 variations (1.35%) via SNP analysis were found and studied in detail. All related data are shown in Figure S1 in the supplementary material. The multiple alignments of identified proteins (PPX and PPK) revealed two mutations in PPX and one mutation in PPK (Text S1 and S2 [supplementary material]). The identified mutations in the PPX protein corresponded to R286K and S465N, and were conservative and semi-conservative replacements, respectively. The catalytic domain of this enzyme is located in the region between residues 37 to 308 that includes the R286K conservative mutation, which may not affect protein function. In the case of the PPK amino acid sequence, the A36V semi-conservative mutation is not located in any of the identified catalytic domains of the enzymes and may not affect enzyme activity as well.

3.3 Relationship between polyP production and Cr(III) concentration in O. anthropi DE2010

Previous studies have noted that one gene, *ppk,* is mainly responsible for polyP production. For this study, the polyphosphate kinase (PPK) activity of cell extracts was tested using cells exposed to Cr(III) contamination in accordance with the evidence that has shown

that polyP inclusions have a significant chelating effect on metal cations. The data collected indicated that under these stress conditions, *O. anthropi* DE2010 synthesised and accumulated polyP in a concentration-dependent manner (Figure 1 and Figure S2 [supplementary material]). A 23.08% change in the polyP concentration was achieved between 0 mmol/L (control) and 10 mmol/L of Cr(III). The statistical analysis showed that there was a significant difference between control and both 7 and 10 mmol/L Cr(III) samples (Figure 1).

3.4 Electron microscopy

In a previous study, we demonstrated the colocalisation of Cr(III) with intracytoplasmic polyP inclusions using scanning transmission electron microscopy (STEM) coupled with EDX (Villagrasa et al. 2020). Nevertheless, the abundance of these inclusions in relation with the presence of chromium was not considered. In the present work, a semiquantitative analysis regarding the relative abundances of P and Cr (in atomic %) in non-contaminated (control) and contaminated (10 mmol/L Cr(III)) samples was carried out using TEM-EDX (Figure S3 and Table S1 [supplementary material]). Comparing data from 1 and 3 EDX spectra, corresponding to polyP inclusions without and with Cr(III), respectively, an increment in the atomic percentage of Cr(III), from 0.1 to 3.59, and P, from 0.01 to 1.51, was detected. Moreover, the data from the EDX spectra 2 (grid) and 4 (cytoplasm in contaminated conditions) demonstrated that P and Cr were not present outside the cells and instead, were dispersed by the bacterial cytoplasm, indicating that the metal was only accumulated in the intracytoplasmic inclusions of polyP (Figure S3 and Table S1 [supplementary material]). At the same time, it was verified that the titanium grids used in these experiments only contained Ti (Figure S3A and Table S1 [supplementary material]).

In order to correlate the number of electrodense inclusions with Cr(III) concentrations in *O. anthropi* DE2010 cultures, a TEM study combined with an image analysis software (ImageJ) was carried out (Figure 2 and Table 3). An increase in the presence of pleomorphic cellular forms and more destructured cytoplasm were observed as the metal concentration increased (Figure 2). The circularity measurements indicated that polyP inclusions are circular. A 6-fold increase in the number of inclusions along with different morphometric parameters assessed (diameter, area, and volume) between 0 mmol/L and 10 mmol/L samples were detected (Table 3). Statistically significant differences were obtained for comparisons between the 0 mM (control) and 10 mmol/L Cr(III) samples in terms of the diameter (F = 903.41) ($p < 0.05$), area (F = 66.15) ($p < 0.05$), and volume (F = 5,209.24) ($p < 0.05$) results. Using the Tukey multiple comparisons post-hoc test, statistically significant differences ($p < 0.05$) were determined (Table 3).

These results suggest that the accumulation of polyP in cytoplasmatic inclusions may be one of the factors providing tolerance and resistance to *O. anthropi* DE2010 against Cr(III) via the formation of cation and polyP complexes.

4. Discussion

Several reports have explored the capacity of some microorganisms to sequester heavy metals via the polyP metabolism (Orell et al. 2012, Acharya and Apte, 2013, Andreeva et al. 2014, Kulakovskaya 2018a). In addition, our research group isolated three heterotrophic microorganisms from Ebro Delta microbial mats with the capacity to immobilise heavy metals, namely, *Paracoccus* sp. DE2007 (Diestra et al. 2007), *Micrococcus luteus* DE2008 (Maldonado et al. 2010), and *Ochrobactrum anthropi* DE2010 (Villagrasa et

al. 2019). *Paracoccus* sp. DE2007 and *Micrococcus luteus* DE2008 can immobilise heavy metals in extracellular polymeric substances (EPS) (Baratelli et al. 2010; Maldonado et al. 2010; Puyen et al. 2012), whilst *O. anthropi* DE2010 is able to capture heavy metals extra- and intra-cellularly in EPS and polyP inclusions, respectively (Villagrasa et al. 2020). Here, we reported the whole genome sequence of *O. anthropi* DE2010 and analysed the response of this strain to Cr(III) in contaminated cultures. The sequencing of the *O. anthropi* DE2010 genome revealed the presence of the key genes involved in polyP and PPi metabolism (Figure 3), including *ppk* and *ppx* genes that comprise part of an operon, as expected. This configuration is maintained in the *O. anthropi* ATCC49188 genome, which was used as a reference in this study (Chain et al. 2011). Moreover, the genome of *O. anthropi* DE2010 contains a gene of the chromium/chromate efflux pump named *chr*A with the accession number DNK03_01860 (DDBJ/EMBL/GenBank). This gene is relevant in the sensitivity of *O. tritici* to transition metals (Almeida et al. 2020) and may have an important role in Cr(III) tolerance in *O. anthropi* DE2010.

The comparative genomics analysis between *O. anthropi* ATCC49188 and *O. anthropi* DE2010 revealed interesting findings regarding bacterial genome composition. Under selective or non-selective pressures, bacterial strains accumulate SNPs that lead to inter- and intra-strain diversity (Gohil et al. 2016). The present SNP study showed an average variability of < 1.6% between the analysed genomes (ATCC and DE2010 strains), which was slightly lower in the sequences of *ppx* and *ppk* genes, the most important polyP metabolic gene cluster. Aujoulat et al. (2014) studied genomic variations between different species of the same genus *(O. intermedium* and *O. ciceri)* and found higher percentages of polymorphic sites in different housekeeping genes such as *dnaK* (3.6%), *recA* (5.7%) and *rpoB*

(7.4%). The low values obtained here in the *ppx* and *ppk* genes indicate that the polyP operon can be under selective pressure due to its evolutionary relevance wherein the genes enhance the capacity of *O. anthropi* DE2010 to survive toxic heavy metal contamination. Although several SNPs were located in the *ppx* and *ppk* genes, Clustal Omega results revealed that only a small fraction was present in the alignment of the corresponding protein sequences. In fact, the detected amino acid changes may not have profound influences on the activity of resultant enzymes, suggesting that polyP metabolism is preserved to cope with stress conditions such as the Cr(III) contamination assessed in this study (Text S1 and S2 [supplementary material]).

On the other hand, previous studies demonstrated the polyP production in response to numerous stress factors such as (i) nutrient starvation in the *Paracoccus* sp. strain (Lee and Park, 2008); (ii) wastewater phosphorus removal by *Chlorella* sp., *Lyngbya* sp., and *Anabaena* sp. (Mukherjee et al 2015); and (iii) heavy metal toxicity by bacteria, microalgae, or cyanobacteria, among others (Suzuki and Banfield, 2004; Millach et al. 2015; Kulakovskaya 2018a). The results obtained in this study demonstrated that *O. anthropi* DE2010 is a significant candidate that has the potential to minimise Cr(III) toxicity by chelating the metal in polyP inclusions, producing a 4-fold increase in polyP concentration and 6-fold increase in polyP inclusion numbers, both in 10 mmol/L Cr(III) cultures with respect to control cultures (0 mmol/L). These results are in agreement with those obtained by Andreeva et al. (2014), which demonstrated that the concentration of polyP in *C. humicola* cells in cultures contaminated with other metals including Cd(II) and Mn(II) increased 3.9- and 3.4-fold, respectively, in comparison with non-contaminated controls. Moreover, the studies by Boswell et al. (1999), Choudhary and Sar (2011), and Acharya and

Apte (2013) corroborated the results indicating that electrodense polyP inclusions were increased in heavy metal contaminated cultures using high-resolution electron microscopy techniques. Similar evidence was found by Kulakovskaya et al. (2018b) in yeast. Taken together, these results indicate that polyP production of *O. anthropi* DE2010 in Cr(III) contaminated cultures seems to be regulated in a concentration dependent manner.

In conclusion, our results demonstrate the genome sequence of *O. anthropi* DE2010 is a valuable source of information that can be used to analyse the metabolic response of the bacteria to Cr(III). In this study, heavy metal contamination of *O. anthropi* DE2010 cultures resulted in dose-dependent polyP accumulation; and an increment in the number of polyP inclusions was observed in contaminated cultures. According to the results obtained in this work, future investigations of processes and metabolic polyP pathways involved in Cr(III) removal in *O. anthropi* DE2010 are required and may facilitate the use of this bacteria in bioremediation efforts.

Funding

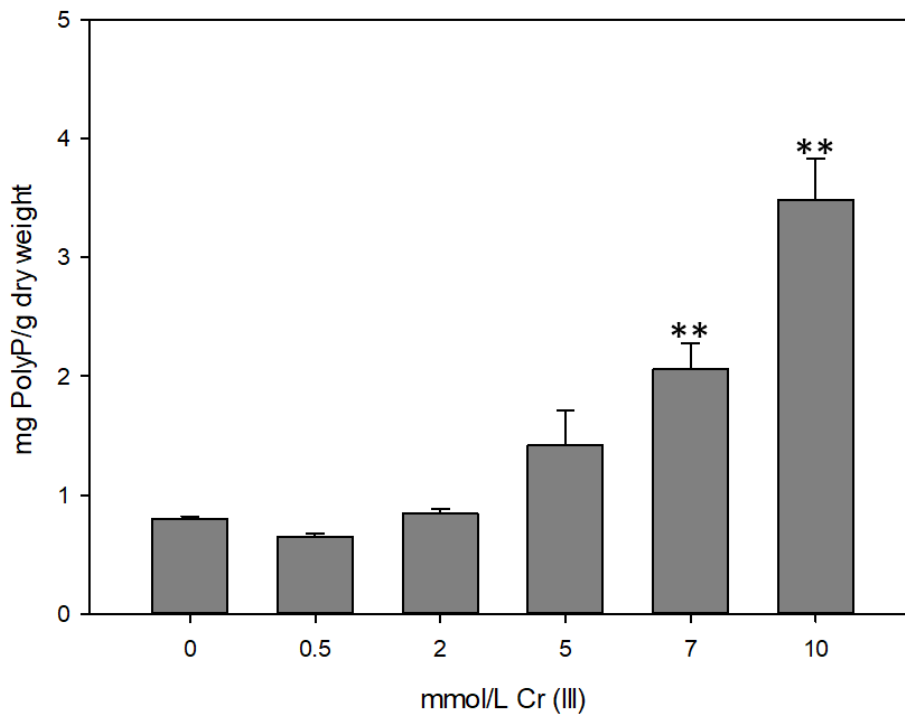Polyphosphate accumulation in Cr (III) contaminated cultures

Figure 1. Polyphosphate content (mg polyP/g dry weight) in the *O. anthropi* DE2010 cultures grown at increasing concentrations of Cr(III). Data from contaminated vs. non-contaminated samples were analysed using one-way ANOVA; values of **$p < 0.005$ were considered statistically significant. Data were expressed as mean ± SD (n= 3).
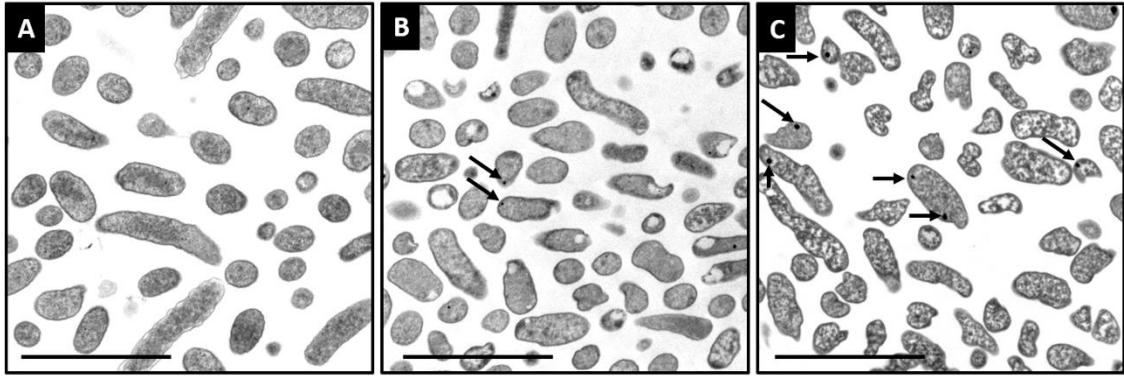
Figure 2. TEM images of *O. anthropi* grown in 0 mmol/L (A), 5 mmol/L (B), and 10 mmol/L (C) Cr(III) contaminated cultures. The arrows indicate intracytoplasmic electrodense inclusions. The scale bars represent 5 μm.
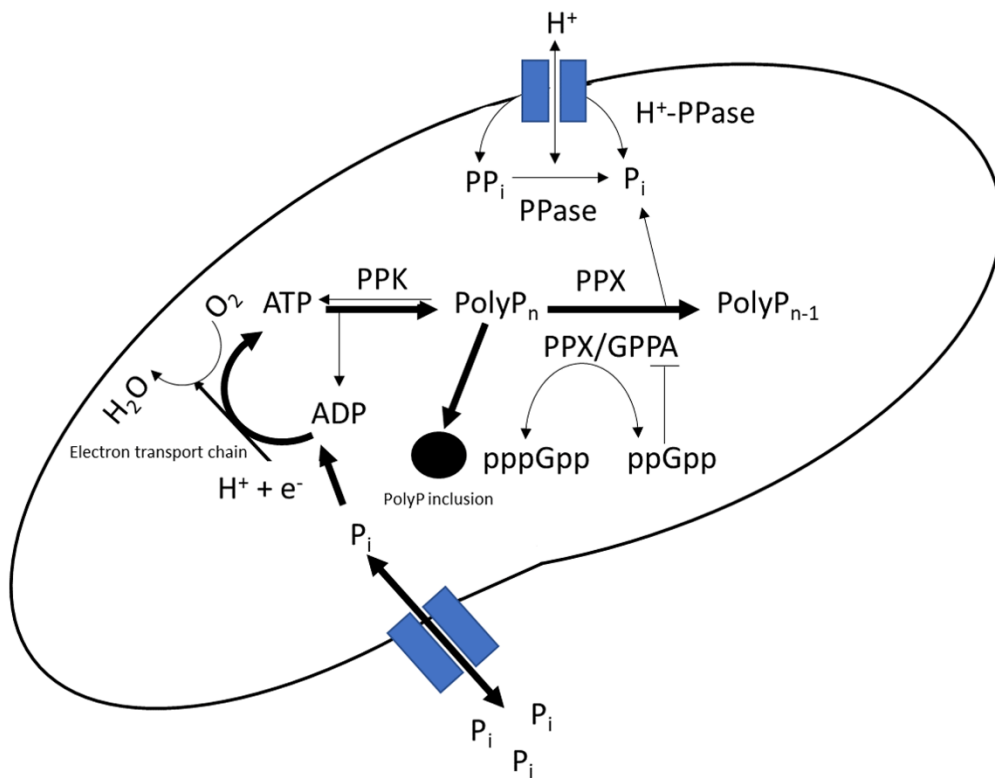
Figure 3. Graphic representation of proposed metabolic pathways for polyP and PPi metabolism within *O. anthropi* DE2010. Abbreviations: Inorganic phosphate (P_i), inorganic pyrophosphate (PP_i), K^+-insensitive pyrophosphate-energized proton pump (H^+PPase), inorganic pyrophosphatase (PPase), guanosine pentaphosphate (pppGpp), guanosine tetraphosphate (ppGpp), polyphosphate kinase (PPK), exopolyphosphatase (PPX), and exopolyphosphatase/pppGpp phosphohydrolase (PPX/GPPA).

Table 1. General features of *O. anthropi* DE2010 and genome information

Item	Description or value
Features of *O. anthropi* DE2010 (MIGS)	
Classification	*Bacteria; Proteobacteria; Alphaproteobacteria; Rhizobiales; Brucellaceae; Ochrobactrum; Ochrobactrum anthropi*
Gram stain	Negative
Cell shape	Rod shaped and pleomorphic forms
Motility	Peritrichous flagellation
Sporulation	Non-sporulating
Temperature optimum	27 ºC
pH range	5 – 9
Salinity range	0 – 70 ‰ NaCl
Relationship to oxygen	Strictly aerobic
Pathogenicity	Opportunistic human pathogen
Sample collection	2010
Geographic location	Spain: Tarragona
Latitude and Longitude	40.33 N 0.35 E
Environment (biome and feature)	Marine soil and wetland (Ebro Delta)
Genome features	
Genome size (Mb)	4.9
GC content (%)	56.52
Total number of genes	4,683
Coding sequence (CDS)	4,519
rRNAs	3
tRNA	48
tmRNA	1
ncRNAs	4
Pseudo Genes	109

Table 2. Genes and encoded proteins for polyP and PPi metabolism in *O. anthropi* DE2010

Gene	GenBank accession number	Gene product	Activity
PolyP and PPi metabolisms			
ppk1	DNK03_06690	**Polyphosphate kinase 1**	Transfers the terminal phosphate residue of ATP to a growing chain of polyP in a reversible reaction.
ppx	DNK03_06685	**Exopolyphosphatase**	Mediates polyP degradation releasing orthophosphate from chain end.
hppa	DNK03_06575	**K$^+$-insensitive pyrophosphate-energized proton pump**	Proton transmembrane pump that utilizes the energy of pyrophosphate hydrolysis as the driving force for proton movement.
ppx/gpp a	DNK03_08775	**Exopolyphosphatase/pp pGpp phosphohydrolase**	Hydrolyses guanosine pentaphosphate (pppGpp) to guanosine tetraphosphate (ppGpp).
ppk2	DNK03_11830	**Polyphosphate kinase 2**	*ppk2*, at least in isolated form, seems to be designed for synthesis of GTP from polyP in contrast to *ppk1*, which strongly favors synthesis of polyP and exclusively from ATP.
ppa	DNK03_19225	**Inorganic pyrophosphatase**	Inorganic pyrophosphatase (PPase) catalyzes the hydrolysis of inorganic pyrophosphate to form orthophosphate

Table 3. Count and morphometric parameters of electrodense inclusions in *O. anthropi* DE2010 Cr(III) contaminated cultures.

Sample	Number	Diameter (μm)	Area (μm^2)	Volume (μm^3)	Circularity (arbitrary units)
0 mmol/L	5	$0.011 \pm 2.45 \cdot 10^{-4}$	$3.80 \cdot 10^{-4} \pm 5.02 \cdot 10^{-7}$	$6.95 \cdot 10^{-7} \pm 1.88 \cdot 10^{-11}$	0.938 ± 0.006
0.5 mmol/L	6	$0.013 \pm 3.67 \cdot 10^{-4}$	$5.31 \cdot 10^{-4} \pm 1.13 \cdot 10^{-6}$	$1.14 \cdot 10^{-6} \pm 6.36 \cdot 10^{-11}$	0.950 ± 0.008
2 mmol/L	8	$0.020 \pm 0.003^{**+}$	$0.001 \pm 1.11 \cdot 10^{-4\ **+}$	$4.17 \cdot 10^{-6} \pm 6.36 \cdot 10^{-8\ **+}$	0.945 ± 0.004
5 mmol/L	20	$0.042 \pm 0.008^{**++\$\$}$	$0.005 \pm 8.04 \cdot 10^{-3\ **++\$\$}$	$3.86 \cdot 10^{-5} \pm 1.20 \cdot 10^{-6\ **++\$\$}$	0.931 ± 0.010
7 mmol/L	24	$0.049 \pm 0.007^{**++\$\$\&\&}$	$0.007 \pm 6.15 \cdot 10^{-4\ **++\$\$\&\&}$	$6.14 \cdot 10^{-5} \pm 8.08 \cdot 10^{-7\ **++\$\$\&\&}$	0.945 ± 0.007
10 mmol/L	31	$0.052 \pm 0.009^{**++\$\$\&\&\wedge}$	$0.008 \pm 0.001^{**++\$\$\&\&\wedge}$	$7.34 \cdot 10^{-5} \pm 1.71 \cdot 10^{-6\ **++\$\$\&\&\wedge}$	0.941 ± 0.005

Data are expressed as mean ± standard deviation (SD)

*p <0.05; **p <0.01: 0.5, 2, 5, 7, and 10 mmol/L treatments vs. control (0 mmol/L)

+p <0.05; ++p <0.01: 2, 5, 7, and 10 mmol/L treatments vs. 0.5 mmol/L treatment

$\$\$$$p$ <0.01: 5, 7, and 10 mmol/L treatments vs. 2 mmol/L treatment

$\&\&$$p$ <0.01: 7, and 10 mmol/L treatments vs. 5 mmol/L treatment

^p <0.05: 7 treatment mmol/L vs. 10 mmol/L treatment

References

Acharya C and Apte SK (2013) Novel surface associated polyphosphate bodies sequester uranium in the filamentous, marine cyanobacterium, *Anabaena torulosa*. Metallomics, 5(12): 1595-1598.

Andreeva N, Ryazanova L, Dmitriev V, Kulakovskaya T, Kulaev I (2014) Cytoplasmic inorganic polyphosphate participates in the heavy metal tolerance of *Cryptococcus humicola*. Folia Microbiol 59 (5):381-389. https://doi.org/10.1007/s12223-014-0310-x

Akiyama M, Crooke E, Kornberg A (1993) An exopolyphosphatase of *Escherichia coli*. The enzyme and its *ppx* gene in a polyphosphate operon. J Biol Chem 268(1):633-639

Albi T and Serrano A (2016) Inorganic polyphosphate in the microbial world. Emerging roles for a multifaceted biopolymer. World J Microbiol Biotechnol 32:27. https://doi.org/10.1007/s11274-015-1983-2

Ali, H., Khan, E., Sajad, M.A. 2013. Phytoremediation of heavy metals—Concepts and applications. Chemosphere 91(7):869-881. https://doi.org/10.1016/j.chemosphere.2013.01.075.

Almeida MC, Branco R, Morais PV (2020) Response to vanadate exposure in *Ochrobactrum tritici* strains. PLOS ONE 15(2): e0229359. https://doi.org/10.1371/journal.pone.0229359.

Alvarez S and Jerez, CA (2004) Copper ions stimulate polyphosphate degradation and phosphate efflux in *Acidithiobacillus ferrooxidans*. Appl Environ Microbiol 70(9):5177–5182. https://doi.org/10.1128/AEM.70.9.5177-5182.2004

Anschutz P and Deborde J (2016) Spectrophotometric determination of phosphate in matrices from sequential leaching of sediments. Limnol Oceanogr Methods 14:245–256. https://doi.org/10.1002/lom3.10085

Aschar-Sobbi R, Abramov AY, Diao C, Kargacin ME, Kargacin JG, French JR, Pavlov E (2008) High sensitivity, quantitative measurements of polyphosphate using a new DAPI-based approach. J Fluoresc 18:859–866. https://doi.org/10.1007/s10895-008-0315-4

Aujoulat F, Romano-Bertrand S, Masnou A, Marchandin H, Jumas-Bilak E (2014) Niches, Population Structure and Genome Reduction in *Ochrobactrum intermedium*: Clues to Technology-Driven Emergence of Pathogens. PLoS ONE 9(1): e83376. https://doi.org/10.1371/journal.pone.0083376.

Bankevich A, Nurk S, Antipov D, Gurevich AA, Dvorkin M, Kulikov AS, Lesin VM, Nikolenko SI, Pham S, Prjibelski AD, Pyshkin AV, Sirotkin AV, Vyahhi N, Tesler G, Alekseyev MA, Pevzner PA (2012) SPAdes: A new genome assembly algorithm and its applications to single-cell sequencing. J. Comput Biol 19(5):455–477. https://doi.org/10.1089/cmb.2012.0021

Baratelli M, Maldonado J, Esteve I, Solé A, Diestra E (2010) Electron microscopy techniques and energy dispersive X-ray applied to determine the sorption of lead in *Paracoccus* sp. DE2007, in: Menendez-Vilas, A. (Ed), Current Research Technology and Education topics in Applied Microbiology and Microbial Biotechnology. Formatex Research Center, Badajoz, pp. 1601-1608.

Baxter M and Jensen TH (1980) Uptake of magnesium, strontium, barium, and manganese by *Plectonema boryanum (*Cyanophyceae) with special reference to polyphosphate bodies. Protoplasma 104:81-89

Boswell, CD, Dick RE, Macaskie LE (1999) The effect of heavy metals and other environmental conditions on the anaerobic phosphate metabolism of *Acinetobacter johnsonii*. Microbiology 145:(7):1711-1720. https://doi.org/10.1099/13500872-145-7-1711.

Brown MR, Kornberg A (2004) Inorganic polyphosphate in the origin and survival of species. Proc Natl Acad Sci USA. 101:16085–16087. https://dx.doi.org/10.1073/pnas.0406909101

Burgos A, Maldonado J, De los Rios A, Solé A, Esteve I (2013) Effect of copper and lead on two consortia of phototrophic microorganisms and their capacity to sequester metals. Aquat Toxicol (140–141): 324-336. https://doi.org/10.1016/j.aquatox.2013.06.022.

Chain PSG, Lang DM, Comerci DJ, Malfatti SA, Vergez LM, Shin M, Ugalde RA, Garcia E, Tolmasky ME (2011) Genome of *Ochrobactrum anthropi* ATCC 49188T, a Versatile Opportunistic Pathogen and Symbiont of Several Eukaryotic Hosts. J Bacteriol 193(16):4274-4275. https://doi.org/10.1128/JB.05335-11

Cheng Y, Yan F, Huang F, Chu W, Pan D, Chen Z, Zheng J, Yu M, Lin Z, Wu Z (2010) Bioremediation of Cr(VI) and immobilization as Cr(III) by *Ochrobactrum anthropi*. Environ Sci Technol 44(16):6357-6363. https://doi.org/10.1021/es100198v.

Chojnacka K (2010) Biosorption and bioaccumulation—the prospects for practical applications. Environ Int 36:299–307

Choudhary S and Sar P (2011) Uranium biomineralization by a metal resistant *Pseudomonas aeruginosa* strain isolated from contaminated mine waste. J Hazard Mater 186(1): 336-343. https://doi.org/10.1016/j.jhazmat.2010.11.004.

Chourey K, Thompson MR, Morrell-Falvey J, VerBerkmoes NC, Brown SD, Shah M, Zhou J, Doktycz M, Hettich RL, Thompson DK (2006) Global molecular and morphological effects of 24-hour chromium(VI) exposure on *Shewanella oneidensis* MR-1. Appl Environ Microbiol 72:6331–6344

Diestra E, Esteve I, Burnat M, Maldonado J, Solé A (2007) Isolation and characterization of a heterotrophic bacterium able to grow in different environmental stress conditions, including crude oil and heavy metals. Communicating Current Research and Educational Topics and Trends in Applied Microbiology, A. Méndez-Vilas (Ed.) FORMATEX

Eixler S, Selig U, Karsten U (2005) Extraction and detection methods for polyphosphate storage in autotrophic planktonic organisms. Hydrobiologia 533(1–3):135–143. https://doi.org/10.1007/s10750-004-2406-9

Fathima A and Rao JR (2018) Is Cr(III) toxic to bacteria: toxicity studies using *Bacillus subtilis* and *Escherichia coli* as model organism. Arch Microbiol 200:453–462 (2018). https://doi.org/10.1007/s00203-017-1444-4.

Gerber U, Zirnstein I, Krawczyk-Bärsch E, Lünsdorf H, Arnold T, Merroun ML (2016) Combined use of flow cytometry and microscopy to study the interactions between the gram-negative betaproteobacterium *Acidovorax facilis* and uranium(VI). J Hazard Mater 317:127–134. https://doi.org/10.1016/j.jhazmat.2016.05.062

Gohil KN, Neurgaonkar PS, Paranjpe A, Dastager SG, Dharne MS (2016) Peeping into genomic architecture by re-sequencing of *Ochrobactrum intermedium* M86 strain during laboratory adapted conditions. Genom Data 8:72-76. https://doi.org/10.1016/j.gdata.2016.04.003

Hansda A, Kumar V, Anshumali (2016) A comparative review towards potential of microbial cells for heavy metal removal with emphasis on biosorption and bioaccumulation. World J Microbiol Biotechnol 32:170. https://doi.org/10.1007/s11274-016-2117-1

Harold FM (1966) Inorganic polyphosphates in biology: structure, metabolism, and function. Bacteriol Rev 30:772-794

Jacobs JA, Testa SM (2005) Overview of chromium (VI) in the environment: background and history. In: Guertin J, Jacobs JA, Avakian CP, editors. Chromium (VI) Handbook. Boca Raton, Fl: CRC Press. pp. 1–22.

Jensen TE, Rachlin JW, Jani V, Warkentine BE (1986) Heavy metal uptake in relation to phosphorus nutrition in *Anabaena variabilis* (Cyanophyceae). Environ Pollut (Series A) 42(1986):261-271

Keasling JD, Bertsch L, Kornberg A (1993) Guanosine pentaphosphate phosphohydrolase of *Escherichia coli* is a long-chain exopolyphosphatase. Proc Natl Acad Sci USA. 90(15):7029-7033. https://doi.org/10.1073/pnas.90.15.7029

Kornberg A, Rao NN, Ault-Riche D (1999) Inorganic polyphosphate: a molecule of many functions. Annu Rev Biochem 68:89-125. https://doi.org/10.1016/j.str.2006.06.009

Kulakovskaya T (2018a) Inorganic polyphosphates and heavy metal resistance in microorganisms. World J Microbiol Biotechnol 34:139. https://doi.org/10.1007/s11274-018-2523-7

Kulakovskaya T, Ryazanova L, Zvonarev A, Khokhlova G, Ostroumov V, Vainshtein M (2018b) The biosorption of cadmium and cobalt and iron ions by yeast *Cryptococcus humicola* at nitrogen starvation. Folia Microbiol 63:507-510. https://doi.org/10.1007/s12223-018-0583-6.

Kuroda A, Nomura K, Ohtomo R, Kato J, Ikeda T, Takiguchi N, Ohtake H, Kornberg A (2001) Role of inorganic polyphosphate in promoting ribosomal protein degradation by the ion protease in *E. coli*. Science 27:705-708. https://doi.org/10.1126/science.1061315

Lahti R, Pitkäranta T, Valve E, Ilta I, Kukko-Kalske E, Heinonen J (1988) Cloning and characterization of the gene encoding inorganic pyrophosphatase of *Escherichia coli* K-12. J Bacteriol 170(12):5901-7.

Langmead B and Salzberg S (2012) Fast gapped-read alignment with Bowtie 2. Nat Methods 9:357-359. https://doi.org/10.1038/nmeth.1923

Lee S, Lee Y, Lee Y, Choi Y (2006) Molecular characterization of polyphosphate (PolyP) operon from *Serratia marcescens*. J. Basic Microbiol. 46:108-115. https://doi.org/10.1002/jobm.200510038

Lee HW and Park YK (2008) Characterizations of denitrifying polyphosphate-accumulating bacterium *Paracoccus* sp. strain YKP-9. J Microbiol Biotechnol 18(12):1958–1965. https://doi.org/10.4014/jmb.0800.162

Li H, Handsaker B, Wysoker A, Fennell T, Ruan J, Homer N, Marth G, Abecasis G, Durbin R (2009) 1000 Genome project data processing subgroup. The sequence alignment/map format and SAMtools. Bioinformatics. 25(16):2078-9. https://doi.org/10.1093/bioinformatics/btp352

Masindi V. and Muedi, K.L. 2018. Environmental contamination by heavy metals. Heavy Metals, Hosam El-Din M. Saleh and Refaat F. Aglan, IntechOpen. https://doi.org/10.5772/intechopen.76082.

Maldonado J, Diestra E, Domènech AM, Villagrasa E, Puyen ZM, Esteve I, Solé A (2010) Isolation and identification of a bacterium with high tolerance to lead and copper from a marine microbial mat in Spain. Ann Microbiol 60(1):113-120. https://doi.org/10.1007/s13213-010-0019-2

Millach L, Solé A and Esteve I (2015) Role of *Geitlerinema* sp. DE2011 and *Scenedesmus* sp. DE2009 as bioindicators and immobilizers of chromium in a contaminated natural environment. BioMed Res Int 519769. https://doi.org/10.1155/2015/519769.

Milloning G (1961) A modified procedure for lead staining of thin sections. J Biophys Biochem Cytol 11:736-739

Mukherjee C, Chowdhury R, Ray K (2015) Phosphorus Recycling from an Unexplored Source by Polyphosphate Accumulating Microalgae and Cyanobacteria-A Step to Phosphorus Security in Agriculture. Front Microbiol 6:1421. https://doi.org/10.3389/fmicb.2015.01421

Narancic T, Djokic L, Kenny ST, O'Connor KE, Radulovic V, Nikodinovic-Runic J, Vasiljevic B (2012) Metabolic versatility of Gram-positive microbial isolates from contaminated river sediments. J Hazard Mater 215–216:243-251. https://doi.org/10.1016/j.jhazmat.2012.02.059

Oehmen A, Carvalho G, Lopez-Vazquez CM, van Loosdrecht MCM, Reis MAM (2010) Incorporating microbial ecology into the metabolic modelling of polyphosphate accumulating organisms and glycogen accumulating organisms. Water Res 44(17):4992-5004. https://doi.org/10.1016/j.watres.2010.06.071

Oliveira H (2012) Chromium as an environmental pollutant: insights on induced plant toxicity. J Botany Article ID 375843. https://doi.org/10.1155/2012/375843

Orell A, Navarro CA, Rivero M, Aguilar JS, Jerez CA (2012) Inorganic polyphosphates in extremophiles and their possible functions. Extremophiles 16: 573. https://doi.org/10.1007/s00792-012-0457-9.

Páez PL, Bazán CM, Bongiovanni ME, Toneatto J, Albesa I, Becerra MC, Argüello GA (2013) Oxidative stress and antimicrobial activity of chromium(III) and ruthenium(II) complexes on *Staphylococcus aureus* and *Escherichia coli*. BioMed Res Int 906912. https://doi.org/10.1155/2013/906912.

Plaper, A., S. Jenko-Brinovec, A. Premzl, J. Kos, and P. Raspor (2002) Genotoxicity of trivalent chromium in bacterial cells. Possible effects on DNA topology. Chem Res Toxicol 15:943-949. https://doi.org/10.1021/tx010096q

Puyen ZM, Villagrasa E, Maldonado J, Diestra E, Esteve I, Solé A (2012) Biosorption of lead and copper by heavy-metal tolerant *Micrococcus luteus* DE2008. Bioresour Technol 126:233–237. https://doi.org/10.1016/j.biortech.2012.09.036.

Rao NN and Kornberg A (1996) Inorganic polyphosphate supports resistance and survival of stationary-phase *Escherichia coli*. J Bacteriol 178:1394–1400. https://doi.org/10.1128/jb.178.5.1394-1400.1996

Rao NN, Gomez-Garcia MR, Kornberg A (2009) Inorganic polyphosphate: essential for growth and survival. Annu Rev Biochem 78:60. https://doi.org/10.1146/annurev.biochem.77.083007.093039

Rea PA and Poole RJ (1993) Vacuolar H+-Translocating Pyrophosphatase. Annu Rev Plant Physiol Plant Mol Biol 44:157-180. https://doi.org/10.1042/bj0221446

Rubio-Rincón FJ, Lopez-Vazquez CM, Welles L, van Loosdrecht MCM, Brdjanovic D (2017) Cooperation between Candidatus Competibacter and Candidatus Accumulibacter clade I, in denitrification and phosphate removal processes. Water Res 120:156-164. https://doi.org/10.1016/j.watres.2017.05.001.

Ruiz FA, Rodrigues CO, Docampo R (2001) Rapid changes in polyphosphate content within acidocalcisomes in response to cell growth, differentiation, and environmental stress in *Trypanosoma cruzi*. J Biol Chem 276:26114–26121. https://doi.org/10.1074/jbc.M102402200.

Sayers EW, Agarwala R, Bolton EE, Brister JR, Canese K, Clark K, Connor R, Fiorini N, Funk K, Hefferon T, Holmes JB, Kim S, Kimchi A, Kitts PA, Lathrop S, Lu Z, Madden TL, Marchler-Bauer A, Phan L, Schneider VA, Schoch CL, Pruitt KD, Ostell J (2019) Database resources of the National Center for Biotechnology Information. Nucleic Acids Res 47:23-28. https://doi.org/10.1093/nar/gky1069

Sievers F, Higgins DG (2018) Clustal Omega for making accurate alignments of many protein sciences. Protein Sci 27:135-145. https://doi.org/10.1002/pro.3290

Suzuki Y and Banfield JF (2004) Resistance to, and accumulation of, uranium by bacteria from uranium-contaminated site. Geomicrobiol J 21:113-121.

Villagrasa E, Ferrer-Miralles N, Millach L, Obiol A, Creus J, Esteve I, Sole A (2019) Morphological responses to nitrogen stress deficiency of a new heterotrophic isolated strain of Ebro Delta microbial mats. Protoplasma 256:105-116. https://doi.org/10.1007/s00709-018-1263-8

Villagrasa E, Ballesteros B, Olbiol A, Millach L, Esteve I, Sole A (2020) Multi-approach analysis to assess the chromium(III) immobilization by *Ochrobactrum anthropi* DE2010. Chemosphere 238:124663. https://doi.org/10.1016/j.chemosphere.2019.124663

Wilbur S, Abadin H, Fay M, Yu D, Tencza B, Ingerman L, Klotzbach J, James S (2012) Toxicological Profile for Chromium. Atlanta (GA): Agency for Toxic Substances and Disease Registry (US). https://www.ncbi.nlm.nih.gov/books/NBK158855/.

Zhang H, Ishige K, Kornberg A (2002) A polyphosphate kinase (PPK2) widely conserved in bacteria. Proc Natl Acad Sci USA 99:16678–83. https://doi.org/10.1073/pnas.262655199

Complete bibliographical reference of article from 2.3 thesis section:

Villagrasa, E., Egea, R., Ferrer-Miralles, N., Solé, A. 2020b. Genomic and biotechnological insights in stress-linked polyphosphate production induced by chromium(III) in *Ochrobactrum anthropi* DE2010. World J Microbiol Biotechnol 36:97. https://doi.org/10.1007/s11274-020-02875-6.

Chapter II. 2.4 Cellular strategies against metal exposure and metal localization patterns linked to phosphorus pathways in *Ochrobactrum anthropi* DE2010

Cellular strategies against metals exposure and metal localization patterns linked to phosphorus pathways in *Ochrobactrum anthropi* DE2010

Eduard Villagrasa[1], Cristina Palet[2], Irene López-Gómez[1], Diana Gutiérrez[1], Isabel Esteve[1], Alejandro Sánchez-Chardi[3,4*], and Antonio Solé[1*]

[1] *Departament de Genètica i Microbiologia. Facultat de Biociències. Universitat Autònoma de Barcelona. Bellaterra, Cerdanyola del Vallès, 08193 Barcelona, Spain*

[2] *GTS-UAB Research Group, Department of Chemistry. Facultat de Ciències. Universitat Autònoma de Barcelona. Bellaterra, Cerdanyola del Vallès, 08193 Barcelona, Spain*

[3] *Departament de Biologia Evolutiva, Ecologia i Ciències Ambientals, Facultat de Biologia, Universitat de Barcelona. 08028 Barcelona, Spain*

[4] *Servei de Microscòpia, Universitat Autònoma de Barcelona, Bellaterra, Cerdanyola del Vallès, 08193 Barcelona, Spain*

Abstract

Cytotoxic, chemical, biochemical, compositional, and morphometric responses were analyzed against heavy metal exposure in *Ochrobactrum anthropi* DE2010, an heterotrophic bacterium isolated from Ebro Delta microbial mats (Tarragona, NE Spain). Several parameters of effect and exposure were evaluated to determine tolerance to a range of cadmium (Cd), lead (Pb(II)), copper (Cu(II)), chromium (Cr(III)), and zinc (Zn) concentrations. Additionally, removal efficiency, polyphosphate production and metal localization patterns were also analyzed. *O. anthropi* DE2010 showed high resistance to the tested metals, supporting concentrations of up to 20 mM for Zn and 10 mM for the rest of the elements. The bacterium also demonstrated a high removal capacity of metals—up to 90% and 40% for Pb(II) and Cr(III), respectively. Moreover, polyphosphate production was strongly correlated with heavy metal concentration, and three clear cell localization patterns

of metals were evidenced using compositional and imaging techniques: (i) extracellular in polyphosphate granules for Cu(II); (ii) in periplasmic space forming crystals with phosphorus for Pb(II); and (iii) intracytoplasmic in polyphosphate inclusions for Pb(II), Cr(III), and Zn. The high resistance and metal sequestration capacity of *O. anthropi* DE2010 both highlight its great potential for bioremediation strategies, especially in Pb and Cr polluted areas.

Keywords: bioaccumulation; biomineralization; heavy metal; polyphosphate production; sequestration

1. Introduction

Heavy metals are persistent pollutants widely spread in ecosystems worldwide. Of the heavy metals, non-essential metals such as lead (Pb) and cadmium (Cd) have no known biological role in living organisms, often inducing highly toxic effects in biota even at low concentrations and over short exposure times (Olmedo et al. 2013; revision in Abtahi et al. 2017; revision in Yilmaz et al. 2018; Rani et al. 2019; Zhu et al. 2020). In contrast, although small levels of essential metals such as copper (Cu), chromium (Cr), and zinc (Zn) are necessary for the right metabolic functioning of plant and animal cells, they are hazardous when their environmental levels and/or body burdens increase (revision in Nagajyoti et al. 2010; Prashanth et al. 2015; Hirve et al. 2020).

Especially sensitive areas such as deltas are fragile coastal wetlands with unique species and ecosystems highly disturbed both by pollutants transported through rivers and by *in situ* anthropogenic impacts (Bruins et al. 2000; Selvin et al. 2009; Masindi and Muedi 2018). The protected area of Ebro Delta (Tarragona, NE Spain) has historically been polluted by industry, agriculture, hunting, and domestic effluents, representing the environmental

status of deltas worldwide (Mañosa et al. 2001; Sánchez-Chardi and López-Fuster, 2009; Dhanakumar et al. 2015). Consequently, an increase in metals such as Cd, Pb, Cu, Cr and Zn has been reported in the waters, soils, plants and animals of this protected coastal wetland (revision in Mañosa et al. 2001). Deltas are also the suitable habitats for microbial mats formed by different microorganisms, mainly phototrophs (algae and cyanobacteria) and heterotrophs (bacteria), with crucial ecological functions such as sediment stabilization (Seder-Colomina et al. 2013; Millach et al. 2019). Several microorganisms have also been reported to be highly efficient in capturing heavy metals both in natural habitats and axenic laboratory cultures (Zhang et al. 2013; Coelho et al. 2015; Chaturvedi et al. 2015; Yin et al. 2016; Li et al. 2018; Maleke et al. 2019; revision in Yin et al. 2019). However, little is known about their specific strategies of immobilization and localization patterns or their morphological responses against metal exposure. Some phototrophic (*Microcoleus chthonoplastes* DE2006, *Scenedesmus* sp. DE2009, *Geiltherinema* sp. DE2011) and heterotrophic (*Paracoccus* sp. DE2007, *Micrococcus luteus* DE2008, *Ochrobactrum anthropi* DE2010) microorganisms from Ebro Delta mats have been tested in axenic laboratory cultures to analyze their ability capturing metals such as Cr(III), Pb(II), and Cu(II) (e.g. Burnat et al. 2009; Burgos et al. 2013; Maldonado et al. 2010a,b; Puyen et al. 2012; Millach et al. 2015; Villagrasa et al. 2019, 2020a). Interestingly, all these isolated microorganisms have the capacity to sequester metals externally (biosorption) in extracellular polymeric substances (EPS), with this ability becoming especially high in *Micrococcus luteus* DE2008 for Cu(II) and Pb(II) metals (Puyen et al. 2012). Additionally, some of them, mainly phototrophic microorganisms, have also demonstrated the capacity to accumulate metals intracellularly (bioaccumulation) in polyphosphate (polyP) inclusions, which is especially

interesting for bioremediation of contaminated environments. Among such microorganisms, the gram-negative heterotrophic bacterium *O. anthropi* DE2010 has recently emerged as an interesting species due to relevant genomic findings concerning polyP production and heavy metal concentration and its high efficiency in removing and accumulating Cr(III) in intracytoplasmic polyphosphate (polyP) inclusions and EPS (Villagrasa et al. 2020a,b). This species grows easily in liquid and solid cultures and could become a suitable model for experimental studies of heavy metals. However, despite the great interest in understanding the capacity of microbiota in microbial mats for capturing and accumulating essential and non-essential heavy metals, this aspect lacks adequate research. Taking this into consideration, a multi-analytical approach assessing several parameters related to the effects of exposure to Cd, Pb, Cu, Cr, and Zn was performed using microbiological cell counts by means of an optical profilometer (OP), growth curves, minimal inhibitory concentration (MIC), and half-maximal inhibitory concentration (IC$_{50}$). Moreover, analytical chemistry (inductively coupled plasma optical emission spectrometer (ICP-OES)), and analytical and morphometric high-resolution (HR) microscopy, (transmission electron microscopy (TEM), and field emission scanning electron microscopy (FESEM)) techniques have been applied from both qualitative and quantitative assessments. With all this in mind, the main goals of the present study with this bacterium *O. anthropi* DE2010 exposed to a range of Cd, Pb(II), Cu(II), Cr(III), and Zn concentrations were as follows: (i) to analyze bacterial responses against metal exposure quantifying cell survival, uptake efficiency, and removal capacity at 24 h after being exposed to a single metal dose; (ii) to evaluate ultrastructural changes due to metal exposure; (iii) to localize metals at nanoscale showing patterns related to polyP production and structure as a mechanism to

immobilize potentially toxic elements; and (iv) to discuss the potential applications of this species in metal immobilization.

2. Materials and methods

2.1 Microorganism, single heavy metal stock solutions, and culture sample preparation

O. anthropi DE2010 isolated from *Scenedemus* consortium from Ebro Delta microbial mats was recently characterized and identified (Villagrasa et al. 2019). The bacterium was cultured in Luria-Bertani (LB) medium containing tryptone (10 g L^{-1}), yeast extract (5 g L^{-1}), sodium chloride (10 g L^{-1}), and bacteriological agar (15 g L^{-1}) at 27 °C (pH 7.0).

Stock solutions of each heavy metal (50 mM) were prepared in sterile double deionized water from the following salts: Cd from cadmium chloride (Acros Organics), Pb(II) from lead nitrate (Merk), Cu(II) from copper sulphate (Merk), Cr(III) from chromium nitrate (Sigma-Aldrich), and Zn from zinc sulphate (Riedel-deHäen). Then, experimental solutions were freshly prepared by diluting the stock solutions in LB medium to obtain the tested concentrations: 0.5, 2, 5, 7, and 10 mM for Cd, Pb(II), Cu(II), and Cr(III); and 2, 5, 10, 15, and 20 mM for Zn. The pH of all experimental solutions was adjusted at 5.5 to prevent heavy metal precipitation.

For all experiments, unpolluted (0 mM) and polluted cultures were prepared in the same conditions for each heavy metal in the following manner: 2 mL of 24 h culture of *O. anthropi DE2010* grown in LB (OD_{600}) ranging between 1.4 and 1.6 (approximately 10^{10} cfu mL^{-1}) was inoculated into 18 mL of LB liquid medium with the different tested concentrations for each heavy metal (final volume 20 mL). All cultures were incubated in an

orbital shaker (Infors HT, Ecotron) (150 rpm) at 27 ºC for 24 h. The pH of all the cultures was adjusted at 5.5 to prevent heavy metal precipitation.

2.2 Minimal inhibitory concentration (MIC), growth curves, and half maximal inhibitory concentration (IC$_{50}$)

The MIC of each heavy metal tested was determined in triplicate by adding 10 μL (one drop) of each experimental metal solution (concentrations tested in a range of 0.5–25 mM) onto LB agar plate surfaces over which *O. anthropi* DE2010 had just been spread. MIC was considered as the metal concentration at which no bacterial growth was detected in the drop zone (Luli et al. 1983) after bacterial growing at 2 ºC during 48 h.

For growth curves assays, aliquots *of O. anthropi* DE2010 were dispensed in a 96-well microplate (20 μL per well), achieving the different tested metal concentrations (0, 0.5, 2, 5, 7, and 10 mM for Cd, Pb(II), Cu(II), and Cr(III); and 0, 2, 5, 10, 15, and 20 mM for Zn) in final volume per well of 200 μL. Blank samples (bacteria-free LB medium with or without metals) and a control (bacterial LB medium without metals) were included in each 96-well microplate (Villagrasa et al. 2020a). The *O. anthropi* DE2010 growth was determined in a Varioskan plate reader (Thermo Fisher Scientific) by turbidity measurements (λ= 600 nm) every 30 min at 27 ºC, over 24 h. The half maximal inhibitory concentration (IC$_{50}$) from samples was determined for each heavy metal sample, as described by Volpe et al. (2014).

2.3 Cell counts by optical profilometer (OP)

All exposed and non-exposed *O. anthropi* DE2010 samples were prepared in glass slides coated with poly-L-lysine (Sigma-Aldrich) by depositing 8 μL of the sample inside a 1 cm^2 square and then spreading it onto the surface, creating a thin monolayer of bacterial cells. The samples were fixed with temperature and coated with a thin layer of Au-Pd using

the E5000 Sputter Coater (Bio-Rad) to improve their contrast. The quantitative surface measurements of bacterial cells were obtained using an OP Leica DCM 3D (Leica microsystems) with dual technology (confocal and interferometric). The triplicates of vertical scanning interferometry images with an area of 250.64x190.90 μm^2 were randomly obtained for each sample and analyzed in quality topography mode using Leica map DCM 3D, version 6.2.6561 (Leica Microsystems).

2.4 Metal quantification by inductively coupled plasma optical emission spectrometry (ICP-OES)

Cd, Pb(II), Cu(II), Cr(III), and Zn concentrations immobilized into the cells were quantified in *O. anthropi* DE2010 cultures to measure both the cellular uptake efficiency and removal capacity of metals. All the samples were centrifuged at 5,000x g at 4 ºC for 20 min (Eppendorf 5804R) and the resulting supernatants were analyzed as described by Villagrasa et al. (2020a). Cd, Pb(II), Cu(II), Cr(III), and Zn concentrations were quantified at 228.80, 220.40, 327.40, 267.72, and 206.20 nm, respectively, in triplicate assays using an ICP-OES spectrometer Optima 4300Dv (Perkin Elmer).

2.5 Cell lysis and quantification of polyphosphate (PolyP) production

For polyP extraction, the metal and control cultures were centrifuged at 5,500x g at 4ºC for 15 min, the supernatants discarded, and the pellets resuspended in 50 mM Tris-HCl buffer (pH 7.0). Samples were then ultrasonicated in SONOREX (Bandelin) in an ice bath for 15 min, followed by centrifugation at 5,500x g at 4 ºC for 20 min to remove cell debris. The resultant supernatants were treated with a protease inhibitor cocktail tablet (Roche). The polyP content was determined through the reaction of molybdenum blue method (Ansvhutz et al. 2016) with reactive phosphorus content. All assays were performed in

triplicate for each sample, and polyP production (μmol of polyP per g^{-1} dry weight of biomass) results were obtained by taking into account the difference between total and soluble cellular phosphorus following the protocol described by Eixler et al. (2005).

2.6 Ultrastructural and analytical assessment with electron microscopy

A complete evaluation of ultrastructural morphometry and sub-cellular metal localization was performed using four high-resolution (HR) electron microscopy techniques. Metal exposed and non-exposed cultures of *O. anthropi* DE2010 were centrifuged at 5,000x *g* during 20 min at 4 ºC in a refrigerated centrifuge (Eppendorf 5804R). The resulting pellets were included in soft agar (3% agarose) and processed following conventional transmission electron microscopy (TEM) procedures optimized to this type of samples (Maldonado et al. 2010a; Villagrasa et al. 2019; Solé et al. 2019). Briefly, samples were fixed with 2.5% glutaraldehyde (Merck) in 0.1 M Millonig buffer (Millonig 1961) for 2 h, postfixed in 1% osmium tetroxide containing 0.8% potassium hexoferrocyanide in Millonig buffer for 1 h, dehydrated in acetone, embedded in Spurr resin, and polymerized at 60 ºC for 48 h. Ultrathin sections (70 nm) of selected areas from semithin sections (1 μm) were obtained with an ultramicrotome UCT7 (Leica Microsystems).

For ultrastructural studies with TEM, a set of ultrathin sections was placed in carbon coated Cu grids (200 mesh) and contrasted following a routine protocol of uranyl acetate and lead citrate solutions. Randomly distributed sections of at least 2 grids of each sample were analyzed in a TEM JEM-1400 (Jeol) equipped with an Erlangshen CCD camera (Gatan) and operating at 80kV.

For analytical studies, with TEM and field emission scanning electron microscope (FESEM), another set of samples was placed in carbon coated Au grids (100 mesh) and

observed without contrasting in HR microscopes. For HR-TEM, samples were analyzed in a TEM JEM-2011 (Jeol) equipped with an 895 USC 4000 CCD camera (Gatan) and operating at 200 kV. Compositional and crystallographic studies of polyP aggregates (granules and inclusions) were performed using an energy dispersive X-ray (EDX) analysis and selected area electron diffraction (SAED), respectively. The obtained diffraction powder ring patterns allowed us to know the kind of sample, following this description: (i) amorphous (diffuse rings), (ii) crystalline (bright spots), and (iii) polynanocrystalline (small spots making up rings) (Meshi, 2012). For HR-SEM, the same samples were observed in a FESEM Merlin (Zeiss) operating at 2 kV and equipped with a backscattered (BSE) detector.

2.7 Statistical analysis

Quantitative data were tested for both normal distribution and homogeneity of variances, using Kolmogorov-Smirnov and Levene's tests, respectively. The statistical comparisons between groups were carried out using one-way analysis of variance (ANOVA), Bonferroni's pairwise test and Tukey's multiple comparison *posthoc* test. Significant differences in ANOVA, Bonferroni's, and Tukey's test were accepted at $p \leq 0.05$. The analyses were performed using SPSS software (version 20.0 for Windows 7). All quantitative data are expressed as mean ± standard error (SE) of the mean.

3. Results and discussion

In the present study, a combination of qualitative and quantitative microbiological, morphological, and analytical techniques was selected to provide a comprehensive overview of the bacterium *O. anthropi* DE2010's responses to heavy metals exposure.

3.1 Cytotoxic effect of heavy metals

The cytotoxic effect of heavy metals exposure in *O. anthropi* DE2010 cultures was determined using IC_{50} and MIC values (Fig. S1, supplementary material). Results from both parameters showed the same cellular responses against each metal exposure. Then, the IC_{50} values remained in the same range (3.5 mM in Cd to 5 mM in Pb(II)), but were highest for Zn (10 mM). These values in *O. anthropi* DE2010 were slightly higher than those obtained in environmental bacteria for Cu(II) and Cd (2.65 and 4.30 mM, respectively) (Nweke et al. 2007), in *Salmonella* sp. for Zn (0.8 mM) (Bestawy et al. 2013), and for Cd, Pb(II), and Cu(II) of 0.005, 0.006, 0.03 mM respectively for *Photobacterium phosphoreum* T3S (Zeb et al. 2017). The MIC values obtained for *O. anthropi* DE2010 were 10 mM for Cd, Pb(II), Cu(II), and Cr(III), and 20 mM for Zn. These values exceed the MIC obtained for *Escherichia coli* ATCC25922, which has been treated as a reference in MIC assays (Bhardwaj et al. 2018). All this information pointed to the high resistance of *O. anthropi* DE2010 to exposure at high concentrations of heavy metals, especially to Zn, considered toxic for other microbial species. These findings highlight a plethora of effective resistance mechanisms in these bacterial cells, such as extracellular sequestration, intracellular sequestration, active export and enzymatic detoxification, which help them interact with metals as well as tolerate rapid environmental changes in metal levels (revision in Yin et al. 2019).

The descriptive statistics of cell counts at each metal concentration evaluated with an OP are shown in Figure 1. Interestingly, the cell numbers decrease when metal concentrations increase, reaching the minimum values at the highest metal concentrations (10 mM for Cd, Pb(II), Cu(II), and Cr(III), and 20 mM for Zn). From this perfect correlation, the most pronounced cytotoxic effect resulting in an abrupt cell decrease of around 40%

and 25% was detected between 0.5 and 2 mM for Cd and Pb(II) respectively, and of more than 30% between 2 and 5 mM for the rest of the metals.

Significant differences ($p < 0.05$) in cell counts obtained with ANOVA comparison were found among all the metal concentrations for Cd (F=68.76), Pb(II) (F= 56.25), Cu(II) (F= 107.1), Cr(III) (F= 330.4), and Zn (F= 16.39). Significant reductions in cell count of 85% for Cd, 80% for Pb(II), 79% for Cu(II), 84% for Cr(III), and 47% for Zn were observed upon comparing controls with samples exposed to 10 mM of each metal. These percentages agree with those obtained for IC_{50} and MICs and strongly suggest that metal toxicity for *O.anthropi* DE2010 is Cd>Cr(III)>Pb(II)>Cu(II)>Zn, cadmium being the most toxic and zinc the least. Moreover, the presence of live cells at all metal concentrations demonstrates the high tolerance of this bacterium to the deleterious effects of each of the five heavy tested metals strongly suggesting a similar behavior against exposure to other potentially toxic elements.

3.2 Heavy metals removal and uptake efficiencies

The descriptive statistics of metal removal and uptake efficiency of *O. anthropi* DE2010 for each metal and concentration are shown in Tables 1 and S1 (supplementary material). The highest removal capacity found in *O. anthropi* DE2010 was around 90% for Pb(II), followed by around 40% for Cr(III). Lower capacities of 20%, 10%, and 3.0% were detected for removal of Zn, Cd, and Cu(II), respectively. Moreover, similar ranges of metal removal (Pb(II)>Cr(III)>Cd>Zn>Cu(II)) and uptake efficiency (Pb(II)>Cr(III)>Cu(II)>Cd>Zn) were found at the highest common concentration for all metals (10 mM). Significant differences ($p < 0.05$) obtained with ANOVA comparison were found among all the metal concentrations for Cd (F= 20.66), Pb(II) (F=13,271), Cu(II) (F= 19.53), Cr(III) (F= 1,190), and

Zn (F= 22.76). Moreover, the Tukey multiple comparisons are labelled in Table 1. Comparing

between metals, *O. anthropi* DE2010 is able to capture 82-fold more Pb than Cu, and *q*

values are 15-fold more for Pb (*q*= 1,548 mg g^{-1}) than for Zn (*q*= 102 mg g^{-1}). Removal

rates of 36% for Cd, 18% for Pb(II),13% for Cu(II), 39% for Cr, 9.0% for Zn (Chatterjee et al.

2010), and of 15% for Cr (Joutey et al. 2014) have been previously described in an

environmental isolate bacterium and *Serratia proteamaculans*. Moreover, *q* values of

around 200 mg g^{-1} for Pb(II) in *Klebsiella* strain R19 (Bowman et al. 2018) and of 29.80 mg

g^{-1} in *Exiguobacterium* sp. ZM-2 for Cr were reported (Alam and Ahmad, 2011). Comparing

these species, *O. anthropi* DE2010 emerges as an extremely efficient bacterium to remove

heavy metals, especially Pb and Cr.

3.3 Heavy metals induction of polyP production

PolyP production in *O. anthropi* DE2010 cultures varied according to the heavy

metal and its concentration (Fig. 2). Significant differences (*p* <0.05) obtained with ANOVA

comparison were found for Pb(II) (F= 77.50), Cu(II) (F= 521.7), Cr(III) (F= 671.9), and Zn (F=

679.7). The levels of polyP (μmol of polyP per g^{-1} dry weight of biomass) were clearly

correlated with the increment of Pb(II), Cu(II), Cr(III), and Zn, being 3, 3.5, 4, and 4.5-fold

more in higher metal concentrations compared to control. These findings agree with those

obtained by Francisco et al. (2011) and Andreeva et al. (2014), demonstrating that polyP

concentration increased in microbial cultures exposed to heavy metals. In marked contrast,

the concentration of polyP is practically unvarying among all ranges of Cd concentrations

(Fig 2A) in spite of 10% of Cd being captured by *O. anthropi* DE2010. Neither induced polyP

production nor Cd bioaccumulation in intracytoplasmic polyP inclusions strongly suggests

a different bacterial response for Cd. This metal probably could be adsorbed in EPS also

due to the sorption ability of *O. anthropi* DE2010, as reported recently for Cr (Villagrasa et al. 2020).

3.4 Heavy metals localization patterns and cellular survival strategies

The imaging of morphological alterations and cellular localization of heavy metals in *O. anthropi* DE2010 at nanoscale was performed with four high-resolution microscopy techniques (Fig. 3). The ultrastructure of unpolluted cultures showed typical morphology (size and shape) of bacterial cells with scarce or small polyP inclusions (Figs. 3 A1 and A2), as reported in Villagrasa et al. (2019). Those inclusions act as a phosphorus reservoir without metal content detectable by EDX or BSE and with amorphous structure by SAED (Figs. 3 A2-A4). In contrast, heavy metals exposure disturbed normal cell metabolism, altering the bacterial morphology. Moreover, intracellular ultrastructure indicated different degrees of alteration, including evident cytoplasm disorganization and retraction (Figs. 3 B1-F1), as well as an increase of pleomorphic cells in Pb(II), Cr(III), and Cu(II) exposed cells (Figs. 3 C1-E1). The high toxicity of these metals in aquatic environments and their relationship with the presence of pleomorphic cells have been reported in microbial species (e.g., Hasnain and Sabri, 1992; Villegas et al. 2013; Bulaev et al. 2017).

The analytical studies with EDX and BSE demonstrated that polyP aggregates containing phosphorus are the main storage structures of metals in *O. anthropi* DE2010 cells and have metal-specific patterns of sub-cellular localization (Figs. 3 B2-E2, B4-E4). Cu(II) induced granules are mainly located extracellularly in the outer membrane surface (Fig. 3 D2), besides Cr(III) and Zn induced inclusions, mostly in the cell cytoplasm (Figs. 3 E2 and F2, respectively), and Pb(II) in both the periplasmic space and the cytoplasm (Fig. 3 C2). In marked contrast, the results in Cd(II) exposed cultures showed no evident morphological

changes and polyP inclusions evidenced no metal content (Fig. 3 B2). It must be noted that the different electron diffraction/SAED patterns obtained from the polyP aggregates showed a general amorphous type of crystallographic structure, (Figs. 3 B3, D3-F3), as often occurs in biological systems, except for Pb(II), which is crystalline (Fig. 3 C3). This particular result indicates that *O. anthropi* DE2010 is not only able to bioaccumulate Pb(II) but can also biomineralize it highly efficiently, as a mechanism to reduce its bioavailability and consequently its biological impact in bacterial cells.

Overall, these results show rapid, varied, and specific responses to different metal stressors and the great importance of polyP production in metal chelation and sequestration by active processes of bacterial bioaccumulation and/or biomineralization. This metal bioimmobilization is an effective mechanism in reducing metal bioavailability, preventing and/or avoiding toxic effects. Moreover, this ultrastructural information about metal toxicity can be confirmed by metal localization in bacterial cells.

3.5 Potential applications in metal immobilization

O. anthropi DE2010 cells can rapidly respond to metals exposure using different strategies such as bioaccumulation and biomineralization in combination with biosorption. These pathways were extremely efficient in chelating Pb and Cr. Also, the cellular bioaccumulation of Zn and the ability to store Cu(II) in external polyphosphate granules were evidenced. All of these processes can be considered for potential applications in the reduction of bioavailability of these metals that are often highly toxic for biota in aquatic environments (Sánchez-Chardi et al. 2007; Sánchez-Chardi and López-Fuster, 2009; Seder-Colomina et al. 2013). Finally, Cd biosorption in EPS physicochemical binding could be easily broken by other competitors (e.g., cations, chelators, etc.), resulting in secondary pollution

when used in bioremediation strategies. All our findings with *O. anthropi* DE2010 point to the high efficiency of this bacterial species in chelating metals from the environment using different metabolic pathways. These data suggest a high metabolic plasticity in *O. anthropi* DE2010 (e.g. Comte et al. 2013, Guerrero and Berlanga, 2016).

In addition to our promising results, more specific studies are needed to evaluate the advantages of each bacterial strategy to localize and bind specific metals and different chemical species. Moreover, further analysis of the capacity of *O. anthropi* DE2010 to remove them in mixed metal solutions and microcosm experiments are also crucial to consider the feasibility of this bacterium in bioremediation processes in natural ecosystems. Up to now, our results with individually high concentrations of five widely distributed heavy metals strongly suggest that this bacterial species can be considered as a valuable player in future bioremediation strategies with biological systems, especially in Pb and Cr polluted environments, more so when concentrations of these metals are lethal for other prokaryotic and eukaryotic organisms.

4. Conclusions

O. anthropi DE2010, isolated from polluted Ebro Delta microbial mats, exhibited resistance to high concentrations of heavy metals and an unusual ability to sequestrate Pb(II) and Cr(III), which is especially high for Pb(II). In an active process, bacterial cells immobilized heavy metals in polyP inclusions and/or granules, besides phosphorus crystalline structures, to reduce their biological toxic effects. Those structures followed a metal-specific pattern in cell distribution.

In summary, *O. anthropi* DE2010 revealed specific responses as survival strategies for each heavy metal exposure, including bioaccumulation (for Pb(II), Cu(II), Cr(III), and Zn), biosorption (for Cd), and biomineralization (for Pb(II)).
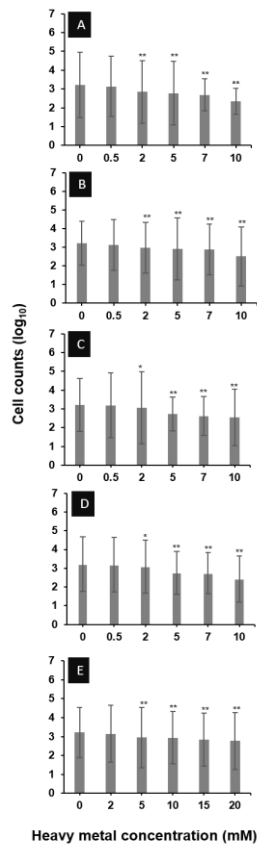
Figure 1. Cell counts (log$_{10}$) in the *O. anthropi* DE2010 cultures grown at increasing concentrations of Cd (A), Pb(II) (B), Cu(II) (C), Cr(III) (D), and Zn (E). Data are expressed as mean ± SE (n=3). Significant differences between control and metal exposed samples (* $p < 0.05$, ** $p < 0.01$).

Figure 2. Polyphosphate content (µmol of polyP per g^{-1} dry weight of biomass) in the *O. anthropi* DE2010 cultures grown at increasing concentrations of Cd (A), Pb(II) (B), Cu(II) (C), Cr(III) (D), and Zn (E). Data are expressed as mean ± SE (n=3). Significant differences between control and metal exposed samples (* $p < 0.05$, ** $p < 0.01$).
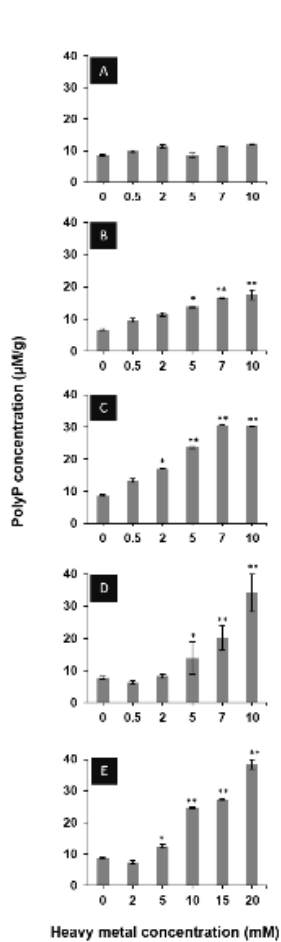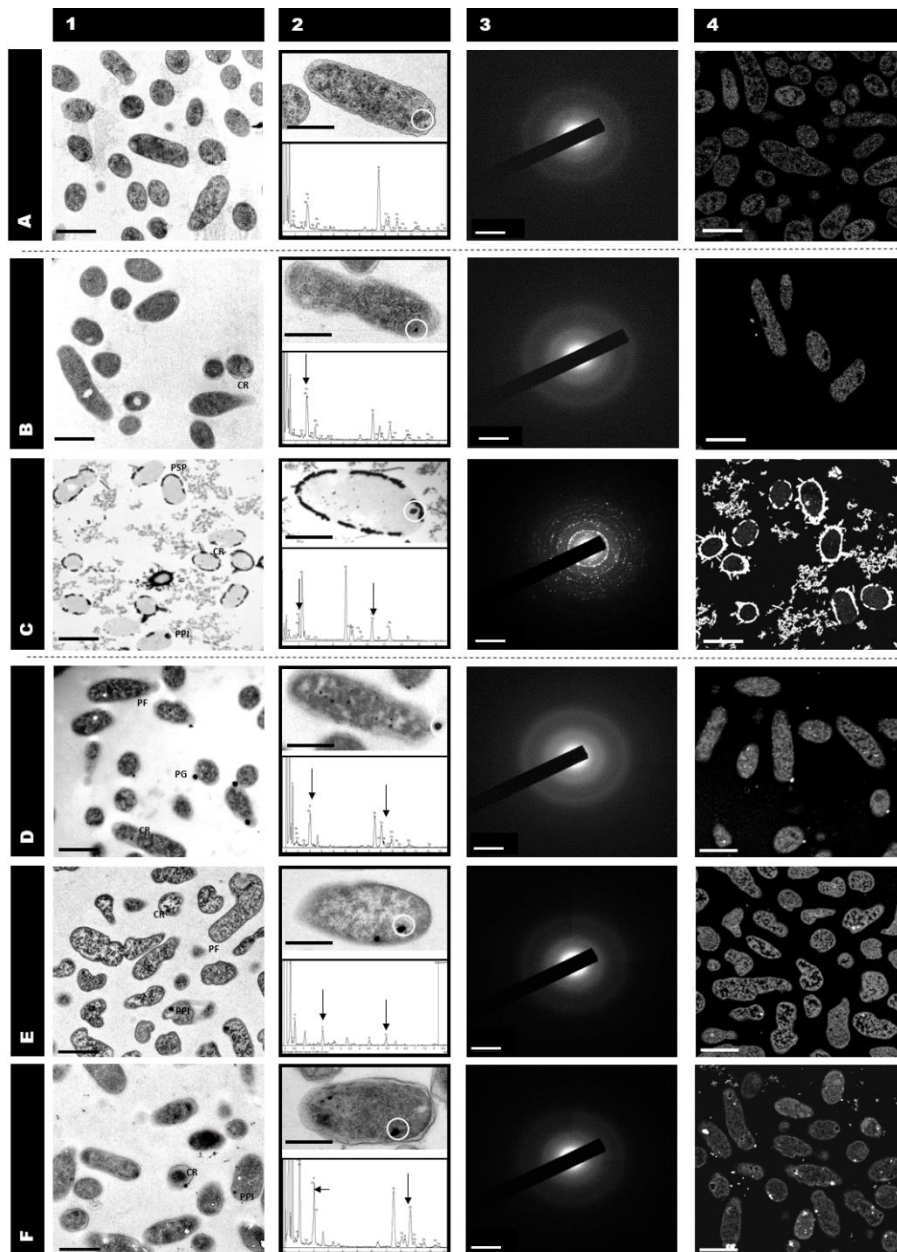
Figure 3. High resolution imaging by electron microscopy techniques: TEM (1), TEM-EDX (2), TEM-SAED (3), and FESEM BSE (4) in the *O. anthropi* DE2010 unexposed (A); and those exposed to 10 mM of Cd (B), Pb(II) (C), Cu(II) (D), Cr(III) (E), and 20 mM of Zn (F) cultures. The arrows of EDX analyses show the representative peak of phosphorus and the assayed heavy metal, respectively. The scale bars represent 1 μm, 0.5 μm, 5 nm^{-1}, and 1 μm for TEM, TEM-EDX, TEM-SAED, and FESEM BSE, respectively. In the TEM figures: Cytoplasm retraction (CR); periplasmic space precipitate (PSP); pleomorphic forms (PF); polyP granules (PG); and polyP inclusions (PPI).

Table 1. Metal removal capacities by ICP-OES in *O. anthropi* DE2010 cultures grown at increasing concentrations of Cd, Pb(II), Cu(II), Cr(III) and Zn

Metal removed (mg L^{-1})

[mM]	Cd	Pb(II)	Cu(II)	Cr(III)*	[mM]	Zn
0	0	0	0	0	0	0
0.5	0	26 ± 0.2	0	7.5 ± 0.6	2	17.0 ± 0.5
2	5.00 ± 0.01	117 ± 2**[++]	5 ± 3	16 ± 2**	5	31 ± 20
5	20 ± 3	331 ± 19**[++$$]	12 ± 1*[+]	58 ± 6**[++$$]	10	51 ± 31
7	15.00 ± 0.04	1,340 ± 2**[++$$&&]	10 ± 1*[+]	148 ± 3**[++$$&&]	15	147 ± 10**[++$$&&]
10	66 ± 12**[++$$&&^^]	1,629 ± 22**[++$$&&^^]	20 ± 2**[++$$^^]	190 ± 9**[++$$&&^^]	20	133 ± 51**[++$$&&]

*All of these Cr(III) uptake results have been taken from Villagrasa et al. 2019
Data are expressed as mean ±SE (n=3)

*p <0.05; **p <0.01: For Cd, Pb(II), Cu(II), and Cr(III): 0.5, 2, 5, 7 and 10 mM treatments vs. control (0 mM); and for Zn: 2, 5, 7, 10, 15 and 20 mM treatments vs. control (0 mM).

[+]p <0.05; [++]p <0.01: For Cd, Pb(II), Cu(II), and Cr(III): 2, 5, 7, and 10 mM treatments vs. 0.5 mM treatment; and for Zn: 5, 7, 10, 15 and 20 mM treatments vs. 2 mM treatment.

[$$]p <0.01: For Cd, Pb(II), Cu(II), and Cr(III): 5, 7, and 10 mM treatments vs. 2 mM treatment; and for Zn: 7, 10, 15 and 20 mM treatments vs. 7 mM treatment.

[&&]p <0.01: For Cd, Pb(II), Cu(II), and Cr(III): 7 and 10 mM treatments vs. 5 mM treatment; and for Zn: 15 and 20 mM treatments vs. 10 mM treatment.

[^^]p <0.01: For Cd, Pb(II), Cu(II), and Cr(III): 10 mM treatment vs. 7 mM treatment and for Zn: 20 mM treatment vs. 15 mM treatment

References:

Abtahi, M., Fakhri, Y., Conti, G.O., Keramati, H., Zandsalimi, Y., Bahmani, Z., Pouya, R.H., Sarkhosh, M., Bigard Moradi, Amanidaz, N., Ghasemi, S.M. 2017. Heavy metals (As, Cr, Pb, Cd and Ni) concentrations in rice (*Oryza sativa*) from Iran and associated risk assessment: a systematic review, Toxin Reviews 36:(4)331-341. http://dx.doi.org/10.1080/15569543.2017.1354307

Alam, M.Z. and Ahmad, S. 2011. Chromium removal through biosorption and bioaccumulation by bacteria from tannery effluents contaminated soil. Clean (Weinh) 39: 226-237. https://doi.org/doi:10.1002/clen.201000259.

Andreeva, N., Ryazanova, L., Dmitriev, V., Kulakovskaya, T., Kulaev, I. 2014. Cytoplasmic inorganic polyphosphate participates in the heavy metal tolerance of *Cryptococcus humicola*. Folia Microbiol 59 (5):381-389. https://doi.org/10.1007/s12223-014-0310-x.

Bestawy, E.E., Helmy, S., Hussien, H., Fahmy, M., Amer, R. 2013. Bioremediation of heavy metal-contaminated effluent using optimized activated sludge bacteria. Appl Water Sci 3:181–192. https://doi.org/10.1007/s13201-012-0071-0.

Bhardwaj, R., Gupta, A., Garg, J.K. 2018. Impact of heavy metals on inhibitory concentration of *Escherichia coli*—a case study of river Yamuna system, Delhi, India. Environ Monit Assess 190:674. https://doi.org/10.1007/s10661-018-7061-0.

Bowman, N., Patel, D., Sanchez, A. et al. 2018. Lead-resistant bacteria from Saint Clair River sediments and Pb removal in aqueous solutions. Appl Microbiol Biotechnol 102, 2391–2398. https://doi.org/10.1007/s00253-018-8772-4

Bruins, M.R., Kapil, S., Oehme, F.W. 2000. Microbial resistance to metals in the environment. Ecotoxicol Environ Saf 45 (3): 198–207. https://doi.org/10.1006/eesa.1999.1860.

Bulaev, A.G., Erofeeva, T.V., Labyrich, M.V., Mel'nikova, E. A. 2017. Resistance of *Acidiplasma* archaea to heavy metal ions. Microbiology 86:583–589. https://doi.org/10.1134/S002626171705006X.

Burgos, A., Maldonado, J., De los Rios, A., Solé, A., Esteve, I. 2013. Effect of copper and lead on two consortia of phototrophic microorganisms and their capacity to sequester metals. Aquat Toxicol 140–141:324–336. https://doi.org/10.1016/j.aquatox.2013.06.022.

Burnat, M., Diestra, E., Esteve, I., Sole, A. 2009. In situ determination of the effects of lead and copper on cyanobacterial populations in microcosms. PLoS ONE 4(7):e6204. https://doi.org/10.1371/journal.pone.0006204.

Chatterjee, S.K., Bhattcharjee, I., Chandra, G. 2010. Biosorption of heavy metals from industrial waste water by *Geobacillus thermodenitrificans*. J Hazard Mater 175(1):117-125. https://doi.org/10.1016/j.jhazmat.2009.09.136.

Chaturvedi, A.D., Pal, D., Penta, S., Kumar, A. 2015. Ecotoxic heavy metals transformation by bacteria and fungi in aquatic ecosystem. World J Microbiol Biotechnol (2015) 31: 1595. https://doi.org/10.1007/s11274-015-1911-5

Coelho, L.M., Rezende, H.C., Coelho, L.M., de Sousa, P.A.R., Melo D.F.O., Coelho, N.M.M. 2015. Chapter 1: Bioremediation of polluted waters using microorganisms. In Advances in Bioremediation of Wastewater and Polluted Soil. InTech. https://doi.org/10.5772/60770.

Comte, J., Fauteux, L., del Giorgio, P. 2013. Links between metabolic plasticity and functional redundancy in freshwater bacterioplankton communities. Frontiers in Microbiology 4:112. https://doi.org/10.3389/fmicb.2013.00112.

Dhanakumar, S., Solaraj, G., Mohanraj, R. 2015. Heavy metal partitioning in sediments and bioaccumulation in commercial fish species of three major reservoirs of river Cauvery delta region India. Ecotoxicol Environ Saf 113: 145-151. https://doi.org/10.1016/j.ecoenv.2014.11.032.

Eixler, S., Selig, U., Karsten, U. 2005. Extraction and detection methods for polyphosphate storage in autotrophic planktonic organisms. Hydrobiologia 533(1–3):135–143. https://doi.org/10.1007/s10750-004-2406-9.

Francisco, R., de Abreu, P., Plantz, B.A., Schlegel, V.L., Carvalho, R.A., Vasconcelos-Morais, P. 2011. Metal-induced phosphate extracellular nanoparticulate formation in *Ochrobactrum tritici* 5bvl1. J Hazard Mater 198:31-39. https://doi.org/10.1016/j.jhazmat.2011.10.005.

Guerrero, R., Berlanga, M. 2016. From the Cell to the Ecosystem: The Physiological Evolution of Symbiosis. Evol Biol 43:543–552. https://doi.org/10.1007/s11692-015-9360-5.

Hasnain, S and Sabri, N.A. 1992. Effects of temperature and pH on conjugal transfer of zinc-resistant plasmids residing in Gram-negative bacteria isolated from industrial effluents. Environ Pollut 76(3): 245-249. https://doi.org/10.1016/0269-7491(92)90143-X.

Hirve, M., Jain, M., Rastogi, A., Kataria, S. 2020. Chapter 8 - Heavy metals, water deficit, and their interaction in plants: an overview. Editor(s): Durgesh Kumar Tripathi, Vijay Pratap Singh, Devendra Kumar Chauhan, Shivesh Sharma, Sheo Mohan Prasad, Nawal Kishore Dubey, Naleeni Ramawat. Plant Life Under Changing Environment. Academic Press p. 175-206. https://doi.org/10.1016/B978-0-12-818204-8.00009-6.

Joutey, N.T, Bahafid, W., Sayel, H., Ananou, S., El Ghachtouli, N. 2014. Hexavalent chromium removal by a novel *Serratia proteamaculans* isolated from the bank of Sebou River (Morocco). Environ Sci Pollut Res 21:3060–3072. https://doi.org/10.1007/s11356-013-2249-x.

Li, F., Wang, W., Li, C., Zhu, R., Ge, F., Zheng, Y., Tang, Y. 2018. Self-mediated pH changes in culture medium affecting biosorption and biomineralization of Cd2+ by *Bacillus cereus* Cd01. J Hazard Mater 358:178-186. https://doi.org/10.1016/j.jhazmat.2018.06.066.

Luli, G.W., Talnagi, J.W., Strohl, W.R., Pfister. R.M. 1983. Hexavalent chromium-resistant bacteria isolated from river sediments. Appl Environ Microbiol 46(4):846-854.

Maldonado, J., Diestra, E., Domènech, A.M., Villagrasa, E., Puyen, Z.M., Esteve, I., Solé, A. 2010a. Isolation and identification of a bacterium with high tolerance to lead and copper from a marine microbial mat in Spain. Ann Microbiol 60(1):113-120. https://doi.org/10.1007/s13213-010-0019-2.

Maldonado, J., de los Rios, A., Esteve, I., Ascaso, C., Puyen, Z.M., Brambilla, C., Solé, A. 2010b. Sequestration and in vivo effect of lead on DE2009 microalga, using high-resolution microscopic techniques. J Hazard Mater 183 (1–3):44-50. https://doi.org/10.1016/j.jhazmat.2010.06.085.

Maleke, M., Valverde, A., Vermeulen, J.G., Cason, E., Moloantoa, K., Swarth, H., Van Heerden, E., Castillo, J. 2019. Biomineralization and bioaccumulation of europium by a thermophilic metal resistant bacterium. Front Microbiol 10:81. https://doi.org/10.3389/fmicb.2019.00081.

Mañosa, S., Mateo, R., Guitart, R. 2001. A review of the effects of agricultural and industrial contamination on the Ebro Delta biota and wildlife. Environ Monit Assess 71:187–205. https://doi.org/10.1023/A:1017545932219.

Masindi V. and Muedi, K.L. 2018. Environmental contamination by heavy metals. Heavy Metals, Hosam El-Din M. Saleh and Refaat F. Aglan, IntechOpen, https://doi.org/10.5772/intechopen.76082.

Meshi, L. 2012. Image formation in the electron microscope. In: Kolb U., Shankland K., Meshi L., Avilov A., David W. (eds). Uniting electron crystallography and powder diffraction. NATO science for peace and security series B: physics and biophysics. Springer, Dordrecht

Millach, L., Solé, A., Esteve, I. 2015. Role of *Geitlerinema* sp. DE2011 and *Scenedesmus* sp. DE2009 as bioindicators and immobilizers of chromium in a contaminated natural environment. BioMed Res Int Article ID 519769. https://doi.org/10.1155/2015/519769.

Millach, L., Villagrasa, E., Solé, A., Esteve, I. 2019. Combined confocal laser scanning microscopy techniques for a rapid assessment of the effect and cell viability of *Scenedesmus* sp. DE2009 under metal stress. Microsc Microanal 25(4):998-1003. https://doi.org/10.1017/S143192761901465X.

Millonig, G.1961. A modified procedure for lead staining of thin sections. J Biophys Biochem Cytol 11(3):736–739.

Nagajyoti, P.C., Lee, K.D., Sreekanth, T.V.M. 2010. Heavy metals, occurrence and toxicity for plants: a review. Environ Chem Lett 8 :199–216. https://doi.org/10.1007/s10311-010-0297-8

Nweke, C.O., Alisi, C.S., Okolo, J.C., Nwanyanwu, C.E. 2007. Toxicity of zinc to heterotrophic bacteria from a tropical river sediment. Appl Eco Environ Res 5(1):123–132.

Olmedo, P., Pla, A., Hernández, A.F., Barbier, F., Ayouni, L., Gil. F. 2013. Determination of toxic elements (mercury, cadmium, lead, tin and arsenic) in fish and shellfish samples. Risk assessment for the consumers. Environ Int 59: 63-72. https://doi.org/10.1016/j.envint.2013.05.005.

Prashanth, L., Kattapagari, K.K., Chitturi, R.T., Baddam, V.R.R., Prasad, L.K. 2015. A review on role of essential trace elements in health and disease. J. Dr. NTR Univ Health Sci 4: 75. https://doi.org/10.4103/2277-8632.158577.

Puyen, Z.M., Villagrasa, E., Maldonado, J., Diestra, E., Esteve, I., Solé, A. 2012. Biosorption of lead and copper by heavy-metal tolerant *Micrococcus luteus* DE2008. Bioresour Technol 126:233–237. https://doi.org/10.1016/j.biortech.2012.09.036.

Rani, P., Upadhaye, S.P. 2019. Review article: Status and prospects of bacterial/strains to cadmium resistant and their diversity isolated from waste sludge, Plant Archives, 19(1):827-844. e-ISSN:2581-6063 (online), ISSN:0972-5210.

Sánchez-Chardi, A., López-Fuster, M.J., Nadal, J. 2007. Bioaccumulation of lead, mercury, and cadmium in the greater white-toothed shrew, *Crocidura russula*, from the Ebro Delta (NE Spain): Sex- and age-dependent variation. Environ Pollut 145(1):7-14. https://doi.org/10.1016/j.envpol.2006.02.033.

Sánchez-Chardi, A., López-Fuster, M.J., 2009. Metal and metalloid accumulation in shrews (Soricomorpha, Mammalia) from two protected Mediterranean coastal sites. Environ Pollut 157(4), 1243-1248 . https://doi.org/10.1016/j.envpol.2008.11.047.

Seder-Colomina, M., Burgos, A., Maldonado, J., Solé, A., Esteve, I. 2013. The effect of copper on different phototrophic microorganisms determined in vivo and at cellular level by confocal laser microscopy. Ecotoxicology 22:199–205. https://doi.org/10.1007/s10646-012-1014-0.

Selvin, J., Priya, S.S., Kiran, G.S., Thangavelu, T., Bai, N.S. 2009. Sponge-associated marine bacteria as indicators of heavy metal pollution. Microbiol Res 164(3):352-363. https://doi.org/10.1016/j.micres.2007.05.005.

Solé, A., Calvo, M.A., Lora, M.J., Sánchez-Chardi, A. 2019. Chapter 12- Electron microscopy techniques applied to bioremediation and biodeterioration studies with molds. Araceli Tomasini Campocosio and Hector Hugo Leon Santiesteban. Fungal Bioremediation: Fundamentals and applications. CRC press. p 354. https://doi.org/10.1201/9781315205984.

Villagrasa, E., Ferrer-Miralles, N., Millach, L., Obiol, A., Creus, J., Esteve, I., Solé, A. 2019. Morphological responses to nitrogen stress deficiency of a new heterotrophic isolated strain of Ebro Delta microbial mats. Protoplasma 256:105-116. https://doi.org/10.1007/s00709-018-1263-8.

Villagrasa, E., Ballesteros, B., Obiol, A., Millach, L., Esteve, I., Solé, A. 2020a. Multi-approach analysis to assess the chromium(III) immobilization by *Ochrobactrum anthropi* DE2010. Chemosphere 238:124663. https://doi.org/10.1016/j.chemosphere.2019.124663

Villagrasa, E., Egea, R., Ferrer-Miralles, N., Solé, A. 2020b. Genomic and biotechnological insights in stress-linked polyphosphate production induced by chromium(III) in *Ochrobactrum anthropi* DE2010. World J Microbiol Biotechnol 36:97. https://doi.org/10.1007/s11274-020-02875-6.

Villegas, L.B., Pereira, C.E., Colin, V.L., Abate, C.M. 2013. The effect of sulphate and phosphate ions on Cr(VI) reduction by *Streptomyces* sp. MC1, including studies of growth and pleomorphism. Int Biodeter Biodegr 82:149-156. https://doi.org/10.1016/j.ibiod.2013.01.017.

Volpe, D.A., Hamed, S.S., Zhang, L.K. 2014. Use of different parameters and equations for calculation of IC50 values in efflux assays: potential sources of variability in IC50 determination. AAPS J 16:172. https://doi.org/10.1208/s12248-013-9554-7.

Yilmaz, A., Yanar, A., Alkan, E. 2018. Review of heavy metal accumulation in aquatic environment of northern east mediterranean sea. Part II: Some non-essential metals. Pollution, 4(1), pp. 143-181. https://doi.org/10.22059/poll.2017.236121.287.

Yin, K., Lv, M., Wang, Q., Wu, Y., Liao, C., Zhang, W., Chen, L. 2016 Simultaneous bioremediation and biodetection of mercury ion through surface display of carboxylesterase E2 from *Pseudomonas aeruginosa* PA1. Water Res 103:383-390. https://doi.org/10.1016/j.watres.2016.07.053.

Yin, K., Wang, Q., Lv, M., Chen, L. 2019. Microorganism remediation strategies towards heavy metals. Chem Eng J 360:1553-1563. https://doi.org/10.1016/j.cej.2018.10.226.

Zeb, B., Ping, Z., Mahmood, Q., Lin, Q., Pervez, A., Irshad,M., Bilal, M., Bhatti, Z.A., Shaheen, S. 2017. Assessment of combined toxicity of heavy metals from industrial wastewaters on *Photobacterium phosphoreum* T3S. Appl Water Sci 7:2043–2050. https://doi.org/10.1007/s13201-016-0385-4.

Zhang, W., Yin, K., Li, B., Chen, L. 2013. A glutathione S-transferase from *Proteus mirabilis* involved in heavy metal resistance and its potential application in removal of Hg^{2+}. J Hazard Mater 261:646-652. https://doi.org/10.1016/j.jhazmat.2013.08.023.

Zhu, Q.L., Bao, J., Liu, J., Zheng, J.L. 2020. High salinity acclimatization alleviated cadmium toxicity in *Dunaliella salina*: Transcriptomic and physiological evidence. Aquat Toxicol 223:105492. https://doi.org/10.1016/j.aquatox.2020.105492.

Complete bibliographical reference of article from 2.4 thesis section:

Villagrasa, E., Palet, C., López-Gómez, I., Gutiérrez, D., Esteve, I., Sánchez-Chardi, A., Solé, A. 2021. Cellular strategies against metals exposure and metal localization patterns linked to phosphorus pathways in *Ochrobactrum anthropi* DE2010. J Hazard Mater 402:123808. https://doi.org/10.1016/j.jhazmat.2020.123808.
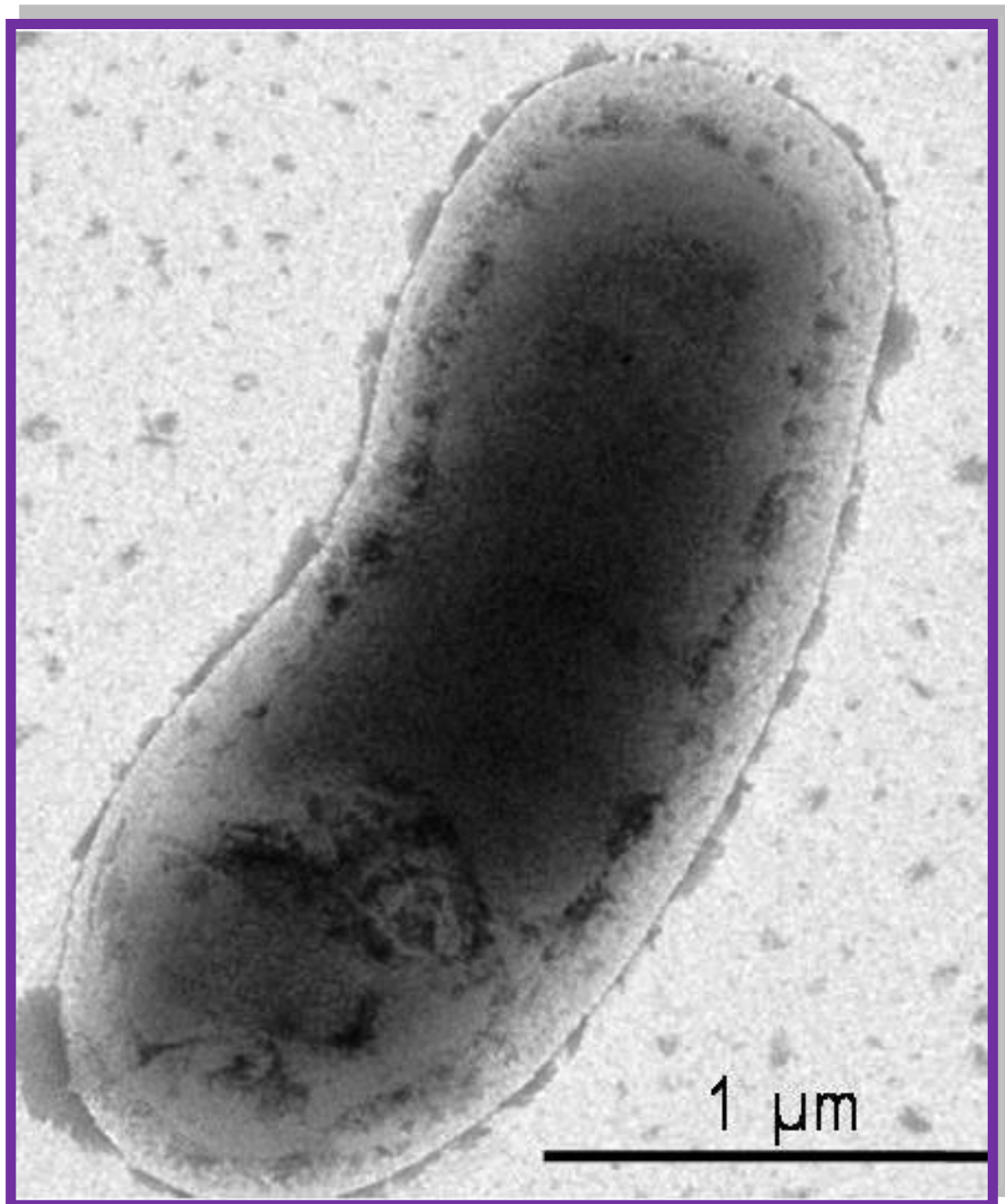
Chapter III. Summary of results and discussion

3.1 SUMMARY OF RESULTS

Section 2.1 **Morphological responses to nitrogen stress deficiency of a new heterotrophic isolated strain of Ebro Delta microbial mats**

The colonies of *Ochrobactrum anthropi* DE2010 grown on LB plate medium for 24 h at 27°C are circular, convex, smooth, and opaque, with entire margins, no pigmentation, and a diameter of 0.8–1 mm. Strain DE2010 is gram-negative, aerobic, non-spore forming, rod shaped, 1–3 μm in length, 0.5 μm wide, and motile, with peritrichous flagella. The isolated bacterium was positive in oxidase, urease and catalase activities and negative in indole and H_2S production. Strain DE2010 was grown on VBE/glucose medium without nitrate or ammonia source after 72 h at 27ºC, indicating that it is able to fix atmospheric nitrogen. The antibiogram results indicate that strain DE2010 is resistant to chloramphenicol, tetracycline, and ampicillin and sensitive to nalidixic acid and erythromycin.

To identify the strain DE2010, the sequence analysis of *16S r*RNA gene was performed. *16S r*RNA gene of strain DE2010 showed that it belongs to the genus *Ochrobactrum* with a 100% probability and, also a high degree of gene sequence similarity with *O. anthropi* ATCC49188 (99.85%) and *O. anthropi* strain AOB (99.85%) using the Ribosomal Database Project website at Michigan State University (RDP-II) and the Basic Local Alignment Search Tool (BLAST), respectively. The Tamura three-parameter model neighbor-joining phylogenetic tree indicated that the strain DE2010 clearly belongs to the genus *Ochrobactrum* and was closely related to the species *O. anthropi*. On the other hand,

to further characterize the strain DE2010, the *nuo*C gene was amplified from the genomic DNA and as with the results obtained for the 16S rRNA gene sequence a high degree of *nuo*C gene sequence similarity was found with *O. anthropi* ATCC49188 (99.85%).

In LB growth conditions cells of *O. anthropi* DE2010, which reproduce by binary fission, were rod shaped and surrounded by extracellular polymeric substances (EPS). In addition, as indicated above, they had a width of 0.5 μm and a length ranging from 1 to 3 μm. Under nitrogen-deficient source growth conditions, cells had a smaller size and exhibit different morphological types, on the one hand, the typical rod shape, and on the other hand, bulging or branched forms shaped like the letter L or V. The biomass of *O. anthropi* DE2010 varied significantly depending on the growth medium used (LB or VBE without nitrogen source), showing a difference of 39.08% in biomass. A reduction in length of 46.4% and in area of 34%, as well as a change of 31% in circularity, was observed in nitrogen-deprived conditions. Moreover, the presence of the genomic nitrogen fixing gene *fixH* was confirmed using specific primers. The DNA sequence of this gene also confirmed the identity of the isolated strain as belonging to the species *O. anthropi*.

Section 2.2 Multi-approach analysis to assess the chromium(III) immobilization by *Ochrobactrum anthropi* DE2010

The effect of Cr(III) in *O. anthropi* DE2010 varied significantly depending on the concentration, although is more evident at the highest metal concentrations. This is evidenced by a reduction in the number of cfu mL^{-1}, cell viability and biomass, and an increase in dormant cells (DC)% and duplication time. The maximum values of the four

biological parameters were obtained at 0mM Cr(III) (9.26·10^9 cfu mL^{-1} of cultivable cells, 4.02 h duplication time, 99.82% of live cells and 46.76 mg C (cm^3)$^{-1}$ of biomass) and the minimum were recovered out for 7mM (<10 cfu mL^{-1} of cultivable cells, 21 h duplication time, 62.72% of live cells and 3.30 mg C (cm^3)$^{-1}$ of biomass). Decreasing values from 0mM to 7mM Cr (III) corresponding to reductions in cfu mL^{-1} of 99.99%, cell viability of 37.1% and biomass of 92.94%, were also noted. On the other hand, results of cell viability and biomass at 10mM Cr(III) could not be determined from fluorochromes-confocal laser scanning microscopy (FLU-CLSM) images due to the formation of cellular aggregates, but a minimal cfu mL^{-1} value was achieved at this concentration. The number of DC increases with the metal concentration. These results were significant at 5mM Cr(III), with a relative ratio of DC of 96.68%. This can be seen even more clearly at 7mM and 10mM Cr(III), where the values were 99.98% and 99.89%, respectively.

Changes in the EPS composition in *O. anthropi* DE2010 were observed as a response to an increase in Cr(III) concentration. At lower concentrations of Cr(III) (0-2 mM) the major EPS component is carbohydrates (88.89%), followed by proteins (5.7%) and uronic acids (3.5%). However, at 5mM Cr(III) the most drastic metal effect was assessed. At this concentration, a considerable increase of 37.88% in proteins was observed in contrast to a significant reduction in 35.45% in carbohydrates, with as well as a slight decrease in uronic acid content. A decreasing value in carbohydrates and proteins content is observed from 7mM Cr(III), reaching a similar value between both EPS components, although a slight increase was observed at 10 mM, as result of cell aggregation. As regards the EPS production, a maximum increase in EPS concentration in relation to cell concentration

(7.82%) was obtained from 0mM (10.17%) to 5mM (17.99%) Cr(III) coinciding with the increment in the protein content.

Removal capacity for Cr(III) results of *O. anthropi* DE2010 indicate that there is a strong correlation between the initial concentration of metal and the total of chromium taken from the cells, reaching maximum values of removal of 40.83% at 7mM and of 38.38% at 10mM Cr(III). In addition, practically all the chromium removed was detected inside the cells (cytoplasm), with values ranging between 97% and 99%, depending on the metal concentration, with the rest of the metal being found in the EPS extracts (1-3%). The uptake efficiency (*q*) values also increase by increasing the initial metal concentration, and a maximum value of 950 mg g^{-1} was reached at 10mM Cr(III). However, the most notable increase in *q* values (590 mg g^{-1}) was observed from 5mM to 7mM Cr(III). The highest *q* value reported here could be related to the cellular aggregation monitored by CLSM imaging at 10mM. This cellular organization is more efficient to capture Cr(III) and to protect the cells from the cytotoxic effect of the metal than the individual cells observed at the other metal concentrations.

The High Angle Annular Dark Field (HAADF) Scanning Transmission Electron Microscopy (STEM) imaging exhibited in *O. anthropi* DE2010 samples discernible changes in cells (changes in cell morphology, an increase in bright inclusions, and the appearance of cellular pleomorphic forms) due to the Cr (III), mainly at the highest concentration (10mM Cr(III)). The Energy Dispersive X-ray spectroscopy (EDX) microanalyses of samples showed that chromium was not detectable, either externally or internally, in control samples (0 mM) and up to 2mM Cr(III). However, results obtained from 5mM to 10mM indicated that the chromium was detected together with an important phosphorous signal in intracellular

bright inclusions. STEM EDX results demonstrate that *O. anthropi* DE2010 accumulates Cr(III) externally in EPS, and internally mainly in cytoplasmic polyphosphate inclusions.

Section 2.3 Genomic and biotechnological insights on stress-linked polyphosphate production induced by chromium(III) in *Ochrobactrum anthropi* DE2010

The genomic assembly of *O. anthropi* DE2010 has a total length of 4.9 Mb, consisting of 26 contigs with an N_{50} length of 688,210 bp. Its GC content is 56.52% and it contains 4683 genes. Further, six genes related to polyphosphate (polyP) and pyrophosphate (PPi) metabolism were found named polyphosphate kinase 1 (*ppk*), exopolyphosphatase (*ppx*), K^{+}-insensitive pyrophosphate-energized proton pump (*hppa*), exopolyphosphatase/pppGpp phosphohydrolase (*ppx/gppa*), polyphosphate kinase 2 (*ppk2*), and inorganic pyrophosphatase (*ppa*). The single nucleotide polymorphism (SNP) calling of *O. anthropi* DE2010 against *O. anthropi* ATCC49188 revealed 72,465 SNPs (1.51% of the total genome length). From these variants, 2527 positions were polymorphic within the *O. anthropi* DE2010.

The multiple alignments of identified proteins (PPX and PPK) revealed two mutations in PPX and one mutation in PPK. The identified mutations in the PPX protein corresponded to R286K and S465N, and were conservative and semi-conservative replacements, respectively. The catalytic domain of this enzyme is in the region between residues 37 to 308 that includes the R286K conservative mutation, which may not affect

protein function. In the case of the PPK amino acid sequence, the A36V semiconservative mutation is not located in any of the identified catalytic domains of the enzymes and may not affect enzyme activity as well.

The data collected indicated that under Cr(III) culture exposed conditions, *O. anthropi* DE2010 synthesized and accumulated polyP in a concentration-dependent manner. An increment of 23.08% in the polyP concentration in *O. anthropi* DE2010 was achieved between 0mM (control) and 10mM of Cr(III) exposure culture conditions.

Analyzing the obtained results by TEM imaging in Cr(III) exposed cultures of *O. anthropi* DE2010, an increase in the presence of pleomorphic cellular forms and more destructured cytoplasm were observed as the metal concentration increased. The results of image analysis about cellular electrodense inclusions showed that they are circular and 6-fold increase in the number between 0mM and 10mM exposed cultures.

These results suggest that the bioaccumulation of polyP in cytoplasmatic inclusions may be one of the strategies providing tolerance and resistance to *O. anthropi* DE2010 against Cr(III) via the formation of cation and polyP complexes.

Section 2.4 Cellular strategies against metal exposure and metal localization patterns linked to phosphorus pathways in *Ochrobactrum anthropi* DE2010

The obtained results from IC_{50} and MIC showed the same cellular responses against each metal exposure. Then, the IC_{50} values remained in the same range (3.5mM in Cd to 5mM in Pb(II)), but were highest for Zn (10mM). The MIC values obtained for *O. anthropi*

DE2010 were 10mM for Cd, Pb(II), Cu(II), and Cr(III), and 20mM for Zn. These values exceed the MIC obtained for *Escherichia coli* ATCC25922, which has been treated as a reference in MIC assays. All this information pointed to the high resistance of *O. anthropi* DE2010 to exposure at high concentrations of heavy metals, especially to Zn, considered toxic for other microbial species.

The cell numbers decrease when metal concentrations increase, reaching the minimum values at the highest metal concentrations (10mM for Cd, Pb(II), Cu(II), and Cr(III), and 20mM for Zn). From this perfect correlation, the most pronounced cytotoxic effect resulting in an abrupt cell decrease of around 40% and 25% was detected between 0.5 and 2mM for Cd and Pb(II) respectively, and of more than 30% between 2 and 5mM for the rest of the metals. Significant reductions in cell counts of 85% for Cd, 80% for Pb(II), 79% for Cu(II), 84% for Cr(III), and 47% for Zn were observed upon comparing controls with samples exposed to 10mM of each metal. These percentages agree with those obtained for IC_{50} and MICs and strongly suggest that metal toxicity for *O. anthropi* DE2010 is Cd>Cr(III)>Pb(II)>Cu(II)>Zn, cadmium being the most toxic and zinc the least. Moreover, the presence of live cells at all metal concentrations demonstrates the high tolerance of this bacterium to the detrimental effects of each of the five heavy tested metals strongly suggesting a similar behavior against exposure to other potentially toxic elements.

The highest removal capacity found in *O. anthropi* DE2010 was around 90% for Pb(II), followed by around 40% for Cr(III). Lower capacities of 20%, 10%, and 3.0% were detected for removal of Zn, Cd, and Cu(II), respectively. Moreover, similar ranges of metal removal (Pb(II)>Cr(III)>Cd>Zn>Cu(II)) and uptake efficiency (Pb(II)>Cr(III)>Cu(II)>Cd>Zn) were found at the highest common concentration for all metals (10mM).

The levels of polyP (μmol of polyP per g^{-1} dry weight of biomass) were clearly correlated with the increment of Pb(II), Cu(II), Cr(III), and Zn, being 3, 3.5, 4, and 4.5-fold more in higher metal concentrations compared to control samples. In marked contrast, the concentration of polyP is practically unvarying among all ranges of Cd concentrations in spite of 10% of Cd being captured by *O. anthropi* DE2010. Neither induced polyP production nor Cd bioaccumulation in intracytoplasmic polyP inclusions strongly suggests a different bacterial response for Cd. This metal probably could be adsorbed in EPS also due to the sorption ability of *O. anthropi* DE2010, as reported recently for Cr (see section 2.2 of the present thesis).

Heavy metals exposure disturbed normal cell metabolism, altering the bacterial morphology. Moreover, intracellular ultrastructure indicated different degrees of alteration, including evident cytoplasm disorganization and retraction, as well as an increase of pleomorphic forms in Pb(II), Cr(III), and Cu(II) exposed cells. The analytical studies with EDX and BSE demonstrated that polyP aggregates containing phosphorus are the main storage structures of metals in *O. anthropi* DE2010 cells and have metal-specific pathways of sub-cellular localization. Cu(II) induced granules are mainly localized extracellularly in the outer membrane surface, besides Cr(III) and Zn induced inclusions, mostly in the cell cytoplasm, and Pb(II) in both the periplasmic space and the cytoplasm. In marked contrast, the results in Cd(II) exposed cultures showed no evident morphological changes and polyP inclusions evidenced no metal content. *O. anthropi* DE2010 is not only able to bioaccumulate Pb(II) but can also biomineralize it highly efficiently, as strategies to reduce its bioavailability and consequently its biological impact in bacterial cells.

3.2 GENERAL DISCUSSION

In this thesis (see section 2.1), the environmental isolated strain DE2010 from microalgae *Scenedesmus* sp. DE2009 consortium has been characterized and identified as *Ochrobactrum anthropi* DE2010. The genus *Ochrobactrum* is a member of the *Brucellaceae* family branch within rRNA superfamily IV, in the class Alphaproteobacteria (Thoma et al. 2009). This genus comprises wild bacteria, rhizosphere members, nitrogen-fixing bacteria, xenobiotic degrading bacteria, and opportunistic human pathogens (Chmelař et al. 2019). The first characterized member within the *Ochrobactrum* genus was named *O. anthropi* (an.thro'pi Gr. n. *anthropos*, a human being; N.L. gen. n. *anthropi*, of a human being, since virtually all strains were recovered from human clinical specimens) by Holmes et al. (1988). However, at present, several strains have been isolated, characterized, and identified within *O. anthropi* species and the ubiquity of these bacteria has been demonstrated (Gohil et al. 2020). They have routinely been isolated from heterogeneous environmental sites such as waters, soils, sludges, plants, and rhizospheres, industrial environments or wastes, and animals including humans (as shown in Table 5). *O. anthropi* is thus a common soil alphaproteobacterium that can colonize a wide spectrum of living organisms. Therefore, it has been recognized as an opportunistic human pathogen.

Based on phenotypic characteristics, *O. anthropi* type strain ATCC49188 exhibits negative results for indole, H_2S, carbohydrate fermentation, and the assimilation of adipate and phenylacetate. Additionally, it shows positive results for oxidase, catalase, urease, and the assimilation of glucose, arabinose, mannose, and malate (Teysser et al. 2005; Huber et al. 2010). The current study results (see section 2.1) demonstrated that *O. anthropi* DE2010

meets all known phenotypic characteristics of the type strain. Moreover, it is also found that

the type strain was highly resistant to all β-lactams (Kulkarni et al. 2017) and *O. anthropi*

DE2010 exhibited resistance to ampicillin (see section 2.1).

Table 5. List of isolated and identified strains of *O. anthropi*.

O. anthropi strains	Isolation sources	References
O. anthropi XM-1	Sludge from a wastewater treatment plant (Hefei, China)	Chen et al. 2019
O. anthropi S1	An anaerobic reactor that treated textile wastewater (Guangdong, China)	Cheng et al. 2020
O. anthropi PBO	Plastics debris from sea coast (Qingdao, China)	GenBank: CP064063.1
O. anthropi CTS-325	Chinese chromate plant (Hangzhou, China)	Cheng et al. 2009
O. anthropi ML7	The nematode *Steinernema longicaudum* species from soil (Me Linh, Vietnam)	Tobias et al. 2015
O. anthropi MP3	Petroleum refinery wastewater (Chennai, India)	Ramasamy et al. 2014
O. anthropi YC152	Sludge from an electroplating wastewater treatment plant (Taoyuan, China)	Wang et al. 2016
O. anthropi GPK 3	Soils (Krasnodar krai, Russia)	Ermakova et al. 2017
O. anthropi sp.	Contaminated sediment from Strážsky canal (Zemplínska šírava, Slovakia)	Murínová et al. 2014
O. anthropi CCUG 33786	Human clinical samples, blood (Jonkoping, Sweden)	Ashford et al. 2020
O. anthropi FRAF13	Farmland soil (Texas, USA).	Iyer and Damania, 2016
O. anthropi B2	The yard of a pesticide factory (Gaomi, China)	Qiu et al. 2006
O. anthropi MCM5/1	Oil contaminated with gasoline from an industrial area (Valencia, Spain).	Barberà et al. 2011
O. anthropi DE2010	Microbial mats in the Ebro Delta area (Tarragona, Spain).	Villagrasa et al. 2019 (current tesis)

Mutualism is defined as a positive biological interaction between two or more

partners of different species that live in proximity and mutually benefit in terms of nutrient

supply, protection, habitat, or transport (Cooper and Smith, 2015). The heterotrophic

microorganism *O. anthropi* DE2010 was isolated from the microalgae *Scenedesmus* sp.

DE2009 consortium of the Ebro Delta microbial mats; the microbiological interaction between these two species is an example of mutualism. The best known and the most documented case of mutualism in a consortium of algae and bacteria is particularly the exchange of micro and macronutrients necessary for cell growth (Ramanan et al. 2016). Examples of such type of microbial interaction involve (i) exchange of vitamin B_{12} and the fixed carbon between microalgae and bacteria (revision in Yao et al. 2019); (ii) bacterial remineralization of sulfur (S), nitrogen (N), and phosphorus (P) that supports further growth of microalgae (revision in Yao et al. 2019); (iii) use of molecular oxygen from algae photosynthesis as an end electron acceptor by bacteria to degrade organic matter (Subashchandrabose et al. 2011); and finally (iv) consumption of typical algae exudates that are rich in carbohydrates by heterotrophic microorganisms such as *O. anthropi* DE2010 (Rodriguez-Celma et al. 2013) (Figure 6). All these examples explain cohabitation (mutualistic relationship) or microalgae-bacteria interrelationship in the same habitat. In fact, microorganisms living in hypersaline microbial mats frequently form consortia under stressful and changing environmental conditions. This relationship could be a possible explanation for microbes surviving in extreme environments under unfavorable conditions.

In a mutualistic relationship concerning nitrogen sources, bacteria often fix nitrogen for non-nitrogen fixing phototrophic microorganisms. As *O. anthropi* DE2010 can grow under stressful conditions lacking N_2 due to the presence of *fix*H gene (metabolic mechanism still not identified), it probably fixes atmospheric nitrogen in the Ebro Delta microbial mats. Therefore, the resulting nitrogen compounds (ammonium, nitrite, and/or nitrate) can be used as a nitrogen source favoring the growth of *Scenedesmus* sp. microalgae.
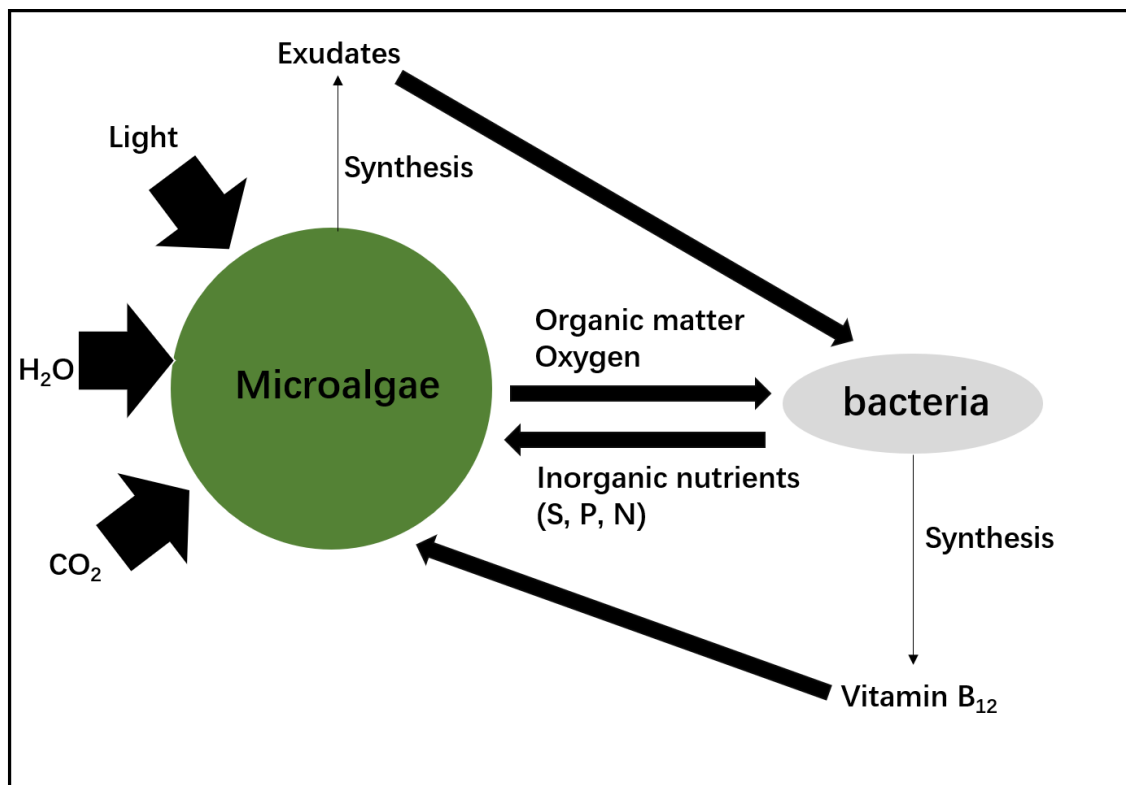
Figure 6. Representation of a mutualistic relationship in a microalgae/bacteria consortium. Source: Property of the thesis author.

Bioremediation is the use of living organisms, mainly microorganisms, to immobilize and/or degrade into less toxic forms of most environmental contaminants (Shanahan, 2004; Asha and Sandeep, 2013). From an ecological point of view, microorganisms are considered the best choice for the treatment of environmental pollution. This is attributable to its widespread in the natural environment with controllable growth conditions and the ability to quickly repair polluted habitats (Ghosh and Mitra, 2018). Consequently, the use of microorganisms for remediation is a promising approach in removing heavy metals (Akinci et al. 2011; Al Hasin et al. 2010; Karthik et al. 2017), owing to the capacity of some microbial species to sequester heavy metals through different strategies and metabolic pathways (Ayangbenro and Babalola, 2017, Gupta and Diwan, 2017; Etesami, 2018). As *O. anthropi*

and other species within the *Ochrobactrum* genus can tolerate and accumulate heavy metals (Table 6), the current thesis investigated these capacities in *O. anthropi* DE2010 strain (see 2.2-2.4 sections).

Table 6. Responses to heavy metal and metalloids exposure by isolated and identified *Ochrobactrum* strains.

Ochrobactrum sp. strains	Features	References
O. anthropic	Heavy metal biosorption in EPS	Ozdemir et al. 2003
O. ciceri BPS-26 and *O. intermedium* BPS-20	Heavy metal bioaccumulation	Sharma and Shukla, 2021
O. anthropic	Uptake Cr(VI)	Li et al. 2008
O. anthropi	Biotransformation of Cr(VI) into Cr(III) and Immobilization as Cr(III)	Cheng et al. 2010
Ochrobactrum sp.	Cadmium resistance	Pandey et al. 2015
Ochrobactrum MT180101	Copper-resistant mechanism	Peng et al. 2019
O. triciti 5bvl1	Chromium induced phosphate extracellular nanoparticulate formation	Francisco et al. 2011
O. triciti AS5	Arsenite biofiltration	Moens et al. 2020
O. anthropi DE2010	Heavy metal bioaccumulation in polyphosphate inclusions or granules, biomineralization in phosphorus crystals, and biosorption in EPS	Villagrasa et al., 2020a Villagrasa et al., 2020b Villagrasa et al. 2021 (current tesis)

The cytotoxic effects (and cellular responses) on the cell viability of *O. anthropi* DE2010 cultures individually exposed to a range of concentrations of five widely distributed essential (Cu, Cr, and Zn) and non-essential (Pb and Cd) heavy metals were assessed. The analysis was performed using a battery of quantitative and analytical methodologies such as growth curves, IC_{50}, MIC, OP cell counts, colony-forming unit counts, FLU-CLSM-IA, and

EPS extraction (see sections 2.1-2.4). The IC$_{50}$ values in *O. anthropi* DE2010 were slightly higher than values in environmental bacteria for Cu(II) and Cd (Nweke et al. 2007), *Salmonella* sp. for Zn (Bestawy et al. 2013), and *Photobacterium phosphoreum* T3S for Cd, Pb(II), and Cu(II) (Zeb et al. 2017). Also, *O. antropi* DE2010 MIC values exceed the MIC values of *Escherichia coli* ATCC25922, which has been treated as a reference in MIC assays (Bhardwaj et al. 2018). For the effect of Cr (III) on cell viability and biomass, cfu mL^{-1} counts varied depending on the concentration; it was more evident at the highest metal concentrations. Here, the confocal analysis also evidenced a high percentage of cells that remained alive (considered as dormant cells). However, minimal growth was detected in plate counts. Furthermore, changes in EPS production and composition were observed for different metal concentrations, being the carbohydrates the major component at lower concentrations and proteins from 5 mM of Cr(III) (see 3.1 section). Comparing these results with those obtained by other authors (Sheng et al. 2005; Yilmazer and Saracoglu, 2008; Yin et al. 2011; Millach et al. 2015; Puyen et al. 2017), *O. anthropi* DE2010 showed greater tolerance and resistance for Cr(III) even at 10 mM. Moreover, with respect to the cytotoxic effects of Cd, Pb(II), Cr(III), Cu(II), and Zn (growth curves and OP cell counts) on *O. anthropi* DE2010, the cell numbers decrease with an increase in metal concentrations, reaching the minimum number at the highest metal concentrations (10 mM for Cd, Pb(II), Cu(II), and Cr(III) and 20 mM for Zn). Other isolated environmental bacteria also demonstrated tolerance/resistance to heavy metals including Cd, Pb(II), Cu(II), Cr(III), and Zn at lower concentrations (Afzal et al. (2017), Deepika and Kannabiran (2010), Domingues et al. (2020), Gillard et al. (2019), Sriram et al. (2011 a, b). These study results pointed to the high resistance of *O. anthropi* DE2010 to the detrimental effects of high concentrations of the

five tested heavy metals, considered toxic for other microbial species. These findings further highlight a possible range of effective resistance mechanisms or strategies of *O. anthropi* DE2010 cells linked to uptake pathways such as extracellular sequestration, intracellular sequestration, active export, and enzymatic detoxification, which help the cells interact with metals as well as tolerate rapid changes in metal levels in the environment (see 1 (Table 3 and 4) and 3.1 sections).

As described before, the intracellular uptake of metals in polyP aggregates is one of the cellular pathways. A polyP is an orthophosphate polymer present in all living organisms (Albi and Serrano, 2016) and its production can be carried out by bacterial cells in response to numerous stress factors such as nutrient starvation, phosphorus removal wastewater, and toxicity of heavy metals (Lee and Park, 2008; Millach et al. 2015; Mukherjee et al. 2015; Kulakovskaya 2018). Various previous studies have explained the metabolic and biological functions of polyP in bacteria (Kornberg et al. 1999; Aschar-Sobbi et al. 2008; Rao et al. 2009; Oehmen et al. 2010; Rubio-Rincón et al. 2017). Specifically, several reports have been explored the ability of some microorganisms to sequester heavy metals intracellularly through polyP-mediated metabolic pathways (Orell et al. 2012, Acharya and Apte, 2013, Andreeva et al. 2014, Kulakovskaya 2018). In the current thesis, the biochemical quantification of intracellular polyP content is considered as the relationship between total and soluble cellular phosphorus. The results showed (see 3.1 section) that polyP production in *O. anthropi* DE2010 cultures varied quantitatively according to heavy metals and their concentrations as described by Andreeva et al. (2014) and Francisco et al. (2011). Furthermore, other authors such as Remonsellez et al. (2006), Perdrial et al. (2008), Martínez et al. (2014), and Jasso-Chávez et al. (2019) have checked the ability of cytosolic

polyphosphates in strains of naturally occurring Archaea and Bacteria to facilitate the intracellular sequestration of Cd, Cu, Pb, and Zn. Moreover, Boswell et al. (1999), Choudhary and Sar (2011), and Acharya and Apte's (2013) studies using electron microscopy imaging indicated that the electrodense polyP inclusions increased in cultures exposed to heavy metals. In this thesis, the genome sequence of *O. anthropi* DE2010 has been widely studied and different genes implied to the metabolism of polyP and PPi were detected. The current study results indicated that *O. anthropi* DE2010 is an important candidate with the potential to minimize heavy metal toxicity by chelating the metal into polyP aggregates.

On the other hand, a chemical analysis on the uptake efficiencies and metal adsorption capacity of *O. anthropi* DE2010 was performed using ICP-OES (see sections 2.2 and 2.4). Quantitative chemical data on the ability of *O. anthropi* DE2010 cells to capture Cd, Pb(II), Cu(II), Cr(III), and Zn, and the corresponding cellular uptake efficiency (q) showed a strong correlation between initial metal concentration and the total amount of metal extracted from the cells. Interestingly, q of *O. anthropi* DE2010 for Cr(III) is higher than those of other prokaryotic (Solisio et al. 2000; Chojnacka et al. 2005; Calfa et al. 2008; Upadhyay et al. 2017; Ramírez et al. 2019) and eukaryotic microorganisms (Ksheminska et al. 2005; Han et al. 2006). The isolated bacterium presented higher removal rates and q values for Pb(II) and Cr(III) around 90% (q= 1548 mg g^{-1}) and 40% (q= 950 mg g^{-1}) respectively and lower for Cu(II) and Zn. However, the overall rates and values are slightly higher than those of other microorganisms (Bowman et al. 2018; Chatterjee et al. 2010; Alam and Ahmad, 2011; Joutey et al. 2014; Li et al. 2020). Comparing with these species, *O. anthropi* DE2010 emerges as an extremely efficient bacterium to remove heavy metals, especially Pb(II), and Cr(III).

Following the objectives of the current thesis, a series of electron microscopy techniques (TEM, TEM-EDX, TEM-SAED, SEM, FESEM-EDX, FESEM-BSE, and STEM-EDX) were applied to determine the localization of metals at the subcellular level. Over the years, electron microscopy imaging has become a crucial tool to visualize the ultrastructure of microorganisms (Golding et al. 2016; Solé et al. 2019) and, coupled to an EDX detector, it is used to analyze the elemental composition and its distribution in the samples (Maldonado et al. 2011, Burgos et al. 2013; Coreño-Alonso et al. 2014; Millach et al. 2015; Povedano-Priego et al. 2017). The analytical studies with EDX and BSE in FESEM and STEM demonstrated that polyP aggregates containing phosphorus are the main storage structures of metals in *O. anthropi* DE2010 cells and have metal-specific patterns for subcellular localization. Initially, STEM-EDX results demonstrated that *O. anthropi* DE2010 accumulates Cr(III) externally in EPS and internally in polyP inclusions which can be removed via biosorption and bioaccumulation strategies (see section 3.1 chapter 2.2). Earlier, it has been indicated that *O. anthropi* DE2010 can not only bioaccumulate Pb(II), Cu(II), Cr(III), and Zn but also biomineralize Pb(II) efficiently (see section 3.1 and chapters 2.2-2.4) as mechanisms to reduce their bioavailability and consequently biological impact on bacterial cells. Overall, these results showed rapid, varied, and specific responses to different metal stressors and the high importance of polyP production in metal chelation and sequestration through active processes of bacterial bioaccumulation and/or biomineralization. Metal bioimmobilization is an effective mechanism to reduce metal bioavailability, prevent and/or avoid toxic effects, and has been described in other microbial species (Yin et al. 2019). Concerning at Cd, only 10% of this metal was captured by *O. anthropi* DE2010 probably also biosorbed in EPS, due to its sorption ability, previously mentioned for Cr(III). However, more

work is needed to show that *O. anthropi* DE2010 indeed captures Cd in its EPS. The study

highlights that this variety of cell strategies and patterns to avoid the toxic effect of heavy

metals have been found in a single bacterium for the first time.

3.3 POTENTIAL APPLICATIONS AND FUTURE PERSPECTIVES OF *O. anthropi* DE2010 IN METAL IMMOBILIZATION

O. anthropi DE2010 cells can rapidly respond to metals exposure using different strategies such as bioaccumulation and biomineralization in combination with biosorption (Figure 7). All of these processes can be considered for potential applications in reducing the bioavailability of heavy metals that are often present at highly toxic levels for biota in aquatic environments (Sánchez-Chardi et al. 2007; Sánchez-Chardi and López-Fuster, 2009; Seder-Colomina et al. 2013). All our findings concerning *O. anthropi* DE2010 point to its high efficiency in chelating metals from the environment using different metabolic pathways. These data suggest high metabolic plasticity of *O. anthropi* DE2010 (Comte et al., 2013; Guerrero and Berlanga, 2016). Apart from our promising results, further specific studies are needed to evaluate the advantages of each bacterial strategy to localize and bind specific metals and different chemical species. Moreover, further analysis of the capacity of *O. anthropi* DE2010 to remove selected heavy metals in mixed solutions (near to real wastewater systems) is essential to consider its feasibility for the development of bioremediation strategies in natural ecosystems. So far, our exposed results, using different concentration levels of five widely distributed heavy metals, strongly suggest that this bacterial species can be considered as a valuable player in future bioremediation strategies that use biological systems such as bacteria strains mainly in Pb(II) and Cr(III) contaminated

environments, especially at high concentration levels where these metals become lethal for
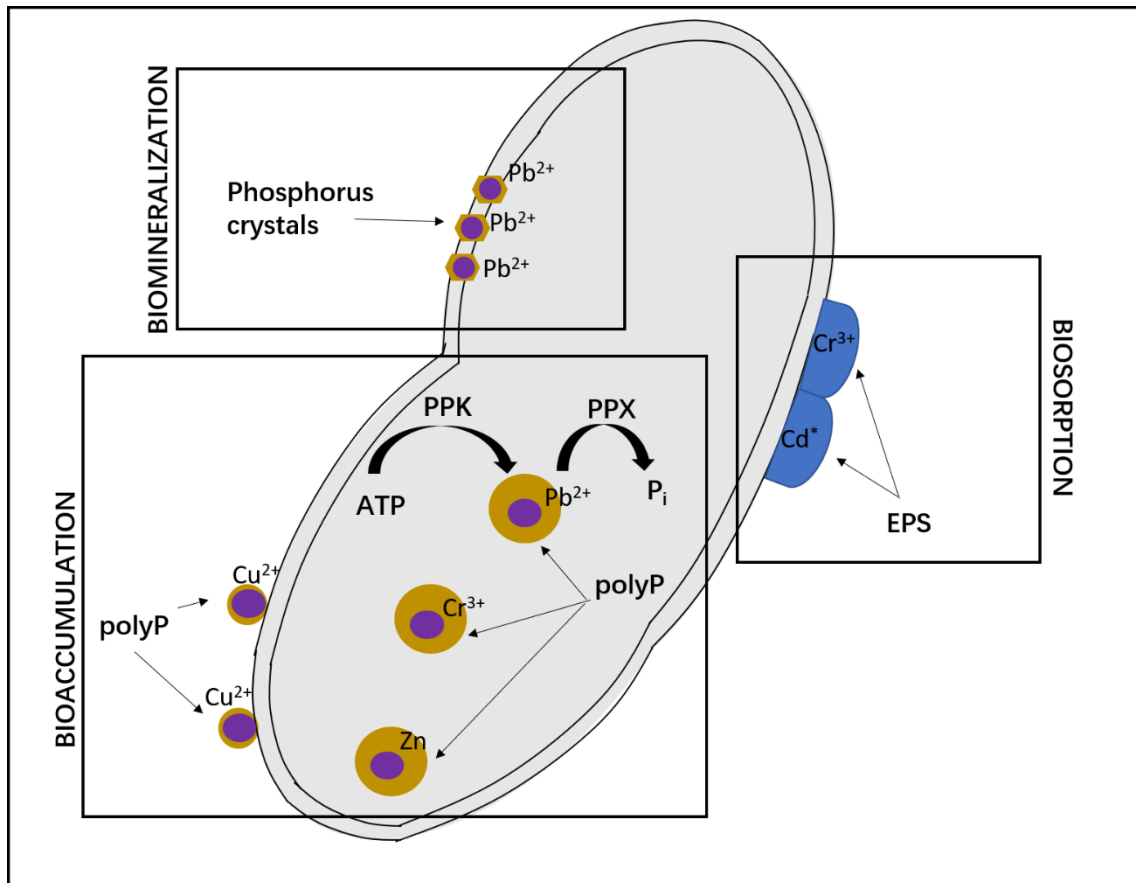
other prokaryotic and eukaryotic organisms.
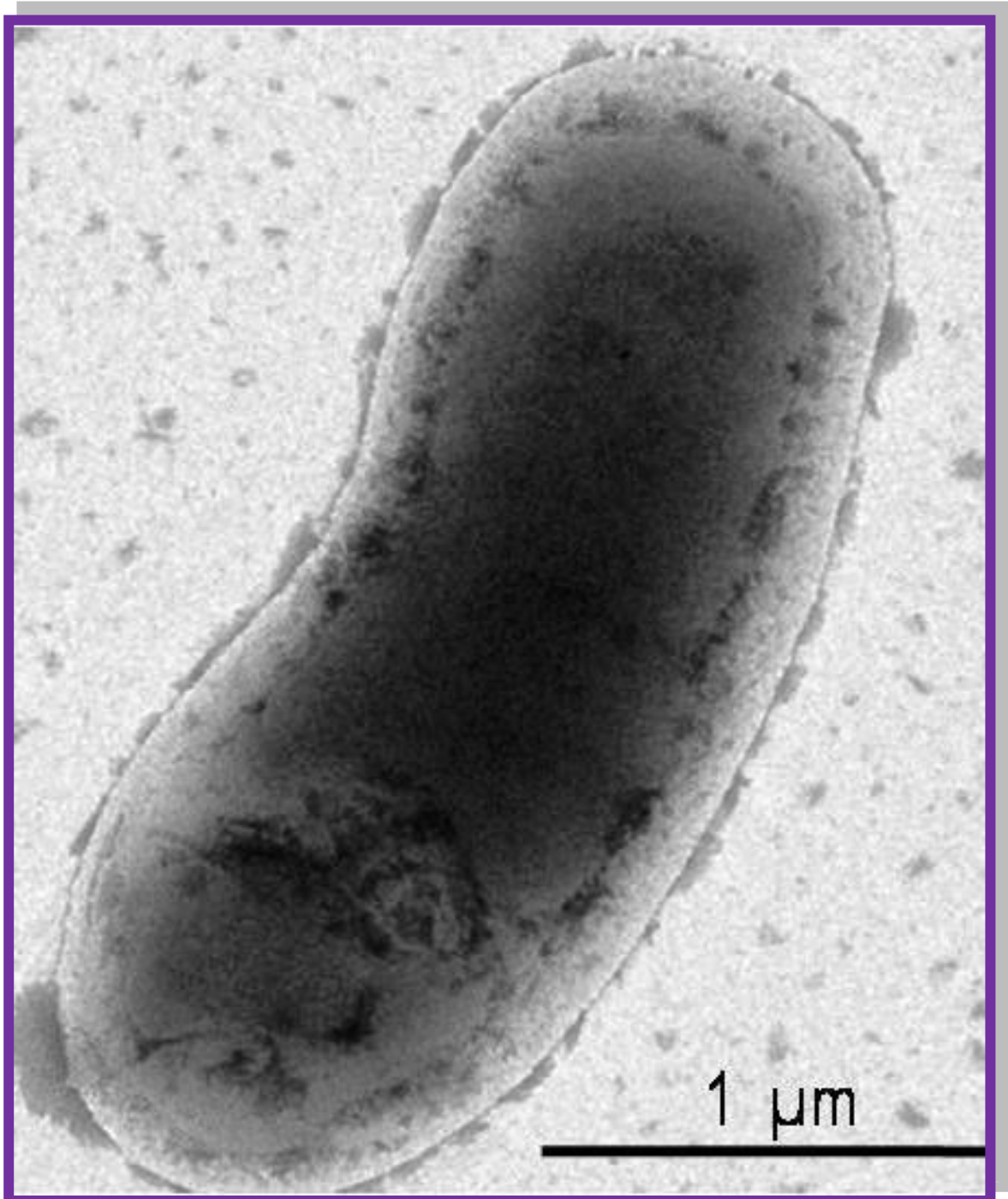

Figure 7. Graphical representation of metal localization patterns and proposed strategies and pathways within *O. anthropi* DE2010 cells in response to heavy metal toxicity. Source: Property of the thesis author.

Chapter IV. Conclusions

Following the objectives of this thesis, the conclusions obtained using quantitative and qualitative methodologies are:

1. The bacterial strain DE2010 isolated from the *Scenedesmus* sp. DE2009 consortium has been genotypically identified (16*S r*RNA, *nuo*C, and *Fix*H genes) as *Ochrobactrum anthropi* DE2010 and confirmed by the phenotypic characterization.

2. *O. anthropi* DE2010 can overcome N_2-limiting conditions through an unidentified *nif*H-independent mechanism, showing changes in shape and size and a great abundance of pleomorphic cells simultaneously.

3. The genome sequence of *O. anthropi* DE2010 has evidenced relevant genomic findings concerning polyP production that includes the presence of six polyphosphates (polyP) and pyrophosphate (PPi) metabolic genes.

4. The bacterium *O. anthropi* DE2010 showed great tolerance and resistance to the presence of heavy metals, surviving at concentrations up to 20 mM for Zn and 10 mM for Cd, Pb(II), Cu(II), and Cr(III). With respect to Cr(III), the bacterium showed changes in production and composition of EPS at increasing metal concentrations.

5. Heavy metal exposure of *O. anthropi* DE2010 cultures induced a dose-dependent polyP production and accumulation, resulting in an increment of polyP aggregates (granules and inclusions).

6. *O. anthropi* DE2010 cells take up Cd, Pb(II), Cr(III), Cu(II), and Zn even at high concentrations and evidence high removal capacities displaying an unusual ability to sequestrate Pb(II) and Cr(III); highlighting up to 90% for Pb(II) and 40% for Cr (III) with maximal removal efficiencies of 1548 mg g^{-1} of Pb(II) and 950 mg g^{-1} of Cr(III) both at 10 mM.

7. *O. anthropi* DE2010 cells immobilized heavy metals in polyP granules and/or inclusions, besides phosphorus crystalline structures, to reduce their deleterious effects on bacterial cells. Those phosphorous structures followed clear metal-specific patterns in cell distribution. Three cell localization patterns and pathways of metals were evidenced using compositional and imaging techniques: (i) extracellular in polyphosphate granules for Cu(II), (ii) in periplasmic space forming crystals with phosphorus for Pb(II), and (iii) intracytoplasmic in polyphosphate inclusions for Pb(II), Cr(III), and Zn. Pleomorphic cellular forms were detected in Pb(II), Cr(III), and Cu(II) exposed cultures, especially at higher concentrations.

8. *O. anthropi* DE2010 revealed specific responses as survival strategies for each heavy metal exposure, including bioaccumulation (for Pb(II), Cu(II), Cr(III), and Zn), biosorption (for Cd and Cr(III)), and biomineralization (for Pb(II)).

9. Considering all the results, it can be concluded that *O. anthropi* DE2010 emerges as an extremely efficient bacterium with a great potential for heavy metals bioremediation, especially in Pb(II) and Cr(III) polluted areas.

REFERENCES

Abdel-Ghani, N.T. and El-Chaghaby, G.A. 2014. Biosorption for metal ions removal from aqueous solutions: a review of recent studies. Int J Lat Res Scie Technol 3(1):24-42.

Abdel-Razik, M.A., Azmy, A.F., Khairalla, A.S., AbdelGhani, S. 2020. Metal bioremediation potential of the halophilic bacterium, *Halomonas* sp. strain WQL9 isolated from Lake Qarun, Egypt. Egypt J of Aquat Res 46(1):19-25. https://doi.org/10.1016/j.ejar.2019.11.009.

Abed, R.M., Klempová, T., Gajdoš, P., Čertík, M. 2015. Bacterial diversity and fatty acid composition of hypersaline cyanobacterial mats from an inland desert wadi. J Arid Environ 115:81-89. https://doi.org/10.1016/j.jaridenv.2015.01.010.

Abed, R.M., Palinska, K.A., Köster, J. 2018. Characterization of microbial mats from a desert Wadi ecosystem in the Sultanate of Oman. Geomicrobiol J 35(7):601-611. https://doi.org/10.1080/01490451.2018.1435755.

Abed R.M., Shanti M., Muthukrishnan T., Al-Riyami Z., Pracejus B., Moraetis, D. 2020. The role of microbial mats in the removal of hexavalent chromium and associated shifts in their bacterial community composition. Front Microbiol 11. https://doi.org/10.3389/fmicb.2020.00012.

Abtahi, M., Fakhri, Y., Oliveri Conti, G., Keramati, H., Zandsalimi, Y., Bahmani, Z., Hosseini, R., Sarkhosh, M., Moradi, B., Amanidaz, N., Ghasemi, S.M. 2017. Heavy metals (As, Cr, Pb, Cd and Ni) concentrations in rice (*Oryza sativa*) from Iran and associated risk assessment: a systematic review. Toxin Rev 36:331-341. https://doi.org/10.1080/15569543.2017.1354307.

Acharya, C. and Apte, S. K. 2013. Novel surface associated polyphosphate bodies sequester uranium in the filamentous, marine cyanobacterium, *Anabaena torulosa*. Metallomics 5(12):1595-1598. https://doi.org/10.1039/C3MT00139C.

Afzal, A.M., Rasool, M.H., Waseem, M., Aslam B. 2017. Assessment of heavy metal tolerance and biosorptive potential of *Klebsiella variicola* isolated from industrial effluents. AMB Expr 7:184. https://doi.org/10.1186/s13568-017-0482-2.

Akinci, G. and Guven, D.E. 2011. Bioleaching of heavy metals contaminated sediment by pure and mixed cultures of *Acidithiobacillus* spp. Desalination 268:221-226. https://doi.org/10.1016/j.desal.2010.10.032.

Al Hasin, A., Gurman, S.J., Murphy, L.M., Perry, A., Smith, T.J., Gardiner, P.H. 2010. Remediation of chromium (VI) by a methane-oxidizing bacterium. Environ Scie Technol 44(1):400-405. https://doi.org/10.1021/es901723c.

Alam, M. Z., Ahmad, S., Malik, A. 2011. Prevalence of heavy metal resistance in bacteria isolated from tannery effluents and affected soil. Environ Monitoring Assess 178(1-4):281-291. https://doi.org/10.1007/s10661-010-1689-8.

Albi, T. and Serrano, A. 2016. Inorganic polyphosphate in the microbial world. Emerging roles for a multifaceted biopolymer. World J Microbiol Biotechnol 32(2):27. https://doi.org/10.1007/s11274-015-1983-2.

Andreeva, N., Ryazanova, L., Dmitriev, V., Kulakovskaya, T., Kulaev, I. 2014. Cytoplasmic inorganic polyphosphate participates in the heavy metal tolerance of *Cryptococcus humicola*. Folia Microbiol 59(5):381–389. https://doi.org/10.1007/s12223-014-0310-x.

Aschar-Sobbi, R., Abramov, A.Y., Diao, C., Kargacin, M.E., Kargacin, J.G., French, J.R., Pavlov, E. 2008. High sensitivity, quantitative measurements of polyphosphate using a new DAPI-based approach. J Fluoresc 18:859–866. https://doi.org/10.1007/s1089 5-008-0315-4.

Asha, L.P. and Sandeep, R.S. 2013. Review on bioremediation-potential tool for removing environmental pollution. Int J Basic Appl Chem Scie 3:21-33.

Ashford, R.T., Muchowski, J., Koylass, M., Scholz, H.C., Whatmore, A.M. 2020. Application of whole genome sequencing and pan-family multi-locus sequence analysis to characterize relationships within the Family *Brucellaceae*. Front Microbiol 11:1329. https://doi.org/10.3389/fmicb.2020.01329.

Atlas, R.M. and Bartha, R. 1993. Microbial ecology: fundamentals and applications. Redwood City.

Ayangbenro, A.S. and Babalola, O.O. 2017. A new strategy for heavy metal polluted environments: a review of microbial biosorbents. Int J Environ Res Public Health 14(1):94. https://doi.org/10.3390/ijerph14010094.

Azimi, A., Azari, A., Rezakazemi, M., Ansarpour, M. 2017. Removal of Heavy Metals from Industrial Wastewaters: A Review. Chem Bio Eng Rev. 4(1):37–59. https://doi.org/10.1002/cben.201600010.

Barberà, M.J., Mateo, E., Monkaityte, R., Constantí, M. 2011. Biodegradation of methyl tert-butyl ether by newly identified soil microorganisms in a simple mineral solution. World J Microbiol Biotechnol 27:813–821. https://doi.org/10.1007/s11274-010-0522-4.

Benaiges-Fernandez, R. and Urmeneta, J. 2018. Use of specific PCR primers for the study of sulfate-reducing bacteria diversity in microbial mats of Ebro Delta, Spain. Int Microbiol 21(4):231-235. https://doi.org/10.1007/s10123-018-0020-3.

Bestawy, E.E., Helmy, S., Hussien, H., Fahmy, M., Amer, R. 2013. Bioremediation of heavy metal-contaminated effluent using optimized activated sludge bacteria. Appl Water Sci 3(1):181-192. https://doi.org/10.1007/s13201-012-0071-0.

Bhardwaj, R., Gupta, A. Garg, J.K. 2018. Impact of heavy metals on inhibitory concentration of *Escherichia coli*—a case study of river Yamuna system, Delhi, India. Environ Monit Assess 190:674. https://doi.org/10.1007/s10661-018-7061-0.

Biswas, J.K., Banerjee, A., Sarkar, B., Sarkar, D., Sarkar, S.K., Rai, M., Vithanage, M. 2020. Exploration of an extracellular polymeric substance from earthworm gut bacterium (*Bacillus licheniformis*) for bioflocculation and heavy metal removal potential. Applied Sciences 10(1):349. https://doi.org/10.3390/app10010349.

Blindauer, C. A. 2008. Zinc-handling in cyanobacteria: an update. Chem Biodivers 5:1990–2013. https://doi.org/10.1002/cbdv.200890183.

Bolhuis, H., Cretoiu, M.S., Stal, L.J. 2014. Molecular ecology of microbial mats. FEMS Microbiol Ecol 90(2):335-350. https://doi.org/0.1111/1574-6941.12408.

Boswell CD, Dick RE, Macaskie LE (1999) The effect of heavy metals and other environmental conditions on the anaerobic phosphate metabolism of *Acinetobacter johnsonii*. Microbiology 145(7):1711–1720. https://doi.org/10.1099/13500872-145-7-1711.

Bowman, N., Patel, D., Sanchez, A., Xu, W., Alsaffar, A., Tiquia-Arashiro, S.M. 2018. Lead-resistant bacteria from Saint Clair River sediments and Pb removal in aqueous solutions. Appl Microbiol Biotechnol 102(5):2391-2398. https://doi.org/10.1007/s00253-018-8772-4.

Burganskaya, E.I., Grouzdev, D.S., Krutkina, M.S., Gorlenko, V.M. 2019. Bacterial communities of microbial mats of the white sea supralittoral and of the littoral of the lakes separated from the sea. Microbiology 88(5):600-612. https://doi.org/10.1134/S0026261719050035.

Burgos, A., Maldonado, J., De los Rios, A., Solé, A., Esteve, I. 2013. Effect of copper and lead on two consortia of phototrophic microorganisms and their capacity to sequester metals. Aquatic Toxicol 140:324-336. https://doi.org/10.1016/j.aquatox.2013.06.022.

Burnat, M., Diestra, E., Esteve, I., Solé, A. 2009. In situ determination of the effects of lead and copper on cyanobacterial populations in microcosms. PLoS One 4(7):e6204. https://doi.org/10.1371/journal.pone.0006204.

Burnat, M., Diestra, E., Esteve, I., Solé, A. 2010. Confocal laser scanning microscopy coupled to a spectrofluorometric detector as a rapid tool for determining the in vivo effect of metals on phototrophic bacteria. Bull Environ Contam Toxicol 84(1):55-60. https://doi.org/10.1007/s00128-009-9907-1.

Calfa, B. A. and Torem, M. L. 2008. On the fundamentals of Cr (III) removal from liquid streams by a bacterial strain. Miner Eng 21(1):48-54.

Cardoso, D.C., Cretoiu, M.S., Stal, L.J., Bolhuis, H. 2019. Seasonal development of a coastal microbial mat. Sci Rep 9(1):1-14. https://doi.org/10.1038/s41598-019-45490-8.

Cervantes, C., Campos-García, J., Devars, S., Gutiérrez-Corona, F., Loza-Tavera, H., Torres-Guzmán, J.C., Moreno-Sánchez, R. 2001. Interactions of chromium with microorganisms and plants. FEMS Microbiol Rev 25(3):335–347. https://doi.org/10.1111/j.15746976.2001.tb00581.x.

Chan, C.S., McAllister, S.M., Leavitt, A.H., Glazer, B.T., Krepski, S.T., Emerson, D. 2016. The architecture of iron microbial mats reflects the adaptation of chemolithotrophic iron oxidation in

freshwater and marine environments. Front Microbiol 7:796. https://doi.org/10.3389/fmicb.2016.00796.

Chaparro-Acuña, S.P., Becerra-Jiménez, M.L., Martínez-Zambrano, J.J., Rojas-Sarmiento, H.A. 2018. Soil bacteria that precipitate calcium carbonate: mechanism and applications of the process. Acta Agron 67(2):277-288. http://dx.doi.org/10.15446/acag.v67n2.66109.

Chatterjee, S. K., Bhattacharjee, I., Chandra, G. 2010. Biosorption of heavy metals from industrial waste water by *Geobacillus thermodenitrificans*. J Hazard Mater 175(1-3):117-125. https://doi.org/10.1016/j.jhazmat.2009.09.136.

Chen, Z., Pan, X., Chen, H., Guan, X., Lin, Z. 2016. Biomineralization of Pb (II) into Pb-hydroxyapatite induced by *Bacillus cereus* 12-2 isolated from Lead–Zinc mine tailings. J Hazard Mater 301:531-537. https://doi.org/10.1016/j.jhazmat.2015.09.023.

Chen, H.W., Xu, M., Ma, X.W., Tong, Z.H., Liu, D.F. 2019. Isolation and characterization of a chlorate-reducing bacterium *Ochrobactrum anthropi* XM-1. J Hazard Mater 380:120873. https://doi.org/10.1016/j.jhazmat.2019.120873.

Cheng, H., Yuan, M., Zeng, Q., Zhou, H., Zhan, W., Chen, H., Mao, Z., Wang, Y. 2020. Efficient reduction of Reactive Black 5 and Cr (VI) by a newly isolated bacterium of *Ochrobactrum anthropi*. J Hazard Mater 124641. https://doi.org/10.1016/j.jhazmat.2020.124641.

Cheng, Y., Yongming, X.I.E., Zheng, J., Zhaoxian, W.U., Zhi, C., Xiaoyan, M.A., Bin, L., Zhang, L. 2009. Identification and characterization of the chromium(VI) responding protein from a newly isolated *Ochrobactrum anthropi* CTS-325. J Environ Scie 21(12):1673-1678. https://doi.org/10.1016/s1001-0742(08)62472-9.

Cheng, Y., Yan, F., Huang, F., Chu, W., Pan, D., Chen, Z., Zheng, J., Yu, M., Lin, Z., Wu, Z. 2010. Bioremediation of Cr(VI) and immobilization as Cr(III) by *Ochrobactrum anthropi*. Environ Scie Technol 44(16):6357-6363. https://doi.org/10.1021/es100198v.

Chevallereau, A., Meaden, S., van Houte, S., Westra, E.R., Rollie, C. 2019. The effect of bacterial mutation rate on the evolution of CRISPR-Cas adaptive immunity. Philos Trans R Soc B 374(1772):20180094. https://doi.org/10.1098/rstb.2018.0094.

Chojnacka, K., Chojnacki, A., Górecka, H. 2005. Biosorption of Cr^{3+}, Cd^{2+} and Cu^{2+} ions by blue-green algae *Spirulina* sp.: kinetics, equilibrium and the mechanism of the process. Chemosphere 59(1):75-84. https://doi.org/10.1016/j.chemosphere.2004.10.005.

Choudhary, S. and Sar, P. 2011. Uranium biomineralization by a metal resistant *Pseudomonas aeruginosa* strain isolated from contaminated mine waste. J Hazard Mater 186(1):336–343. https://doi.org/10.1016/j.jhazmat.2010.11.004.

Chmelař, D., Holý, O., Kasáková, I., Hájek, M., Lazarová, A., Gonzalez-Rey, C., Lasák, J., Raclavský, V., Čižnár, I. 2019. Antibiotic susceptibility and production of endotoxin by *Ochrobactrum*

anthropi isolated from environment and from patients with cystic fibrosis. Folia Microbiol 64:861-865. https://doi.org/10.1007/s12223-019-00700-8.

Colica, G., Mecarozzi, P, De Phillippis, R. 2010. Treatment of Cr(VI)-containing wastewaters with exopolysaccharide-producing cyanobacteria in pilot flow through and batch systems. Appl Microbiol Biotechnol 87:1953–1961. https://doi.org/10.1007/s00253-010-2665-5.

Comte, J., Fauteux, L., del Giorgio, P., 2013. Links between metabolic plasticity and functional redundancy in freshwater bacterioplankton communities. Front Microbiol 4:112. https://doi.org/10.3389/fmicb.2013.00112.

Cooper, M.B. and Smith, A.G. 2015. Exploring mutualistic interactions between microalgae and bacteria in the omics age. Curr Opin Plant Biol 26:147-153. https://doi.org/10.1016/j.pbi.2015.07.003.

Coral, M. U., Korkmaz, H., Arikan, B., Coral, G. 2005. Plasmid mediated heavy metal resistances in Enterobacter spp. isolated from Sofulu landfill, in Adana, Turkey. Ann Microbiol 55(3):175.

Coreño-Alonso, A., Solé, A., Diestra, E., Esteve, I., Gutiérrez-Corona, J.F., López, G.R., Reyna López, G.E., Fernández, F.J., Tomasini, A. 2014. Mechanisms of interaction of chromium with *Aspergillus niger* var *tubingensis* strain Ed8. Biores Technol 158:188-192. https://doi.org/10.1016/j.biortech.2014.02.036.

Davey, M.E. and O'toole, G.A. 2000. Microbial biofilms: from ecology to molecular genetics. Microbiol Mol Biol Rev 64(4):847-867. https://doi.org/10.1128/mmbr.64.4.847-867.2000.

de los Ríos, A., Cary, C., Cowan, D. 2014. The spatial structures of hypolithic communities in the Dry Valleys of East Antarctica. Polar Biol 37:1823–1833. https://doi.org/10.1007/s00300-014-1564-0.

Deepika, L. and Kannabiran, K. 2010. Biosurfactant and heavy metal resistance activity of *Streptomyces* spp. isolated from Saltpan soil. Br J Pharmacol Toxicol 1:33–39.

Dhanakumar, S., Solaraj, G., Mohanraj, R. 2015. Heavy metal partitioning in sediments and bioaccumulation in commercial fish species of three major reservoirs of river Cauvery delta region, India. Ecotoxicol Environ Saf 113:145-151. https://doi.org/10.1016/j.ecoenv.2014.11.032.

Diep, P., Mahadevan, R., Yakunin, A.F. 2018. Heavy metal removal by bioaccumulation using genetically engineered microorganisms. Front Bioeng Biotechnol 6:157. https://doi.org/10.3389/fbioe.2018.00157

Diestra, E., Solé, A., Martí, M., De Oteyza, T.G., Grimalt, J.O., Esteve, I. 2005. Characterization of an oil-degrading *Microcoleus* consortium by means of confocal scanning microscopy, scanning

electron microscopy and transmission electron microscopy. Scanning 27(4):176-180. https://doi.org/10.1002/sca.4950270404.

Diestra, E., Esteve, I., Burnat, M., Maldonado, J., Solé, A. 2007. Isolation and characterization of a heterotrophic bacterium able to grow in different environmental stress conditions, including crude oil and heavy metals. Communicating Current Research and Educational Topics and Trends in Applied Microbiology, 1:90-99.

Domingues, V.S., de Souza Monteiro, A., Júlio, A.D.L., Queiroz, A.L.L., Dos Santos, V.L. 2020. Diversity of metal-resistant and tensoactive-producing culturable heterotrophic bacteria isolated from a copper mine in Brazilian Amazonia. Sci Rep 10:6171. https://doi.org/10.1038/s41598-020-62780-8

Edwardson, C.F., Planer-Friedrich, B., Hollibaugh, J.T. 2014. Transformation of monothioarsenate by haloalkaliphilic, anoxygenic photosynthetic purple sulfur bacteria. FEMS Microbiol Ecol 90(3):858-868. https://doi.org/10.1111/1574-6941.12440.

Engwa, G.A., Ferdinand, P.U., Nwalo, F.N., Unachukwu, M.N. 2019. Mechanism and health effects of heavy metal toxicity in humans. In poisoning in the modern world-new tricks for an old dog? IntechOpen. https://doi.org/10.5772/intechopen.82511.

Ermakova, I.T., Shushkova, T.V., Sviridov, A.V., Zelenkova, N.F., Vinokurova, N.G., Baskunov, B.P., Leontievsky, A.A. 2017. Organophosphonates utilization by soil strains of *Ochrobactrum anthropi* and *Achromobacter* sp. Arch Microbiol 199:665–675. https://doi.org/10.1007/s00203-017-1343-8.

Esteve, I., Martínez-Alonso, M., Mir, J., Guerrero, R. 1992. Distribution, typology and structure of microbial mat communities in Spain: a preliminary study. Limnetica 8:185–195.

Etesami, H. 2018. Bacterial mediated alleviation of heavy metal stress and decreased accumulation of metals in plant tissues: mechanisms and future prospects. Ecotoxicol Environ Saf 147:175-191. https://doi.org/10.1016/j.ecoenv.2017.08.032.

Fakhimi, N., Gonzalez-Ballester, D., Fernández, E., Galván, A., Dubini, A. 2020. Algae-bacteria consortia as a strategy to enhance H_2 production. Cells 9(6):1353. https://doi.org/10.3390/cells9061353.

Fashola, M.O., Ngole-Jeme, V.M., Babalola O.O. 2016. Heavy metal pollution from gold mines: Environmental effects and bacterial strategies for resistance. Int J Environ Res Public Health 13(11):1047. https://doi.org/10.3390/ijerph13111047.

Fernández-Martínez, M.A., Pointing, S.B., Pérez-Ortega, S., Arróniz-Crespo, M., Green, T.A., Rozzi, R., Sancho, L.G., de Los Ríos, A. 2016. Functional ecology of soil microbial communities along a glacier forefield in Tierra del Fuego (Chile). Int Microbiol 19(3):161-173. https://doi.org/10.2436/20.1501.01.274.

Fomina, M., Hillier, S., Charnock, J.M., Melville, K., Alexander, I.J., Gadd, G.M. 2005. Role of oxalic acid overexcretion in transformations of toxic metal minerals by *Beauveria caledonica*. Appl Environ Microbiol 71(1):371-381. https://doi.org/10.1128/aem.71.1.371-381.2005.

Fomina, M. and Gadd, G.M. 2014. Biosorption: current perspectives on concept, definition and application. Biores Technol 160:3-14. https://doi.org/10.1016/j.biortech.2013.12.102.

Francisco, R., de Abreu, P., Plantz, B.A., Schlegel, V.L., Carvalho, R.A., Vasconcelos-Morais, P. 2011. Metal-induced phosphate extracellular nanoparticulate formation in *Ochrobactrum tritici* 5bvl1. J Hazard Mater 198:31–39. https://doi.org/10.1016/j.jhazmat.2011.10.005.

Fu, F. and Wang, Q. 2011. Removal of heavy metal ions from wastewaters: a review. J Environ Manage 92(3):407-418. https://doi.org/10.1016/j.jenvman.2010.11.011.

García-Betancourt, M.L., Ramírez Jiménez, S.I., González-Hodges, A., Nuñez Salazar, Z.E., Escalante-García, I.L., Ramírez Aparicio, J. 2020. Low dimensional nanostructures: Measurement and remediation technologies applied to trace heavy metals in water. IntechOpen. http://doi.org/10.5772/intechopen.93263.

Ghosh, S. and Mitra, D. 2018. Elimination of chromium(VI) from waste water using various biosorbents. In: Sarma A., Singh V., Bhattacharjya R., Kartha S. (eds) Urban Ecology, Water Quality and Climate Change. Water Science and Technology Library, vol 84. Springer, Cham. https://doi.org/10.1007/978-3-319-74494-0_20.

Gillard, B., Chatzievangelou, D., Thomsen, L., Ullrich, M.S. 2019. Heavy-metal-resistant microorganisms in deep-sea sediments disturbed by mining activity: an application toward the development of experimental in vitro systems. Front Mar Sci 6:462. https://doi.org/10.3389/fmars.2019.00462.

Gohil, K., Rajput, V., Dharne, M. 2020. Pan-genomics of *Ochrobactrum* species from clinical and environmental origins reveals distinct populations and possible links. Genomics 112(5): 3003-3012. https://doi.org/10.1016/j.ygeno.2020.04.030.

Golding, J.D. and Dreitz, V.J. 2017. Songbird response to rest-rotation and season-long cattle grazing in a grassland sagebrush ecosystem. J Environ Manage 204:605-612. https://doi.org/10.1016/j.jenvman.2017.09.044.

Gontharet, S., Crémière, A., Blanc-Valleron, M.M., Sebilo, M., Gros, O., Laverman, A.M., Dessailly, D. 2017. Sediment characteristics and microbial mats in a marine mangrove, Manche-à-eau lagoon (Guadeloupe). J Soils Sediments 17(7):1999-2010. https://doi.org/10.1007/s11368-016-1555-6.

Guerrero, R., Urmeneta, J., Rampone, G. 1993. Distribution of types of microbial mats at the Ebro Delta, Spain. BioSystems 31(2-3):135-144.

Guerrero, R., Berlanga, M., 2016. From the cell to the ecosystem: the physiological evolution of symbiosis. Evol Biol 43:543–552. https://doi.org/10.1007/s11692-015-9360-5.

Gupta, P. and Diwan, B. 2016. Bacterial exopolysaccharide mediated heavy metal removal: a review on biosynthesis, mechanism and remediation strategies. Biotechnol Rep 13:58-71. https://doi.org/0.1016/j.btre.2016.12.006.

Han, X., Wong, Y.S., Tam, N.F.Y. 2006. Surface complexation mechanism and modeling in Cr(III) biosorption by a microalgal isolate, *Chlorella miniata*. J Colloid Interface Sci 303(2):365-371. https://doi.org/10.1016/j.jcis.2006.08.028.

Hayashida, G., Schneider, C., Espíndola, L., Arias, D., Riquelme, C., Wulff-Zottele, C., Diaz-Palma, P., Rivas, M. 2017. Characterization of a Chlorophyta microalga isolated from a microbial mat in Salar de Atacama (northern Chile) as a potential source of compounds for biotechnological applications. Phycological Res 65(3):202-211. https://doi.org/10.1111/pre.12176.

He, Z.L., Yang, X.E., Stoffella, P.J. 2005. Trace elements in agroecosystems and impacts on the environment. J Trace Elem Med Biol 19(2-3):125-40. https://doi.org/10.1016/j.jtemb.2005.02.010.

Hickman-Lewis, K., Cavalazzi, B., Foucher, F., Westall, F. 2018. Most ancient evidence for life in the Barberton greenstone belt: Microbial mats and biofabrics of the ~3.47 Ga Middle Marker horizon. Precambrian Res 312:45-67. https://doi.org/10.1016/B978-0-444-63901-1.00042-3.

Hirve, M., Jain, M., Rastogi, A., Kataria, S. 2020. Heavy metals, water deficit, and their interaction in plants: an overview. In Plant Life Under Changing Environment (pp. 175-206). Academic Press.

Hoehler, T.M., Bebout, B.M., Des Marais, D.J. 2001. The role of microbial mats in the production of reduced gases on the early Earth. Nature 412(6844):324-327. https://doi.org/10.1038/35085554.

Holmes, B., Popoff, M., Kiredjian, M., Kersters, K. 1988. *Ochrobactrum anthropi* gen. nov., sp. nov. from human clinical specimens and previously known as group Vd. Int J Syst Bacteriol 38(4):406–416. https://doi.org/10.1099/00207713-38-4-406.

Huber, B., Scholz, H.C., Kámpfer, P., Falsen, E., Langer, S., Busse, H.J. 2010. *Ochrobactrum pituitosum* sp. nov., isolated from an industrial environment. Int J Syst Evol Microbiol 60:321–326. https://doi.org/10.1099/ijs.0.011668-0.

Igiri, B.E., Okoduwa, S.I.R., Idoko, G.O., Akabuogu, E.P., Adeyi, A.O., Ejiogu, I.K. 2018. Toxicity and bioremediation of heavy metals contaminated ecosystem from tannery wastewater: A review. J Toxicol Article ID 2568038. https://doi.org/10.1155/2018/2568038.

Isaji, Y., Kawahata, H., Kuroda, J., Yoshimura, T., Ogawa, N.O., Suzuki, A., Shibuya, T., Jiménez-Espejo, F., Lugli, S., Santulli, A., Manzi, V., Roveri, M., Ohkouchi, N. 2017. Biological and physical modification of carbonate system parameters along the salinity gradient in shallow hypersaline solar salterns in Trapani, Italy. Geochim Cosmochim Acta 208:354-367. https://doi.org/10.1016/J.GCA.2017.04.013.

Iyer, R. and Damania, A. 2016. Draft genome sequence of organophosphate‑degrading *Ochrobactrum anthropi* FRAF13. Genome Announc 4(2). https://doi.org/10.1128/genomeA.00295‑16.

Jaishankar, M., Tseten, T., Anbalagan, N., Mathew, B.B., Beeregowda, K.N. 2014. Toxicity, mechanism and health effects of some heavy metals. Interdiscip Toxicol 7(2):60–72. https://doi.org/10.2478/intox‑2014‑0009.

Jasso‑Chávez, R., Lira‑Silva, E., González‑Sánchez, K., Larios Serrato, V., Mendoza‑Monzoy, D.L., Pérez‑Villatoro, F., Morett, E., Vega‑Segura, A., Torres‑Márquez, M.E., Zepeda‑Rodríguez, A., Moreno‑Sánchez, R. 2019. Marine archaeon *Methanosarcina acetivorans* enhances polyphosphate metabolism under persistent cadmium stress. Front Microbiol 10:2432. https://doi.org/10.3389/fmicb.2019.02432.

Joutey, N.T., Bahafid, W., Sayel, H., Ananou, S., El Ghachtouli, N. 2014. Hexavalent chromium removal by a novel *Serratia proteamaculans* isolated from the bank of Sebou River (Morocco). Environ Sci Pollut Res 21(4):3060‑3072. https://doi.org/10.1007/s11356‑013‑2249‑x.

Jungblut, A.D., Vincent, W.F., Lovejoy, C. 2012. Eukaryotes in Arctic and Antarctic cyanobacterial mats. FEMS Microbiol Ecol 82(2):416‑428. https://doi.org/10.1111/j.1574‑6941.2012.01418.x.

Kanamarlapudi, S.L.R.K., Chintalpudi, V.K., Muddada, S. 2018. Application of biosorption for removal of heavy metals from wastewater. Biosorption 18:69. https://doi.org/10.5772/intechopen.77315.

Kapahi, M. and Sachdeva, S. 2019. Bioremediation options for heavy metal pollution. J Health Pollut 9(24):191203. https://doi.org/10.5696/2156‑9614‑9.24.191203.

Karthik, C., Barathi, S., Pugazhendhi, A., Ramkumar, V.S., Thi, N.B.D., Arulselvi, P.I. 2017. Evaluation of Cr(VI) reduction mechanism and removal by *Cellulosimicrobium funkei* strain AR8, a novel haloalkaliphilic bacterium. J Hazard Mater 333:42‑53. https://doi.org/10.1016/j.jhazmat.2017.03.037.

Keyhani, S., Lopez, J. L., Clark, D.S., Keasling, J.D. 1996. Intracellular polyphosphate content and cadmium tolerance in *Anacystis nidulans* R2. Microbios 88(355):105‑114.

Khan, I., Ali, M., Aftab, M., Shakir, S., Qayyum, S., Haleem, K.S., Tauseef, I. 2019. Mycoremediation: a treatment for heavy metal‑polluted soil using indigenous metallotolerant fungi. Environ Monit Assess 191:622. https://doi.org/10.1007/s10661‑019‑7781‑9.

Khulbe, K.C. and Matsuura, T. 2018. Removal of heavy metals and pollutants by membrane adsorption techniques. Appl Water Scie 8(1):19. https://doi.org/10.1007/s13201‑018‑0661‑6.

Kobayashi, T., Ralph, T.J., Sharma, P., Mitrovic, S.M. 2020. Influence of historical inundation frequency on soil microbes (Cyanobacteria, Proteobacteria, Actinobacteria) in semi‑arid floodplain wetlands. Mar Fresh Res 71(5):617‑625. https://doi.org/10.1071/MF18468.

Kornberg, A., Rao, N.N., Ault-Riche, D. 1999. Inorganic polyphosphate: a molecule of many functions. Annu Rev Biochem 68:89-125. https://doi.org/10.1146/annurev.biochem.68.1.89.

Ksheminska, H., Fedorovych, D., Babyak, L., Yanovych, D., Kaszycki, P., Koloczek, H. 2005. Chromium (III) and (VI) tolerance and bioaccumulation in yeast: a survey of cellular chromium content in selected strains of representative genera. Process Biochem 40(5):1565-1572. https://doi.org/10.1016/j.procbio.2004.05.012.

Kulakovskaya, T., Ryazanova, L., Zvonarev, A., Khokhlova, G., Ostroumov, V., Vainshtein, M. 2018. The biosorption of cadmium and cobalt and iron ions by yeast *Cryptococcus humicola* at nitrogen starvation. Folia Microbiol 63:507–510. https://doi.org/10.1007/s12223-018-0583-6

Kulkarni, G., Gohil, K., Misra, V., Kakrani, A.L., Misra, S.P., Patole, M., Shouche, Y., Dharne, M. 2017. Multilocus sequence typing of *Ochrobactrum* spp. isolated from gastric niche. J Infect Public Health 10:201–210. https://doi.org/10.1016/j.jiph.2016.04.013.

Lavoie, K.H., Winter, A.S., Read, K.J.H., Hughes, E.M., Spilde, M.N., Northup, D.E. 2017. Comparison of bacterial communities from lava cave microbial mats to overlying surface soils from Lava Beds National Monument, USA. PLOS ONE 12(2):e0169339. https://doi.org/10.1371/journal.pone.0169339.

Lee, H.W. and Park, Y.K. 2008. Characterizations of denitrifying polyphosphate-accumulating bacterium *Paracoccus* sp. strain YKP-9. J Microbiol Biotechnol 18(12):1958–1965. https://doi.org/10.4014/jmb.0800.162.

Li, B., Pan, D., Zheng, J., Cheng, Y., Ma, X., Huang, F., Lin, Z. 2008. Microscopic investigations of the Cr (VI) uptake mechanism of living *Ochrobactrum anthropi*. Langmuir 24(17):9630-9635. https://doi.org/10.1021/la801851h.

Li, K. and Ramakrishna, W. 2011. Effect of multiple metal resistant bacteria from contaminated lake sediments on metal accumulation and plant growth. J Hazard Mater 189(1-2):531-539. https://doi.org/10.1016/j.jhazmat.2011.02.075.

Li, M. H., Gao, X. Y., Li, C., Yang, C. L., Fu, C. A., Liu, J., Wang, R., Chen, L.X., Li, J.Q., Liu, X.M., Lin, J.Q 1, Xin Pang, X. 2020. Isolation and identification of chromium reducing *Bacillus cereus* species from chromium-contaminated soil for the biological detoxification of chromium. Int J Environ Res Public Health 17(6):2118. https://doi.org/10.3390/ijerph17062118.

Li, Y., Zhang, H., Chen, X., Tu, C., Luo, Y., Christie, P. 2014. Distribution of heavy metals in soils of the Yellow River Delta: concentrations in different soil horizons and source identification. J Soils Sediments 14:1158–1168. https://doi.org/10.1007/s11368-014-0861-0

Lichtenberg, M., Cartaxana, P., Kühl, M. 2020. Vertical migration optimizes photosynthetic efficiency of motile cyanobacteria in a coastal microbial mat. Front Mar Sci 7:359. https://doi.org/10.3389/fmars.2020.00359.

Liu, S.H., Zeng, G.M., Niu, Q.Y., Liu, Y., Zhou, L., Jiang, L.H., Tan, X-F., Xu, P., Zhang, C., Cheng, M. 2017. Bioremediation mechanisms of combined pollution of PAHs and heavy metals by

bacteria and fungi: A mini review. Biores Technol 224:25-33. https://doi.org/10.1016/j.biortech.2016.11.095.

Luo, S., Cai, T., Liu, C., Zhang, Y., Liu, Y., Ma, J., Wei, Y., Ali, O., Zhang, S. 2017. Fast adsorption of heavy metal ions by waste cotton fabrics based double network hydrogel and influencing factors insight. J Hazard Mater 344:1034–1042. https://doi.org/10.1016/j.jhazmat.2017.11.041.

Madkour, L.H. 2020. Ecotoxicology of environmental heavy metal ions and free radicals on macromolecule cell organisms. In nanoparticles induce oxidative and endoplasmic reticulum stresses (pp. 1-46). Springer, Cham. https://doi.org/10.1007/978-3-030-37297-2_1.

Magnin, J.P., Gondrexon, N., Willison, J.C. 2014. Zinc biosorption by the purple non-sulfur bacterium *Rhodobacter capsulatus*. Can J Microbiol 60(12):829-37. https://doi.org/10.1139/cjm-2014-0231.

Maldonado, J., de los Rios, A., Esteve, I., Ascaso, C., Puyen, Z. M., Brambilla, C., Solé, A. 2010a. Sequestration and in vivo effect of lead on DE2009 microalga, using high-resolution microscopic techniques. J Hazard Mater 183(1-3):44-50. https://doi.org/10.1016/j.jhazmat.2010.06.085.

Maldonado, J., Diestra, E., Huang, L., Domènech, A. M., Villagrasa, E., Puyen, Z. M., Esteve, I., Solé, A. 2010b. Isolation and identification of a bacterium with high tolerance to lead and copper from a marine microbial mat in Spain. Ann Microbiol 60(1):113-120. https://doi.org/10.1007/s13213-010-0019-2.

Malik, A. 2004. Metal bioremediation through growing cells. Environ Int 30(2):261–278. https://doi.org/10.1016/j.envint.2003.08.001.

Mañosa, S., Mateo, R., Guitart, R. 2001. A review of the effects of agricultural and industrial contamination on the Ebro delta biota and wildlife. Environ Monit Assess 71(2):187-205. https://doi.org/10.1023/A:1017545932219.

Martinez, R.J., Beazley, M.J., Sobecky, P.A. 2014. Phosphate-mediated remediation of metals and radionuclides. Adv Ecol https://doi.org/10.1155/2014/786929.

Martínez-Alonso, M., Mir, J., Caumette, P., Gaju, N., Guerrero, R., Esteve, I. 2004. Distribution of phototrophic populations and primary production in a microbial mat from the Ebro Delta, Spain. Int Microbiol 7(1):19–25

Masindi, V. and Muedi, K.L. 2018. Environmental Contamination by Heavy Metals, Heavy Metals, Hosam El-Din M. Saleh and Refaat F. Aglan, IntechOpen, https://doi.org/10.5772/intechopen.76082.

Mehta, H.H., Prater, A.G., Beabout, K., Elworth, R., Karavis, M., Gibbons, H.S., Shamoo, Y. 2019. The essential role of hypermutation in rapid adaptation to antibiotic stress. Antimicrob Agents Chemother 63(7):e00744-19. https://doi.org/10.1128/AAC.00744-19.

Merino, N., Aronson H.S., Bojanova, D.P., Feyhl‑Buska, J., Wong M.L., Zhang, S., Giovannelli, D. 2019. Living at the extremes: Extremophiles and the limits of life in a planetary. Front Microbiol 10:780. https://doi.org/10.3389/fmicb.2019.00780.

Millach, L., Solé, A., Esteve, I. 2015. Role of *Geitlerinema* sp. DE2011 and *Scenedesmus* sp. DE2009 as bioindicators and immobilizers of chromium in a contaminated natural environment. BioMed Res Int. https://doi.org/10.1155/2015/519769.

Millach, L., Villagrasa, E., Solé, A., Esteve, I. 2019. Combined confocal laser scanning microscopy techniques for a rapid assessment of the effect and cell viability of *Scenedesmus* sp. DE2009 under metal stress. Microsc Microanal 25(4):998‑1003. https://doi.org/10.1017/S143192761901465X.

Miranda, P.J., McLain, N.K., Hatzenpichler, R., Orphan, V.J., Dillon, J.G. 2016. Characterization of chemosynthetic microbial mats associated with intertidal hydrothermal sulfur vents in white point, San Pedro, CA, USA. Front Microbiol 7:1163. https://doi.org/10.3389/fmicb.2016.01163.

Moens, M., Branco, R., Morais, P.V. 2020. Arsenic accumulation by a rhizosphere bacterial strain *Ochrobactrum tritici* reduces rice plant arsenic levels. World J Microbiol Biotechnol 36(2):23. https://doi.org/10.1007/s11274‑020‑2800‑0.

Monteiro, C.M., Marques, A.P.G.C., Castro, P.M.L., Malcata, F.X. 2009. Characterization of *Desmodesmus pleiomorphus* isolated from a heavy metal‑contaminated site: biosorption of zinc. Biodegradation 20:629–641. https://doi.org/10.1007/s10532‑009‑9250‑6

Mukherjee, C., Chowdhury, R., Ray, K. 2015. Phosphorus recycling from an unexplored source by polyphosphate accumulating microalgae and cyanobacteria—A step to phosphorus security in agriculture. Front Microbiol 6:1421. https://doi.org/10.3389/fmicb.2015.01421.

Murínová, S., Dercová, K. 2014. Potential use of newly isolated bacterial strain *Ochrobactrum anthropi* in bioremediation of polychlorinated biphenyls. Water Air Soil Pollut 225:1980. https://doi.org/10.1007/s11270‑014‑1980‑3.

Nadal, M., Casacuberta, N., Garcia‑Orellana, J., Ferré‑Huguet, N., Masqué, P., Schuhmacher, M., Domingo, J.L. 2011. Human health risk assessment of environmental and dietary exposure to natural radionuclides in the Catalan stretch of the Ebro River, Spain. Environ Monit Assess 175:455–468. https://doi.org/10.1007/s10661‑010‑1543‑z.

Nagajyoti, P.C., Lee, K.D., Sreekanth, T.V.M. 2010. Heavy metals, occurrence and toxicity for plants: a review. Environ Chem Lett 8(3):199‑216. https://doi.org/10.1007/s10311‑010‑0297‑8.

Navarrete, A., Peacock, A., Macnaughton, S. J., Urmeneta, J., Mas‑Castella, J., White, D.C., Guerrero, R. 2000. Physiological status and community composition of microbial mats of the Ebro Delta, Spain, by signature lipid biomarkers. Microb Ecol 39(1):92‑99. https://doi.org/10.1007/s002489900185.

Nguyen, T.A.H., Ngo, H.H., Guo, W.S., Zhang, J., Liang, S., Yue, Q.Y., Li, Q., Nguyen, T.V. 2013. Applicability of agricultural waste and by-products for adsorptive removal of heavy metals from wastewater. Biores Technol 148:574-585. https://doi.org/10.1016/j.biortech.2013.08.124.

Nübel, U., Bateson, M.M., Madigan, M.T., Kühl, M., Ward, D.M. 2001. Diversity and distribution in hypersaline microbial mats of bacteria related to *Chloroflexus* spp. Appl Environ Microbiol 67(9):4365-4371. https://doi.org/10.1128/AEM.67.9.4365-4371.2001.

Nweke, C.O., Alisi, C.S., Okolo, J.C., Nwanyanwu, C.E. 2007. Toxicity of zinc to heterotrophic bacteria from a tropical river sediment. Appl Ecol Environ Res 5(1):123-132.

Oehmen, A., Carvalho, G., Freitas, F., Reis, M.A. 2010. Assessing the abundance and activity of denitrifying polyphosphate accumulating organisms through molecular and chemical techniques. Water Sci Techno 61(8):2061-2068. https://doi.org/10.2166/wst.2010.976.

Ojuederie, O.B. and Babalola, O.O. 2017. Microbial and Plant-Assisted Bioremediation of Heavy Metal Polluted Environments: A Review. Int J Environ Res Public Health 14(12):1504. https://doi.org/10.3390/ijerph14121504.

Olawoyin, R., Oyewole, S.A., Grayson, R.L. 2012. Potential risk effect from elevated levels of soil heavy metals on human health in the Niger delta. Ecotoxicol Environ Saf 85:120-130. https://doi.org/10.1016/j.ecoenv.2012.08.004.

Orell, A., Navarro, C.A., Rivero, M., Aguilar, J.S., Jerez, C.A. 2012. Inorganic polyphosphates in extremophiles and their possible functions. Extremophiles 16(4):573-583. https://doi.org/ https://doi.org/10.1007/s00792-012-0457-9.

Ozdemir, G., Ozturk, T., Ceyhan, N., Isler, R., Cosar, T. 2003. Heavy metal biosorption by biomass of *Ochrobactrum anthropi* producing exopolysaccharide in activated sludge. Biores Technol 90(1):71-74. https://doi.org/10.1016/S0960-8524(03)00088-9.

Pandey, S., Chakrabarty, J., Maiti, T.K. 2015. The FAME profiles of Cadmium resistant *Ochrobactrum* sp. and Lead and Arsenate resistant *Bacillus* spp. Natl Acad Sci Lett 38(6):507-511. https://doi.org/10.1007/s40009-015-0364-6.

Peng, W., Li, X., Xiao, S., Fan, W. 2018. Review of remediation technologies for sediments contaminated by heavy metals. J soils sediments 18(4):1701-1719. https://doi.org/10.1007/s11368-018-1921-7.

Peng, H., Xie, W., Li, D., Wu, M., Zhang, Y., Xu, H., Liang,Y., Liu, W. 2019. Copper-resistant mechanism of *Ochrobactrum* MT180101 and its application in membrane bioreactor for treating electroplating wastewater. Ecotoxicol Enviro Saf 168:17-26. https://doi.org/10.1016/j.ecoenv.2018.10.066.

Perdrial, N., Liewig, N., Delphin, J.E., Elsass, F. 2008. TEM evidence for intracellular accumulation of lead by bacteria in subsurface environments. Chem Geol 253(3-4):196-204. https://doi.org/10.1016/j.chemgeo.2008.05.008.

Podda, F., Medas, D., De Giudici, G., Ryszka, P., Wołowski, K., Turnau, K. 2014. Zn biomineralization processes and microbial biofilm in a metal-rich stream (Naracauli, Sardinia). Environ Sci Pollut Res 21:6793–6808. https://doi.org/10.1007/s11356-013-1987-0

Povedano-Priego, C., Martín-Sanchez, I., Jroundi, F., Sanchez-Castro, I., Merroun, M.L., 2017. Fungal biomineralization of lead phosphates on the surface of lead metal. Miner Eng 106:46e54. https://doi.org/10.1016/j.mineng.2016.11.007.

Prieto-Barajas, C. M., Valencia-Cantero, E., Santoyo, G. 2018. Microbial mat ecosystems: structure types, functional diversity, and biotechnological application. Electron J Biotechnol 31:48-56. https://doi.org/10.1016/j.ejbt.2017.11.001.

Puyen, Z.M., Villagrasa, E., Maldonado, J., Diestra, E., Esteve, I., Solé, A. 2012. Biosorption of lead and copper by heavy-metal tolerant *Micrococcus luteus* DE2008. Biores Technol 126:233-237. https://doi.org/10.1016/j.biortech.2012.09.036.

Puyen, Z.M., Villagrasa, E., Millach, L., Esteve, I., Maldonado, J., Solé, A. 2017. Multi-approach microscopy techniques to evaluate the cytotoxic effect of chromium (III) on the cyanobacterium Chroococcus sp. PCC 9106. In Microscopy and Imaging Science: Practical Approaches to Applied Research and Education (pp. 602-609). Formatex Research Center Badajoz.

Qiu, X.H., Bai, W. Q., Zhong, Q.Z., Li, M., He, F. Q., Li, B.T. 2006. Isolation and characterization of a bacterial strain of the genus *Ochrobactrum* with methyl parathion mineralizing activity. J Applied Microbiol 101(5):986-994. https://doi.org/10.1111/j.1365-2672.2006.03016.x.

Rai, P.K., Lee, S.S., Zhang, M., Tsang, Y.F., Kim, K.H. 2019. Heavy metals in food crops: Health risks, fate, mechanisms, and management. Environ Int 125:365-385. https://doi.org/10.1016/j.envint.2019.01.067.

Ramanan, R., Kim, B.H., Cho, D.H., Oh, H.M., Kim, H.S. 2016. Algae–bacteria interactions: evolution, ecology and emerging applications. Biotechnol Adv 34(1):4-29. https://doi.org/10.1016/j.biotechadv.2015.12.003.

Ramasamy, S., Mathiyalagan, P., Chandran, P. 2014. Characterization and optimization of EPS-producing and diesel oil-degrading *Ochrobactrum anthropi* MP3 isolated from refinery wastewater. Petroleum Sci 11(3):439-445. https://doi.org/10.1007/s12182-014-0359-9.

Ramírez, V., Baez, A., López, P., Bustillos, R., Villalobos, M.Á., Carreño, R., Contreras, J.L., Muñoz-Rojas, J., Fuentes, L.E., Martínez, J., Munive, J.A. 2019. Chromium hyper-tolerant *Bacillu*s sp. MH778713 assists phytoremediation of heavy metals by mesquite trees (*Prosopis laevigata*). Front Microbiol 10:1833. https://doi.org/10.3389/fmicb.2019.01833.

Rao, A.V., Bested, A.C., Beaulne, T.M., Katzman, M.A., Iorio, C., Berardi, J.M., Logan, A.C. 2009. A randomized, double-blind, placebo-controlled pilot study of a probiotic in emotional symptoms of chronic fatigue syndrome. Gut pathogens 1(1):1-6.

Rajpert, L., Skłodowska, A., Matlakowska, R. 2013. Biotransformation of copper from Kupferschiefer black shale (Fore-Sudetic Monocline, Poland) by yeast *Rhodotorula mucilaginosa* LM9. Chemosphere 91(9):1257-1265. https://doi.org/10.1016/j.chemosphere.2013.02.022.

Reid, R.P., Visscher, P.T., Decho, A.W., Stolz, J.F. 2000. The role of microbes in accretion, lamination and early lithification of modern marine stromatolites. Nature 406(6799):989–992. https://doi.org/10.1038/35023158.

Reinold, M., Wong, H.L., MacLeod, F.I., Meltzer, J., Thompson, A., Burns, B.P. 2019. The vulnerability of microbial ecosystems in a changing climate: Potential impact in Shark Bay. Life 9(3):71. https://doi.org/10.3390/life9030071.

Remonsellez, F., Orell, A., Jerez, C.A. 2006. Copper tolerance of the thermoacidophilic archaeon *Sulfolobus metallicus*: possible role of polyphosphate metabolism. Microbiology 152(1):59-66. https://doi.org/10.1099/mic.0.28241-0.

Rizvi, A. and Saghir Khan, M. 2019. Putative role of bacterial biosorbent in metal sequestration revealed by SEM-EDX and FTIR. Indian journal of microbiology 59(2):246–249. https://doi.org/10.1007/s12088-019-00780-7

Rizvi, A., Ahmed, B., Zaidi, A. Khan, M.S. 2020. Biosorption of heavy metals by dry biomass of metal tolerant bacterial biosorbents: an efficient metal clean-up strategy. Environ Monit Assess 192:801. https://doi.org/10.1007/s10661-020-08758-5

Roane, T.M., Pepper, I.L., Gentry, T.J. 2015. Microorganisms and metal pollutants. In Environmental microbiology (pp. 415-439). Academic Press. https://doi.org/10.1016/B978-0-12-394626-3.00018-1.

Rodríguez-Celma, J., Lin, W.D., Fu, G.M., Abadía, J., López-Millán, A.F., Schmidt, W. 2013. Mutually exclusive alterations in secondary metabolism are critical for the uptake of insoluble iron compounds by *Arabidopsis* and *Medicago truncatula*. Plant Physiol 162(3):1473–1485. https://doi.org/10.1104/pp.113.220426.

Roeselers, G., Norris, T.B., Castenholz, R.W., Rysgaard, S., Glud, R.N., Kühl, M., Muyzer, G. 2007. Diversity of phototrophic bacteria in microbial mats from Arctic hot springs (Greenland). Environ Microbiol 9(1):6-38. https://doi.org/10.1111/j.1462-2920.2006.01103.x.

Rubio-Rincón, F.J., Welles, L., Lopez-Vazquez, C.M., Nierychlo, M., Abbas, B., Geleijnse, M., Nielsen, P.H., van Loosdrecht, M.C.M., Brdjanovic, D. 2017. Long-term effects of sulphide on the enhanced biological removal of phosphorus: the symbiotic role of *Thiothrix caldifontis*. Water Res 116:53-64. https://doi.org/10.1016/j.watres.2017.03.017.

Rügner, H., Schwientek, M., Milačič, R., Zuliani, T., Vidmar, J., Paunović, M., Laschou, S., Kalogianni, E., Skoulikidis, N.T., Diamantini, E., Majone, B., Bellin, A., Chiogna, G., Martinez, E., López de Alda, M., Díaz-Cruz, M.S., Grathwohl, P. 2019. Particle bound pollutants in rivers: Results from suspended sediment sampling in Globaqua River Basins. Sci Total Environ 647:645-652. https://doi.org/10.1016/j.scitotenv.2018.08.027.

Saber, A., James, D.E., Hayes, D.F. 2019. Estimation of water quality profiles in deep lakes based on easily measurable constituents at the water surface using artificial neural networks coupled with stationary wavelet transform. Sci Total Environ 694:133690. https://doi.org/10.1016/j.scitotenv.2019.133690.

Sakai, H.D. and Kurosawa, N. 2016. Exploration and isolation of novel thermophiles in frozen enrichment cultures derived from a terrestrial acidic hot spring. Extremophiles 20(2):207-214. https://doi.org/10.1007/s00792-016-0815-0.

Sánchez-Chardi, A., Marques, C.C., Nadal, J., da Luz Mathias, M. 2007. Metal bioaccumulation in the greater white-toothed shrew, *Crocidura russula*, inhabiting an abandoned pyrite mine site. Chemosphere 67(1):121-130. https://doi.org/10.1016/j.chemosphere.2006.09.009.

Sánchez-Chardi, A. and López-Fuster, M.J. 2009. Metal and metalloid accumulation in shrews (Soricomorpha, Mammalia) from two protected Mediterranean coastal sites. Environ Pollut 157(4):1243-1248. https://doi.org/10.1016/j.envpol.2008.11.047.

Seder-Colomina, M., Burgos, A., Maldonado, J., Solé, A., Esteve, I. 2013. The effect of copper on different phototrophic microorganisms determined in vivo and at cellular level by confocal laser microscopy. Ecotoxicology 22(1):199-205. https://doi.org/10.1007/s10646-012-1014-0.

Şen, A., Pereira, H., Olivella, M.A., Villaescusa, I. 2015. Heavy metals removal in aqueous environments using bark as a biosorbent. Int J Environ Sci Technol 12(1):391-404. https://doi.org/10.1007/s13762-014-0525-z.

Serra, A.V., Botté, S.E., Cuadrado, D.G., La Colla, N.S., Negrin, V.L. 2017. Metals in tidal flats colonized by microbial mats within a South-American estuary (Argentina). Environ Earth Sci 76(6):254. https://doi.org/10.1007/s12665-017-6577-x.

Seufferheld, M.J., Alvarez, H.M., Farias, M.E. 2008. Role of polyphosphates in microbial adaptation to extreme environments. Appl Environ Microbiol 74:5867–5874. https://doi.org/10.1128/AEM.00501-08.

Shadrin, N.V. 2018. Hypersaline lakes as the polyextreme habitats for life. Introduction to salt lake sciences, 180-187.

Shanahan, P. 2004. Bioremediation. Waste Containment and Remediation Technology, Spring 2004, Massachusetts Institute of Technology, MIT OpenCourseWare

Shao, W., Li, M., Teng, Z., Qiu, B., Huo, Y., Zhang, K. 2019. Effects of Pb(II) and Cr(VI) stress on phosphate-solubilizing bacteria (*Bacillus* sp. Strain MRP-3): oxidative stress and bioaccumulation potential. Int J Environ Res Public Health 16(12):2172. https://doi.org/10.3390/ijerph16122172.

Sharma, B. and Shukla, P. 2021. A comparative analysis of heavy metal bioaccumulation and functional gene annotation towards multiple metal resistant potential by *Ochrobactrum*

intermedium BPS-20 and *Ochrobactrum ciceri* BPS-26. Biores Technol 320:124330. https://doi.org/10.1016/j.biortech.2020.124330.

Sheng, G.P., Yu, H.Q., Yue, Z.B., 2005. Production of extracellular polymeric substances from *Rhodopseudomonas acidophila* in the presence of toxic substances. Appl Microbiol Biotechnol. 69 (2):216e222. https://doi.org/10.1007/s00253-005-1990-6.

Singh, R., Gautam, N., Mishra, A., Gupta, R. 2011. Heavy metals and living systems: An overview. Indian J Pharmacol 43(3):246. https://doi.org/10.4103/0253-7613.81505.

Smitha, M.S., Singh, S., Singh, R. 2017. Microbial biotransformation: a process for chemical alterations. J Bacteriol Mycol Open Access 4(2):85. https://doi.org/10.15406/jbmoa.2017.04.00085.

Solé, A., Gaju, N., Esteve, I. 2003. The biomass dynamics of cyanobacteria in an annual cycle determined by confocal laser scanning microscopy. Scanning 25(1):1-7.

Solisio, C., Lodi, A., Converti, A., Del Borghi, M., 2000. The effect of acid pretreatment on the biosorption of chromium(III) by *Sphaerotilus natans* from industrial wastewater. Water Res. 34 (12), 3171e3178. https://doi.org/10.1016/S0043-1354(00)00059-2.

Spetter, C.V., Buzzi, N.S., Fernández, E.M., Cuadrado, D.G., Marcovecchio, J.E. 2015. Assessment of the physicochemical conditions sediments in a polluted tidal flat colonized by microbial mats in Bahía Blanca Estuary (Argentina). Mar Pollut Bull 91(2):491-505. https://doi.org/10.1016/j.marpolbul.2014.10.008.

Sriram, M.I., Kalishwaralal, K., Deepak, V., Gracerosepat, R., Srisakthi, K., Gurunathan, S., 2011a. Biofilm inhibition and antimicrobial action of lipopeptide biosurfactant produced by heavy metal tolerant strain *Bacillus cereus* NK1. Colloids Surf. B. Biointerf. 85:174–181. https://doi.org/10.1016/j.colsurfb.2011.02.026.

Sriram, M.I., Gayathiri, S., Gnanaselvi, U., Jenifer, P.S., Raj, S.M., Gurunathan, S. 2011b. Novel lipopeptide biosurfactant produced by hydrocarbon degrading and heavy metal tolerant bacterium *Escherichia fergusonii* KLU01 as a potential tool for bioremediation. Biores Technol 102(19):9291-9295. https://doi.org/10.1016/j.biortech.2011.06.094.

Subashchandrabose, S.R., Ramakrishnan, B., Megharaj, M., Venkateswarlu, K., Naidu, R. 2011. Consortia of cyanobacteria/microalgae and bacteria: biotechnological potential. Biotechnol Adv 29(6):896–907. https://doi.org/10.1016/j.biotechadv.2011.07.009.

Tang, X., Zheng, H., Teng, H., Sun, Y., Guo, J., Xie, W., Yang, Q., Chen, W. 2016. Chemical coagulation process for the removal of heavy metals from water: a review. Desalin Water Treat 57(4):1733-1748. https://doi.org/10.1080/19443994.2014.977959.

Tank, M., Thiel, V., Ward, D.M., Bryant, D.A. 2017. A panoply of phototrophs: an overview of the thermophilic chlorophototrophs of the microbial mats of alkaline siliceous hot springs in

Yellowstone National Park, WY, USA. In Modern topics in the phototrophic prokaryotes (pp. 87-137). Springer, Cham.

Tchounwou, P.B., Yedjou, C.G., Patlolla, A.K., Sutton, D.J. 2012. Heavy metal toxicity and the environment. Experientia Suppl 101:133–164. https://doi.org/10.1007/978-3-7643-8340-4_6.

Teitzel, G.M., Geddie, A., Susan, K., Kirisits, M.J., Whiteley, M., Parsek, M.R. 2006. Survival and growth in the presence of elevated copper: transcriptional profiling of copper-stressed Pseudomonas aeruginosa. J Bacteriol 188(20):7242-7256. https://doi.org/10.1128/JB.00837-06.

Teyssier, C., Marchandin, H., Jean-Pierre, H., Diego, I., Darbas, H., Jeannot, J.L., Gouby, A., Jumas-Bilak, E. 2005. Molecular and phenotypic features for identification of the opportunistic pathogens *Ochrobactrum* spp. J Med Microbiol 54(10):945–953. https://doi.org/10.1099/jmm.0.46116-0.

Thoma, B., Straube, E., Scholz, H.C., Al Dahouk, S., Zöller, L., Pfeffer, M., Neubauer, H., Tomaso H. 2009. Identification and antimicrobial susceptibilities of *Ochrobactrum* spp. Int J Med Microbiol 299(3):209-220. https://doi.org/10.1016/j.ijmm.2008.06.009.

Tobias, N.J., Mishra, B., Gupta, D.K., Ke, L.P., Thines, M., Bode, H.B. 2015. Draft genome sequence of *Ochrobactrum anthropi* strain ML7 isolated from soil samples in Vinhphuc Province, Vietnam. Genome Announc 3(2). https:///doi.org/10.1128/genomeA.00218-15.

Upadhyay, N., Vishwakarma, K., Singh, J., Mishra, M., Kumar, V., Rani, R., Mishra, R.K., Chauhan, D. K., Tripathi, D.K., Sharma, S. 2017. Tolerance and reduction of chromium(VI) by *Bacillus* sp. MNU16 isolated from contaminated coal mining soil. Front Plant Sci 8:778. https://doi.org/10.3389/fpls.2017.00778.

Verma, P., Raghavan, R. V., Jeon, C. O., Lee, H. J., Priya, P. V., Dharani, G., Kirubagaran, R. 2017. Complex bacterial communities in the deep-sea sediments of the Bay of Bengal and volcanic Barren Island in the Andaman Sea. Mar Genomics 31:33-41. https://doi.org/10.1016/j.margen.2016.08.003.

Vila. A., Pagella, H., Vera Bello, G., Vicente, A. 2016. *Brucella* suis bacteremia misidentified as *Ochrobactrum anthropi* by the VITEK 2 system. J Infect Dev Ctries 10(4):432-6. https://doi.org/10.3855/jidc.7532.

Vilavert, L., Sisteré, C., Schuhmacher, M., Nadal, M., Domingo, J.L. 2015. Environmental concentrations of metals in the catalan stretch of the Ebro river, Spain: assessment of temporal trends. Biol Trace Elem Res 163(1-2):48-57. https://doi.org/10.1007/s12011-014-0140-3.

Villagrasa, E., Ferrer-Miralles, N., Millach, L., Obiol, A., Creus, J., Esteve, I., Solé, A. 2019. Morphological responses to nitrogen stress deficiency of a new heterotrophic isolated strain of Ebro Delta microbial mats. Protoplasma 256:105-116. https://doi.org/10.1007/s00709-018-1263-8.

Villagrasa, E., Ballesteros, B., Obiol, A., Millach, L., Esteve, I., Solé, A. 2020a. Multi-approach analysis to assess the chromium(III) immobilization by *Ochrobactrum anthropi* DE2010. Chemosphere 238:124663. https://doi.org/10.1016/j.chemosphere.2019.124663.

Villagrasa, E., Egea, R., Ferrer-Miralles, N., Solé, A. 2020b. Genomic and biotechnological insights in stress-linked polyphosphate production induced by chromium(III) in *Ochrobactrum anthropi* DE2010. World J Microbiol Biotechnol 36:97. https://doi.org/10.1007/s11274-020-02875-6.

Villagrasa, E., Palet, C., López-Gómez, I., Gutiérrez, D., Esteve, I., Sánchez-Chardi, A., Solé, A. 2021. Cellular strategies against metal exposure and metal localization patterns linked to phosphorus pathways in *Ochrobactrum anthropi* DE2010. J Hazard Mater 123808. https://doi.org/10.1016/j.jhazmat.2020.123808.

Visscher, P.T., Gallagher, K.L., Bouton, A., Farias, M.E., Kurth, D., Sancho-Tomás, M., Philippot, P., Somogyi, A., Medjoubi, K., Vennin, E., Bourillot, R., Walter, M.R., Burns, B.P., Contreras, M., Dupraz, C. 2020. Modern arsenotrophic microbial mats provide an analogue for life in the anoxic Archean. Commun Earth Environ 1:24. https://doi.org/10.1038/s43247-020-00025-2

Wang, C., Jin, H., Zhong, C., Wang, J., Sun, M., Xie, M. 2020. Estimating the contribution of atmosphere on heavy metals accumulation in the aboveground wheat tissues induced by anthropogenic forcing. Environ Res 189:109955. https://doi.org/10.1016/j.envres.2020.109955.

Wang, G.H., Cheng, C.Y., Liu, M.H., Chen, T.Y., Hsieh, M.C., Chung, Y.C. 2016. Utility of *Ochrobactrum anthropi* YC152 in a microbial fuel cell as an early warning device for hexavalent chromium determination. Sensors 16:1272. https://doi.org/10.3390/s16081272.

Wong, H.L., Ahmed-Cox, A., Burns, B.P. 2016. Molecular Ecology of Hypersaline Microbial Mats: Current Insights and New Directions. Microorganisms 4(1):6. https://doi.org/10.3390/microorganisms4010006

Xiao, R., Bai, J., Gao, H., Wang, J., Huang, L., Liu, P. 2012. Distribution and contamination assessment of heavy metals in water and soils from the college town in the Pearl River Delta, China. CLEAN–Soil, Air, Water 40(10):1167-1173. https://doi.org/10.1002/clen.201200016.

Xu, X., Hao, R., Xu, H., Lu, A. 2020. Removal mechanism of Pb(II) by *Penicillium polonicum*: Immobilization, adsorption, and bioaccumulation. Sci Rep 10(1):9079. https://doi.org/10.1038/s41598-020-66025-6.

Yagel, Y., Sestito, S., Motro, Y., Shnaiderman-Torban, A., Khalfin, B., Sagi, O., Navon-Venezia, S., Steinman, A., Moran-Gilad, J. 2020. Genomic characterization of antimicrobial resistance, virulence, and phylogeny of the genus *Ochrobactrum*. Antibiotics 9(4):177. https://doi.org/10.3390/antibiotics9040177.

Yao, S., Lyu, S., An, Y., Lu, J., Gjermansen, C., Schramm, A. 2019. Microalgae–bacteria symbiosis in microalgal growth and biofuel production: a review. J Appl Microbiol 126(2): 359-368. https://doi.org/10.1111/jam.14095.

Yilmaz, A., Yanar, A., Alkan, E. 2018. Review of heavy metal accumulation in aquatic environment of Northern East Mediterrenean Sea part II: Some non-essential metals. Pollution 4(1):143-181. https://doi.org/10.22059/POLL.2017.236121.287.

Yilmazer, P. and Saracoglu, N. 2009. Bioaccumulation and biosorption of copper (II) and chromium (III) from aqueous solutions by Pichia stipitis yeast. Journal of Chemical Technology & Biotechnology: International Research in Process, Environmental & Clean Technology 84(4):604-610. https://doi.org/10.1002/jctb.2088.

Yin, W., Wang, Y., Liu, L., He, J. 2019a. Biofilms: The microbial "protective clothing" in extreme environments. Int J Mol Sci 20(14):3423. https://doi.org/10.3390/ijms20143423.

Yin, K., Wang, Q., Lv, M., Chen, L. 2019b. Microorganism remediation strategies towards heavy metals. Chem Eng J 360:1553-1563. https://doi.org/10.1016/j.cej.2018.10.226.

Yue, Z.B., Li, Q., Li, C.C., Chen, T.H., Wang, J. 2015. Component analysis and heavy metal adsorption ability of extracellular polymeric substances (EPS) from sulfate reducing bacteria. Biores Technol 194:399-402. https://doi.org/10.1016/j.biortech.2015.07.042.

Zeb, B., Ping, Z., Mahmood, Q., Lin, Q., Pervez, A., Irshad, M., Bilal, M., Bhatti, Z.A., Shaheen, S. 2017. Assessment of combined toxicity of heavy metals from industrial wastewaters on *Photobacterium phosphoreum* T3S. Appl Water Sci 7(4):2043-2050. https://doi.org/10.1007/s13201-016-0385-4.

Zhang, L., Sun, Z.L., Geng, W., Cao, H., Qin, Y.C., Xu, C.L., Zhang, X., Li, X., Zhang, X., Song, H.L. 2019. Advances in the microbial mineralization of seafloor hydrothermal systems. China Geol 2(2):227-237. https://doi.org/10.31035/cg2018087.

Zhu, Q.L., Bao, J., Liu, J., Zheng, J.L. 2020. High salinity acclimatization alleviated cadmium toxicity in *Dunaliella salina*: transcriptomic and physiological evidence. Aquat Toxicol 223:105492. https://doi.org/10.1016/j.aquatox.2020.105492.

AGRAïMENTS AGRADECIMIENTOS ACKNOWLEDGEMENTS

Lo tenía claro, desde bien pequeño quería ser biólogo. Cuando llegó el momento me matriculé en la Licenciatura de biología en la Universidad Autónoma de Barcelona, y lo hice por vocación, por ganas de ser aquello que quería ser. En segundo curso de esta Licenciatura realicé la asignatura de Microbiología, y allí me di cuenta de que iba a ser Microbiólogo. Llegó el tercer curso, demasiado rápido y sin mucho tiempo para digerirlo, y escogí la asignatura de Ecología Microbiana. Sin duda, mi punto de inflexión, un claro antes y después en mi crecimiento profesional y personal. Cursando esa asignatura la conocí, entró en clase y desde la proximidad y amabilidad que la caracterizaba nos presentó la asignatura. Isabel Esteve me mostró el universo de la Ecología Microbiana y allí aprendí dos cosas: la primera, que no sería Microbiólogo a secas si no que sería Ecólogo Microbiano y la segunda, que quería del modo que fuera, hacerlo en el grupo de investigación al que Isabel perteneciera. Y así fue, cursé las prácticas de la Licenciatura, las prácticas del Máster y el doctorado en ese laboratorio. Aprendí, disfruté, crecí, descubrí y, principalmente, abrí mi mente a la ciencia. Y ahora, que acabo de escribir mi tesis, ella no está, nos dejó no hace mucho. Durante mi tesis ella ha sido mi tutora, siempre dispuesta a colaborar, a aportar, a dar una palmadita en la espalda cuando las cosas se ponían feas, a debatir sobre todo y sobre nada, a tantas y tantas situaciones, momentos y vivencias que parece imposible plasmarlas en un papel. Isabel quiero dedicarte esta tesis, es un pequeño gesto que no se ajusta a lo que realmente te mereces, pero donde quiera que estés deseo con todas mis fuerzas que te sientas orgullosa de este trabajo. Muchísimas gracias por tanto a cambio de tan poco, siempre estarás en mis recuerdos.

Durante la elaboración de mi tesis doctoral, que ha durado cinco años, he tenido la suerte que estar muy bien acompañado. Estas personas han hecho que mi día a día fuera motivante y una aventura "microbiana" que he disfrutado mucho viviéndola. Tengo tantas y tantas palabras de agradecimiento que espero poder plasmarlas en este papel. En primer lugar, gracias a mi director de tesi el Dr. Antoni Solé por la confianza, por la oportunidad, por tenerme siempre en cuenta, y por las horas dedicadas a hacer ciencia. Sin duda el viaje ha valido mucho la pena. Quiero agradecer también a los y las estudiantes tanto de grado como de máster y doctorado con los que he podido compartir aprendizajes, Malú, Altair, Dani, Diana, Irene, Nadia, Neus y Anna. Mil gracias por las ganas de aprender, por las ganas de ayudar y por aportarme tantas y tantas cosas buenas. También quiero tener palabras de agradecimiento para los que estuvieron a mi lado cuando yo era mucho más joven, mil gracias Joan, Elia, Zully, Álvaro, Maximiliano, Marina, Jordi, Pilar y Sandra. Y, como no, a Laia y Cris. Con vosotras he compartido mi día a día, gracias infinitas por vuestros consejos, por vuestra ayuda y por regalarme momentos que permanecerán siempre en mi memoria. También, y con especial cariño, gracias Alex, Neus, Belén, Núria, Mireia, Raquel y Cristina. Muchas veces pienso que debería valorar mucho más a las buenas personas que el azar cruza en mi vida, espero aprender a hacerlo mejor. Gracias por los consejos desinteresados y por tantos momentos de desconexión para cargar las pilas y volver al trabajo como nuevo. Finalmente, y no por eso menos importantes, gracias a los míos, a mi familia. A mi madre, a mi padre y a mi hermano, os quiero mucho. Infinitas gracias, a mis tres paredes maestras a Estefanía, Luis y Arnau, sin duda sin vosotros no sería yo. Gracias por aguantarme (soportarme), por tener paciencia cuando la mía ya hace rato que no está y por darme fuerza para seguir adelante sin rendirme.